

# Biodegradable Architecture with Mycelium-based Biocomposite Materials

*A Compostable Catenary Vault Design*

by

**Onurcan Sabri Kurt**

In partial fulfilment of the requirements for the degree of

**Master of Engineering**

Master of Integrated Design (MID)

At the Hochschule Ostwestfalen-Lippe

To be presented publicly on Wednesday July 11, 2018 at 10:00 am

Supervisors: Prof. Dipl.-Ing. Schulz, Jens-Uwe

Dipl.-Ing. Lemberski, David

**MID**

**Hochschule Ostwestfalen-Lippe**  
*University of Applied Sciences*

## Abstract

In 1980's, with the evolving understanding of ecological and environmental awareness, the term of sustainability was introduced for the first time which later led to occur a new sub-concept of sustainability which is eco-efficiency. An emerging and relatively more concentrated form of those terms is receiving an increasing interest; biodegradability. Especially, in the construction industry which has an enormous contribution to the current environmental issues, the interests and investments in eco-efficient and biodegradable materials is remarkably high. However, developing biodegradable materials with natural sources and materials for construction industry is relatively expensive. Except mushrooms. There is an emerging type of materials with its remarkably high potential by being completely bio-based and biodegradable with zero trace, as well as low-cost production. These materials are based on *mycelium* which is the vegetative part of fungus/mushroom combined with agricultural waste as a natural reinforcement like straw, sawdust, flax or hemp fibers etc. In this master thesis study, the potential fields of usage of mycelium and mycelium-based biocomposite materials have been represented with a wide range of literature review. Based on the literature knowledge and personal experiences, a variety of experiments have been done in order to produce mycelium-based materials by using different fungi/mushroom species and natural fibers as substrates. As a case study, a catenary vault has been designed using computational parametric design tools in order to provide a wide control over the design. Then, based on the selected material properties data bases from the literature, the catenary vault design has been analyzed and results have been simulated in order to represent the effect of different mechanical properties of mycelium-based biocomposite materials on the design. Through computational analysis tools, it has been proved that by using the appropriate species of mushroom and substrate types it is possible to build the designed catenary vault pavilion which is in a static equilibrium.

*Key words: Mycelium, mycelium-based biocomposite, biodegradable, catenary vault*



## *Preface*

This master thesis project has been written as in partial fulfilment of the requirements for the degree of Master of Engineering in the master program Master of Integrated Design (MID) at the Hochschule Ostwestfalen-Lippe and handed in the summer semester 2018. The story how I ended up working with mushrooms and mycelium is actually going way back to my bachelor studies, to the times that I have had an increasing interest on biomimicry and natural materials. Since then, I was always looking for a way to make any idea or design more eco-friendly and sustainable with biomimetic approaches. Thus, when I was thinking about to design a vault structure, I started to do lots of researches in emerging bio-based and sustainable building materials. However, mycelium-based biocomposite materials immediately amazed me by being completely biodegradable and having a lot of potentials. I have incredibly enjoyed exploring about mushrooms, mycelium and countless applications and possible fields of usages of mycelium and mycelium-based biocomposite materials. It was really educating to explore a new building material and combine it with computational design and analysis tools in order to be able to deeply examine and understand the behavior of the material and the design. This thesis work definitely brought me a completely different and unique point of view in terms of the relationship between material science, biology, nature, biomimicry and computational design tools under architectural design and structural analysis subjects.

## *Acknowledgments*

My first and foremost gratitude is to my thesis advisor Professor Dip.-Ing. Jens-Uwe Schulz who has been my attentive guide and teacher who encouraged me to explore and experiment while providing me a broad range of advices and aspects. I also thank my second supervisor Dip.-Ing. David Lemberski for his encouragement and advice during this thesis work.

I also would like to extend special thanks to Prof. Dr.-Ing. Christoph Barth who is in charge of Plastics Technology Laboratory, under the Department of Production and Economics at Hochschule Ostwestfalen-Lippe, for providing me access to specific tools and materials with his great generosity during the plastic mold production process. I am sincerely thankful to Dip.-Ing. Jens Mannel and M.Eng. George Matthes for guiding me and sharing knowledge during the process of plastic mold production. Also, thanks to Dip.-Ing. Guido Brand and Dip.-Ing. Ingmar Rohlf for their support during the fast prototyping and mold production process.

My dearest loving parents Aynur and Necdet, and my sibling Bora, have been always there when I needed them the most and done everything in their power to help and encourage me the achieve my goals and follow my dreams. My deepest thanks to Cansu for being there when I needed the most.

*Onurcan Sabri KURT*  
*Detmold, June 2018*

## *Declaration of Authorship*

I hereby certify that the thesis I am submitting is entirely my own original work except where otherwise indicated. I am aware of the University's regulations concerning plagiarism, including those regulations concerning disciplinary actions that may result from plagiarism. Any use of the works of any other author, in any forms, is properly acknowledged at their point of use.

*Onurcan Sabri KURT*

*Detmold, June 2018*

# Contents

<i>Abstract</i> .....	2
<i>Preface</i> .....	3
<i>Acknowledgments</i> .....	4
<i>Declaration of authorship</i> .....	5
<i>Contents</i> .....	6
<i>List of figures</i> .....	8
<i>List of tables</i> .....	10
<b>CHAPTER I</b> .....	<b>11</b>
<b>1. Introduction</b> .....	<b>11</b>
<b>1.1 What is biodegradable?</b> .....	<b>13</b>
<b>1.2 Advantages and disadvantages of biodegradable materials</b> .....	<b>14</b>
1.2.1 Landfill saving.....	14
1.2.2 Resource efficiency .....	14
1.2.3 Low embodied energy .....	16
1.2.4 Thermal and acoustic properties .....	16
1.2.5 Biological contamination and pest infestation .....	16
1.2.6 Moisture weakness .....	16
1.2.7 Low tensile strength .....	16
<b>1.3 Biodegradable building materials</b> .....	<b>16</b>
1.3.1 Minimally processed .....	16
1.3.2 Bonded biodegradable materials.....	17
1.3.3 Plastic from natural polymers.....	17
1.3.4 Synthetic biodegradable materials .....	17
<b>CHAPTER II</b> .....	<b>18</b>
<b>2. What is mycelium?</b> .....	<b>18</b>
<b>2.1 A literature review of mycelium and mycelium-based materials</b> .....	<b>19</b>
2.1.1 Medical applications .....	20
2.1.2 Biotechnological applications.....	20
2.1.3 Transportation industry.....	20
2.1.4 Packing .....	20
2.1.5 Building materials.....	21
2.1.6 Furniture .....	22
2.1.7 Textile.....	23
2.1.8 Architecture .....	24
<b>2.2 Potential usages of mycelium and advantages of mycelium-based materials</b> .....	<b>24</b>
2.2.1 Using mycelium to clean oil spills .....	24
2.2.2 Purification of urban streams, lake, and rivers.....	24
2.2.3 Fuel production .....	25
2.2.4 Reforestation.....	25
2.2.5 Locality .....	25
2.2.6 Close-loop cycle .....	25
2.2.7 Fire resistance .....	26

<b>2.3</b>	<b>A literature review of physical and mechanical properties of mycelium-based materials.....</b>	<b>27</b>
2.3.1	Morphology and mechanical aspects of mycelium .....	27
2.3.2	Natural fibers .....	28
2.3.3	Known properties of mycelium-based materials .....	31
2.3.3.1	Compressive strength.....	32
2.3.3.2	Tensile strength .....	33
2.3.3.3	Elastic modulus and shear modulus .....	34
2.3.3.4	Poisson’s ratio.....	34
2.3.3.5	Density.....	34
2.3.4	Comparison of tensile strength and compressive strength values .....	35
<b>CHAPTER III.....</b>		<b>37</b>
<b>3.</b>	<b>How to grow mycelium and mycelium-based materials?.....</b>	<b>37</b>
<b>3.1</b>	<b>Petri dish stage .....</b>	<b>38</b>
3.1.1	Spore print culture .....	40
3.1.2	Mushroom tissue culture .....	41
3.1.3	Mycelium growth .....	41
<b>3.2</b>	<b>Jar stage .....</b>	<b>42</b>
<b>3.3</b>	<b>Bag stage.....</b>	<b>44</b>
3.3.1	Sawdust, sawdust + woodchips.....	44
3.3.2	Straw .....	46
<b>3.4</b>	<b>Forming stage .....</b>	<b>47</b>
<b>3.5</b>	<b>Drying.....</b>	<b>49</b>
<b>3.6</b>	<b>Experiences and deduces of mycelium growing process .....</b>	<b>50</b>
<b>CHAPTER IV .....</b>		<b>54</b>
<b>4.</b>	<b>Biodegradable pavilion design .....</b>	<b>54</b>
<b>4.1</b>	<b>Catenary curve, arch, and vault .....</b>	<b>54</b>
<b>4.2</b>	<b>Parametric catenary vault design .....</b>	<b>56</b>
4.2.1	Hanging chain model.....	56
4.2.2	Adaptive mold system and hyperbolic paraboloid bricks .....	60
4.2.3	Density matching with Karamba3D analysis .....	61
4.2.4	Structural analysis by ANSYS .....	62
4.2.4.1	Catenary vault with the hyperbolic paraboloid bricks with different densities .....	63
4.2.4.2	Catenary vault with the hyperbolic paraboloid bricks based on the data of <i>MycoFoam</i> .....	69
4.2.4.3	Catenary vault with the hyperbolic paraboloid bricks based on the data of Travaglini <i>et al.</i> (2013) .....	71
4.2.4.4	Catenary vault with the hyperbolic paraboloid bricks based on the data of Yang <i>et al.</i> (2017) .....	73
4.2.4.5	Catenary vault with the rectangular shaped bricks based on the data of Yang <i>et al.</i> (2017).....	75
<b>CHAPTER V.....</b>		<b>77</b>
<b>5.</b>	<b>Conclusion.....</b>	<b>77</b>
<b>CHAPTER VI .....</b>		<b>80</b>
<b>6.</b>	<b>Prospects.....</b>	<b>80</b>
<b>CHAPTER VII .....</b>		<b>82</b>
<b>7.</b>	<b>Attachment/Appendix.....</b>	<b>82</b>
<b>BIBLIOGRAPHY/REFERENCES .....</b>		<b>87</b>

## List of Figures

Figure 1: Ganoderma lucidum mycelium structure.....	19
Figure 2: Black arrow: hyphae; White arrows: septa.....	19
Figure 3: Spawn jar with Ganoderma lucidum mycelium growing on wheat grains.....	19
Figure 4: Parts of mushroom and their functions.....	20
Figure 5: Mycelium material injection molding system to produce vehicle pieces by Kalisz and Rocco.....	21
Figure 6: MycoFoam tile and MycoFoam single bottle wine shipper by Ecovative Design.....	22
Figure 7: Greensulate mycelium-based insulation material.....	23
Figure 8: Section of Greensulate by Ecovative Design.....	23
Figure 9: Mycelium char by Philip Ross.....	23
Figure 10: Mycelium lamp by Jonas Edward.....	23
Figure 11: 3D printed mold, filled with mycelium inoculated biomass by Eric Klarenbeek.....	24
Figure 12: Leather-like mycelium textile development by MycoWorks.....	24
Figure 13: Hy-fi mycelium tower FEA by ARUP.....	25
Figure 14: Hy-fi mycelium bricks tower by The Living.....	25
Figure 15: Fire test on mycelium-based insulation material Greensulate by Ecovative Design.....	27
Figure 16: Schematic representation of mycelium physiology at different scales.....	28
Figure 17: Micrographs of strongly branched hyphal networks of.....	29
Figure 18: Hierarch of flax bundles.....	30
Figure 19: Tensile and compressive stress-strain comparison of mycelium-based material.....	37
Figure 20: The effect of different densities on the stress-strain response both under tension and compression.....	37
Figure 21: Ingredients for malt extract agar medium.....	40
Figure 22: Malt extract agar medium mixture.....	40
Figure 23: Petri dish with agar medium.....	40
Figure 24: Spore print of a mushroom cap.....	41
Figure 25: Inoculation of an agar medium in a Petri dish.....	41
Figure 26: Tissue extraction from a mushroom section.....	42
Figure 27: Tissue transformation into an agar Petri dish.....	42
Figure 28: Ingredients to soak the rye grain.....	43
Figure 29: Simmering the soaked rye grain.....	43
Figure 30: Simmered rye grains in the jars.....	44
Figure 31: Polyester filter on the lid of the jars.....	44
Figure 32: Inoculated jar of rye grain with mycelium on an agar medium.....	45
Figure 33: Woodchips.....	46
Figure 34: Woodchips soaked in water.....	46
Figure 35: Oak sawdust pellets.....	46
Figure 36: Autoclave bags.....	46
Figure 37: Straw substrate.....	47
Figure 38: Pasteurization of straw substrate.....	47
Figure 39: Draining the pasteurized straw.....	47
Figure 40: Inoculation with mycelium spawn.....	47
Figure 41: Oak sawdust and woodchips substrate.....	48
Figure 42: Substrate mixtures with different ratios.....	48
Figure 43: Pressure cooker to sterilize the substrate mixtures.....	48
Figure 44: Sterilized substrate mixtures.....	48
Figure 45: Thermoforming machine.....	49
Figure 46: CNC processed MDF negative form and.....	49
Figure 47: Thermoformed plastic and negative forms.....	49
Figure 48: Negative form and thermoformed plastic of hyperbolic paraboloid brick.....	49
Figure 49: Section of the molds for hyperbolic paraboloid bricks.....	49
Figure 50: Hyperbolic paraboloid brick mold.....	49
Figure 51: A sawdust mycelium block before oven drying.....	51
Figure 52: A sawdust mycelium block after oven drying.....	51
Figure 53: Mycelium bricks before oven drying.....	51
Figure 54: Mycelium bricks after oven drying.....	51
Figure 55: Lentinula edodes (Shiitake).....	51
Figure 56: Pleurotus eryngii (King Oyster).....	51
Figure 57: First day of the observation on the sample groups.....	52
Figure 58: 10th day of the observation on the sample groups.....	52
Figure 59: 3 point load mechanical tests.....	53
Figure 60: Failure of the first samples.....	53
Figure 61: Ganoderma lucidum mushroom fruiting on nutritional substrates.....	53
Figure 62: Comparison of different substrates inoculated with different species.....	54

Figure 63: Mycelium growing on the straw substrate.....	54
Figure 64: Mycelium growing on Oak sawdust substrate.....	54
Figure 65: Samples growing in different molds.....	54
Figure 66: Graph of different catenary curves.....	55
Figure 67: An almost catenary arch of Taq Kasra, 6th Century BC.....	56
Figure 68: (A) Poleni's drawing of a hanging chain and an arch, (B) the analysis of the dome of St-Peter's by Poleni.....	56
Figure 69: Hanging chain under only gravitational forces creating undistributed catenary form and chain loaded with different loads creating modified catenary.....	57
Figure 70: Related part of the Grasshopper definition to simulate the hanging chain model.....	58
Figure 71: Steps 1 to 4 to create the hanging chain model with Grasshopper script.....	58
Figure 72: Steps 5 to 8 to create the catenary vault surface with Grasshopper script.....	59
Figure 73: Karamba3D analysis of the catenary vault surface.....	60
Figure 74: Steps 10 to 11 to analyze the displacement on the catenary vault and first brick generation.....	60
Figure 75: Steps 11 to 13 of the adaptive mold system and variations of the vault with each brick type.....	61
Figure 76: Steps 14 to 16 of the adaptive mold system and variations of the vault with each brick type.....	62
Figure 77: Steps 17 to 18 of the Karamba3D analysis and density matching.....	63
Figure 78: Related part of the Grasshopper script to match the densities and the Karamba3D analysis results.....	63
Figure 79: The interface of SpaceClaim where the Rhinoceros 5 model has been imported and grouped according to the densities.....	64
Figure 80: Interface of the "Engineering Data" component of ANSYS Workbench to define material properties.....	65
Figure 81: The schematic interface of ANSYS Workbench.....	66
Figure 82: The interface of ANSYS Mechanical.....	67
Figure 83: (A) Standard Earth Gravity force applied to the catenary vault, (B) Fixed supports of the catenary vault.....	67
Figure 84: Total displacement analysis of the catenary vault with different density bricks.....	68
Figure 85: Equivalent (von-Mises) stress analysis of the catenary vault with different density bricks.....	68
Figure 86: Maximum principal stress analysis of the catenary vault with different density bricks.....	69
Figure 87: Comparison of the deformed and undeformed catenary vault with different density bricks.....	69
Figure 88: Total displacement analysis of the catenary vault with MycoFoam mycelium material.....	70
Figure 89: Equivalent (von-Mises) stress analysis of the catenary vault with MycoFoam mycelium material.....	70
Figure 90: Maximum principal stress analysis of the catenary vault with MycoFoam mycelium material.....	71
Figure 91: Comparison of the deformed and undeformed catenary vault with MycoFoam mycelium material.....	71
Figure 92: Total displacement analysis of the catenary vault with the data of Travaglini et al. (2013).....	72
Figure 93: Equivalent (von-Mises) stress analysis of the catenary vault with the data of Travaglini et al. (2013).....	72
Figure 94: Results of the maximum principal stress analysis of the catenary vault with the data of Travaglini et al. (2013).....	73
Figure 95: Comparison of the deformed and undeformed catenary vault with the data of Travaglini et al. (2013).....	73
Figure 96: Total displacement analysis of the catenary vault with the data of Yang et al. (2017).....	74
Figure 97: Equivalent (von-Mises) stress analysis of the catenary vault with the data of Yang et al. (2017).....	74
Figure 98: Results of the maximum principal stress analysis of the catenary vault with the data of Yang et al. (2017).....	75
Figure 99: Comparison of the deformed and undeformed catenary vault with the data of Yang et al. (2017).....	75
Figure 100: Total displacement analysis of the catenary vault with the regular rectangular shaped bricks based on the data of Yang et al. (2017).....	76
Figure 101: Equivalent (von-Mises) stress analysis of the catenary vault with the regular rectangular shaped bricks based on the data of Yang et al. (2017).....	76
Figure 102: Results of the maximum principal stress analysis of the catenary vault with the regular rectangular shaped bricks based on the data of Yang et al. (2017).....	77
Figure 103: Comparison of the deformed and undeformed catenary vault with the regular rectangular shaped bricks based on the data of Yang et al. (2017).....	77
Figure 104: Grasshopper definition of the acoustic panel.....	82
Figure 105: Steps 1 to 6 of the Grasshopper definition to generate the acoustic panel.....	82
Figure 106: Steps 7 to 8 of the Grasshopper definition to generate the acoustic panel.....	83
Figure 107: Acoustic panel out of Ganoderma lucidum and sawdust-wood chips substrate mixture right after it has been taken out from the mold.....	83
Figure 108: Acoustic absorber panel.....	84
Figure 109: Various materials taken out from their molds with Pleurotus eryngii and straw substrate.....	84
Figure 110: Mycelium growth of various materials after two days outside the molds.....	84
Figure 111: Another acoustic absorber panel.....	85
Figure 112: Mycelium-based biocomposite bricks growing in the molds.....	85
Figure 113: Mycelium-based biocomposite bricks growing in the molds.....	86
Figure 114: Hyperbolic paraboloid mycelium-based biocomposite brick growing in the molds.....	86

## List of Tables

Table 1: Biodegradable Polymers .....	14
Table 2: Kg of landfill in the EU-27 countries.....	15
Table 3: Embodied energy for common building materials.....	16
Table 4: Embodied energy levels in average Australian house.....	16
Table 5: Ecovative Design's MycoFoam material properties.....	21
Table 6: Natural and synthetic fiber classification.....	30
Table 7: Comparison between natural and glass fiber .....	31
Table 8: Mechanical properties of natural fibers .....	31
Table 9: Comparative material properties of mycelium material .....	33
Table 10: Compressive stress-strain response .....	33
Table 11: Collection of different values for compressive strength of different mycelium-based materials.....	34
Table 12: Mechanical characterization .....	34
Table 13: Collection of different values for tensile strength of different mycelium-based materials .....	35
Table 14: Comparison of tensile strength and compressive strength values of mycelium-based materials.....	36
Table 15: Steps of the methodology to create mycelium-based material.....	39
Table 16: Material properties of MycoFoam by Ecovative Design .....	65
Table 17: Material properties of the mycelium-based material by Travaglini et al. (2013).....	65
Table 20: Material properties of the mycelium-based material by Yang et al. (2017).....	66
Table 21: Results of the total displacement analysis of the catenary vault with different density bricks .....	68
Table 22: Results of the Equivalent (von-Mises) stress analysis of the catenary vault with different density bricks.....	68
Table 23: Results of the maximum principal stress analysis of the catenary vault with different density bricks.....	69
Table 24: Results of the total displacement analysis of the catenary vault with MycoFoam mycelium material.....	70
Table 25: Results of the Equivalent (von-Mises) stress analysis of the catenary vault with MycoFoam mycelium material .....	70
Table 26: Results of the maximum principal stress analysis of the catenary vault with MycoFoam mycelium material .....	71
Table 27: Results of the total displacement analysis of the catenary vault with the data of Travaglini et al. (2013) .....	72
Table 28: Results of the Equivalent (von-Mises) stress analysis of the catenary vault with the data of Travaglini et al. (2013).....	72
Table 29: Results of the maximum principal stress analysis of the catenary vault with the data of Travaglini et al. (2013).....	73
Table 30: Results of the total displacement analysis of the catenary vault with the data of Yang et al. (2017) .....	74
Table 31: Results of the Equivalent (von-Mises) stress analysis of the catenary vault with the data of Yang et al. (2017).....	74
Table 32: Results of the maximum principal stress analysis of the catenary vault with the data of Yang et al. (2017).....	75
Table 33: Results of the total displacement analysis of the catenary vault with the regular rectangular shaped bricks based on the data of Yang et al. (2017) .....	76
Table 34: Results of the Equivalent (von-Mises) stress analysis of the catenary vault with the regular rectangular shaped bricks based on the data of Yang et al. (2017) .....	76
Table 35: Results of the maximum principal analysis of the catenary vault with the regular rectangular shaped bricks based on the data of Yang et al. (2017) .....	77



### 1. Introduction

All systems in the biosphere cycle, as the biosphere is literally made of networks of materials and information which continuously recycle. However, recent outrages human activities especially in terms of fossil fuel usage, extreme deforestation, the rapid increase in concrete mass with the urbanization etc. generated a huge impact resulting with a critical level of imbalance in the carbon cycle. As it exceeds the capacities of the natural cycle, this rapid and excessive release of CO<sub>2</sub> to the atmosphere is not compensable with the photosynthesis activity or the dissolution of the natural water sources. As the biggest and most well-known result of this break in the carbon cycle, the impact of global warming increases as the accumulation of CO<sub>2</sub> increases in the atmosphere.

In 1980's, with the evolving understanding of ecological and environmental awareness, the term "sustainability" was introduced for the first time. According to the UN World Commission on Environmental Development in Our Future, sustainability defined as "*a development that meets the needs of the present without compromising the ability of future generations to meet their own needs*". Within the concept of sustainability, a new sub-concept called eco-efficiency was introduced for the first time in 1991 by the World Business Council for Sustainable Development-WBCSD as "*the development of products and services at competitive prices that meet the needs of humankind with quality of life, while progressively reducing their environmental impact and consumption of raw materials throughout their life cycle, to a level compatible with the capacity of the planet*".

Since the last decades, bio-based and biodegradable products are receiving an increasing interest in their high potential of being eco-efficient. For many, this has a strong connection with the expansion of sustainable development policies and decreasing reserve fossil resources as well as expanding environmental concerns. According to Wool and Sun (2005),

*"The conversion of biomass to useful materials such as polymers and composites has considerable economic and environmental value, particularly in times of global warming and diminishing petroleum oil reserves"*.

Being one of the largest and most active sectors in Europe, the obvious contribution of the construction industry to the current environmental issues is literally enormous as it is stated by Pacheco Torgal and Jalali (2011) that it represents about 28.1% in the industry and about 7.5% employment in the European economy. This effect of the construction industry in the environment is mainly constituted with building materials. Clearly, the environmental impacts occurred from the extraction of raw materials are one of the most important environmental issues related to the production of construction materials (Barnett and Morse 1963). Besides the high energy consumption in the manufacturing process of the modern construction materials, another problem is related with their low ability to be recycled or decomposed after their disposal which brings up the massive piles of waste to landfills.

There is an emerging type of materials with its remarkably high potential by being completely bio-based and biodegradable with no environmental impact. These materials are based on *mycelium* which is the vegetative part of fungus and agricultural waste as a natural reinforcement like sawdust, straw, flax or hemp fibers etc. Due to their low-cost production process, nature of being a part of the carbon cycle, renewability, and biodegradability, mycelium-based biocomposite materials have a high potential to replace architectural and structural materials in the building industry.

In this master thesis study, a wide range of current and prospect usages of mycelium and mycelium-based biocomposite materials have been studied through literature review. Furthermore, mycelium generation and producing mycelium-based biocomposite materials have been studied both with an extensive literature review and various personal experiments that have been personally conducted. As the results of the experiments, a variety of mycelium-based biocomposite materials in many different forms have been produced.

As a case study to apply structural analyses and simulations in order to clearly represent the effect of variable material properties of mycelium-based biocomposite materials, a biodegradable pavilion design concept has been brought in. Thus, a catenary vault has been designed through parametric design tools and a variety of finite element analysis have been applied on the different stages of the design, based on the collection of material properties from the literature review.

## 1.1 What is biodegradable?

The simple definition of biodegradable is being able to be broken down into simpler substances and natural materials in the environment without causing any harm to nature or the organism that ingests. More specifically, biodegradation is an event which takes place through the action of enzymes and/or chemical decomposition associated with living organisms (bacteria, fungi, etc.) and their secretion products (Albertsson and Karlsson 1994). It is also necessary to consider abiotic reactions like photo-degradation, oxidation, and hydrolysis which may also alter the polymer before, during or instead of biodegradation because of environmental factors (Mohanty *et al.* 2000).

According to ASTM standard D-5488-94d and European norm EN 13432, “biodegradable” means “*capable of undergoing decomposition into carbon dioxide, methane, water, inorganic compounds, and biomass*”. The table below shows the categories of biodegradable polymers.

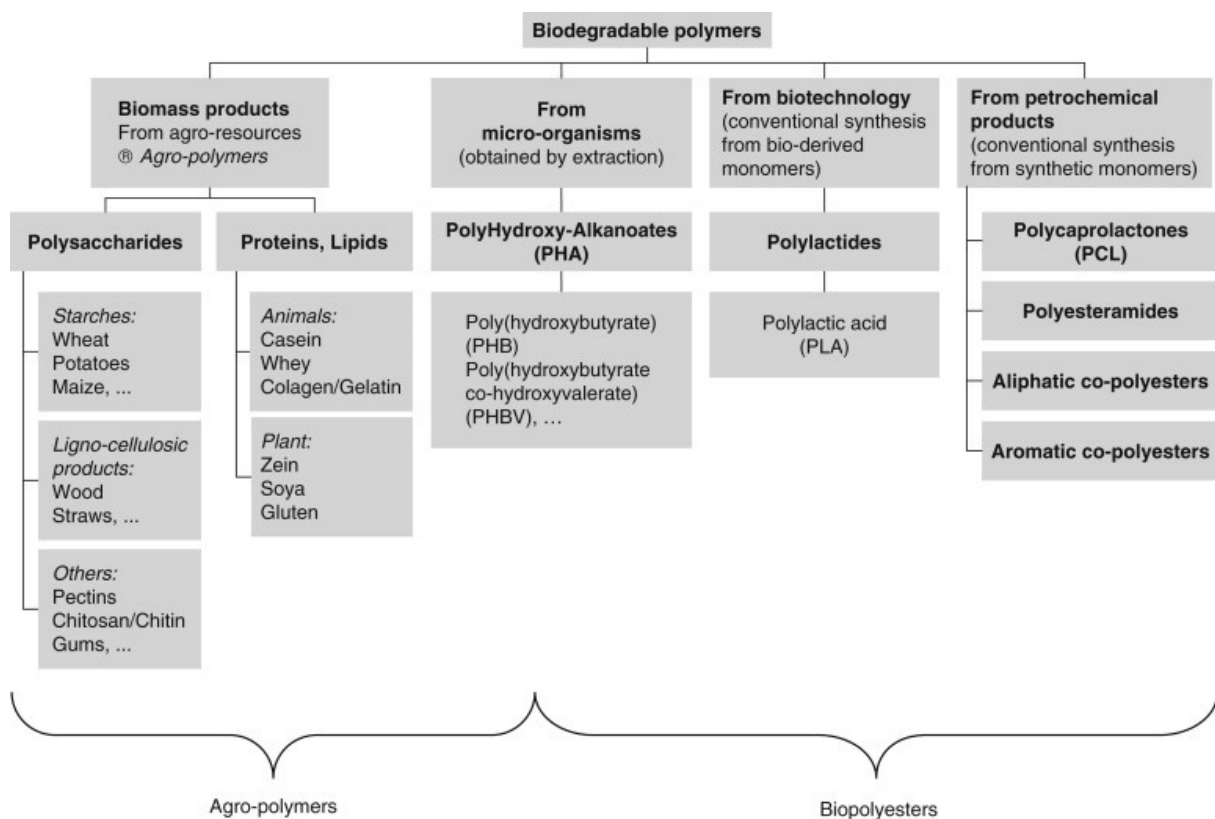


Table 1: Biodegradable Polymers (Bordes *et al.* 2009)

In order to be considered as a true biodegradable material, the period of time to fully break down should be short even on a human scale rather than taking extremely long years. Furthermore, nothing harmful should be left behind at the end of the decomposition process. Although the fact that some items are obviously biodegradable like food waste or chemical free wood and relatively easy to biodegrade materials like paper, some other products like steel may take extremely long years to be biodegraded. At this point, it is hard to avoid the question of how biodegradable are those products.

## 1.2 Advantages and disadvantages of biodegradable materials

As one of the positive results of sustainable and eco-friendly building concepts and policies, there is an increasing demand for biodegradable and bio-based materials in the construction sector. Besides some limitations related to the nature of biodegradable materials, they also bring a wide variety of advantages related to sustainable and environmental aspects, thermal and acoustic performances etc. Some of the primary advantages of biodegradable materials can be listed as in the following sub-categories;

### 1.2.1 Landfill saving

Since the biodegradable materials are part of the biosphere's innate cycle, they are meant to be decomposed once left aside in nature which helps to save an important amount of waste from the landfill areas. The following graph shows the amount of kg of landfilled waste per capita in the EU-27 countries.

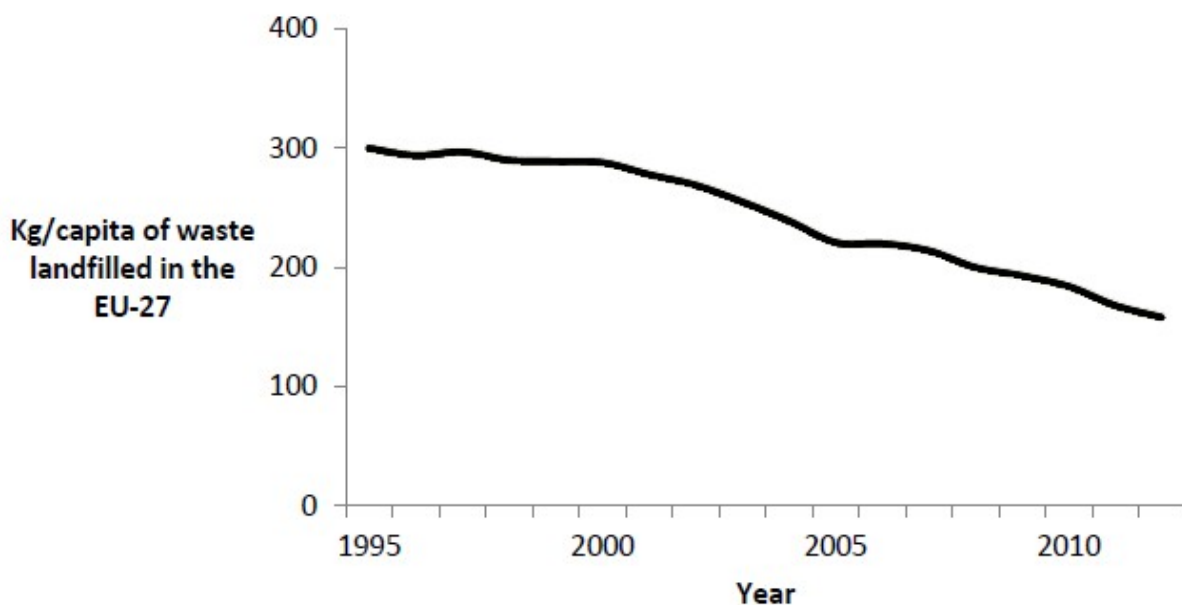


Table 2: Kg of landfill in the EU-27 countries (Lelivelt 2015)

### 1.2.2 Resource efficiency

Almost all of the raw material to produce biodegradable materials is supplied from the earth like soil, fiber-rich plants, and trees or agricultural wastes. Some often used raw materials like hemp, flax or cork have an appreciable short period of time to grow and be produced as well as they can be harvested multiple times with no harm to the plant, these materials are considered as resource efficient.

Similar to the criteria defined by Kralj and Markič (2008), resource efficient biodegradable building materials include an identifiable amount of recycled content while minimizing the resources during the production cycle and reducing the energy consumption.

### 1.2.3 Low embodied energy

Owing to low energy consuming production process of most of the biodegradable materials, they have relatively low embodied-energy and remarkably low CO<sub>2</sub> emission

contrary to modern mass-produced synthetic building materials. In order to have an overall view, some commercial building materials and their embodied energy values are listed in the table below.

Material	PER Embodied Energy (MJ/kg)
Kiln dried sawn softwood	3.4
Kiln dried sawn hardwood	2.0
Air dried sawn hardwood	0.5
Hardboard	24.2
Particleboard	8.0
MDF (medium density fiberboard)	11.3
Plywood	10.4
Glue-laminated timber	11.0
Laminated veneer lumber	11.0
Plastics — general	90.0
PVC (polyvinyl chloride)	80.0
Synthetic rubber	110.0
Acrylic paint	61.5
Stabilized earth	0.7
Imported dimensioned granite	13.9
Local dimensioned granite	5.9
Gypsum plaster	2.9
Plasterboard	4.4
Fiber cement	4.8*
Cement	5.6
In situ concrete	1.9
Precast steam-cured concrete	2.0
Precast tilt-up concrete	1.9
Clay bricks	2.5
Concrete blocks	1.5
Autoclaved aerated concrete (AAC)	3.6
Glass	12.7
Aluminum	170.0
Copper	100.0
Galvanized steel	38.0

Table 3: Embodied energy for common building materials (\*Based on an earlier version by Dr. Lawson) (Lawson 2006)

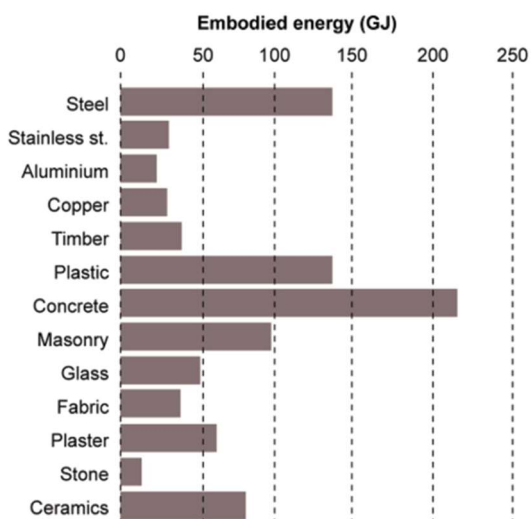


Table 4: Embodied energy levels in average Australian house (by the Commonwealth and Industrial Research Organization)

Some building materials like concrete, timber or bricks are more commonly used in construction industry rather than stainless steel or plastic. This creates the result of highest embodied energy mass in most buildings are from low embodied energy materials. The graph on the left shows the results of a research in Australia that has been done by CSIRO about the levels of embodied energy of building materials in an average Australian house.

#### 1.2.4 Thermal and acoustic properties

In the majority, biodegradable building materials have significant thermal and acoustic properties which can be applied for thermal and sound insulation purposes or etc. A study held by Curtu *et al.* (2012) showed that the study sample made out of wood flakes, wool bind with clay has a potential to be used for absorption of large frequency sounds.

Despite all the benefits of biodegradable materials, it is important to objectively mention their drawbacks and weak points in order to understand the nature of biodegradable materials. Their drawbacks are connected with weathering if unprotected, fire resistance and pest infestations, as well as sometimes dimensional instability (Ganotopoulou 2014).

Some of the disadvantages of biodegradable materials are listed below;

#### 1.2.5 Biological contamination and pest infestation

Depending on the type of biodegradable material, growth of harmful biological organisms like mold, bacteria or microbes can cause several problems. Since most of the biodegradable materials provide a suitable environment, they form a greater risk of biological contamination as a result of their nutrition content for fungi (Tuzcu 2007), mildews or molds. Also, the moisture content and temperature of the surface of the material, as well as the material type and exposure time are most critical factors on pest infestation, mold, bacteria and microbe development (Viitanen *et al.* 2010) on biodegradable building materials.

#### 1.2.6 Moisture weakness

As one of the most known problems of biodegradable materials, their high sensitivity to moisture causes problems related to material failure and biological contamination. Especially, biodegradable materials that include natural fibers with hydrophilic behavior may tend to hold a large amount of moisture if not well isolated.

#### 1.2.7 Low tensile strength

Even though natural fiber based biodegradable materials have better tensile strengths, materials based on soil like rammed earth have very low tensile strength while having a better compressive strength.

### 1.3 Biodegradable building materials

In general, biodegradable materials can be categorized into 4 different groups; natural materials with minimum processing requirements like timber, bamboo etc., and natural materials held together with resin or mesh-like soy boards, sisal carpet etc., biopolymers and adhesives like biodegradable plastics produced from natural compounds; synthetic biodegradable materials (Sassi 2006).

#### 1.3.1 Minimally processed

With the advanced crafting techniques and tools, natural biodegradable materials with minimal processing requirements find more use in contemporary construction beside the traditional areas of utilization within the categories listed below;

- *Structural elements (timber, bamboo, adobe, straw etc.)*
- *Insulation materials (flax, cork, hemp and sheep wool and stone wool etc.)*
- *Floor, wall and roof finishes (bamboo and timber rigid floor finishes, cork oak wall and floor finishes etc.)*
- *Timber fixture and fittings (bathtubs, sinks etc.)*

### 1.3.2 Bonded biodegradable materials

Bonded biodegradable materials consist of natural binding materials like clay, resin, soy-based binders, and lignin etc. and natural fibers and limestone etc. Engineered wood products are one of the biggest members of this group such as MDF, OSB, plywood, particleboard and laminated timber etc. The only contrary about engineered wood is even though they contain up to 90-100% (Lelivelt 2015) biodegradable compounds, the binder adhesive is not always considered as biodegradable depending on its chemical structure. One of the oldest examples of bonded biodegradable building materials is traditional adobe mixture out of clay and natural fibers like straw. Some other examples are listed below;

- *Non-loadbearing walls composed with layers of paper and natural fibers like straw, cotton or hemp*
- *Wall coverings composed with sisal, sheep wool, stone wool, coconut fibers, and seagrass etc.*
- *Floor finishes like linoleum composed with cork, sawdust, limestone powder, linseed oil and bonded with natural fiber*
- *Straw and soy composed boards and finishing*

### 1.3.3 Plastic from natural polymers

Although there are not lots of examples of building materials out of natural polymers with natural binders that performs equal characteristics in mechanical behavior as other biodegradable plastics bonded with synthetic adhesives, there are successful applications of biodegradable plastics composed out of proteins, cellulose, sugar molasses, starch, potato, wheat gluten bonded with natural adhesives like rye and potato flour starch, natural rubber and soy protein (Sassi 2006).

### 1.3.4 Synthetic biodegradable materials

Unlike natural polymers and due to higher production costs, synthetic biodegradable polymers have not achieved significant developments in order to manufacture building products (Sassi 2006). However, there are promising discoveries on petroleum-based plastics which can biodegrade with special additives (Swain *et al.* 2004).

Among all these groups of biodegradable building materials, mycelium-based biodegradable materials can be included within the group of bonded biodegradable materials as they are fully bio-based composite materials consisted of natural fibers and mycelium acting as a binding adhesive.

### 2. What is mycelium?

Lexical meaning of mycelium is “more than one” and actually, it is the plural form of the word “mycelia”. The scientific explanation of mycelium refers it as the vegetative lower part of a fungus, consisting of a mass branching, thread-like hyphae. Hyphae (singular hypha) is tubular filaments constituted by rigid chitin cell walls.

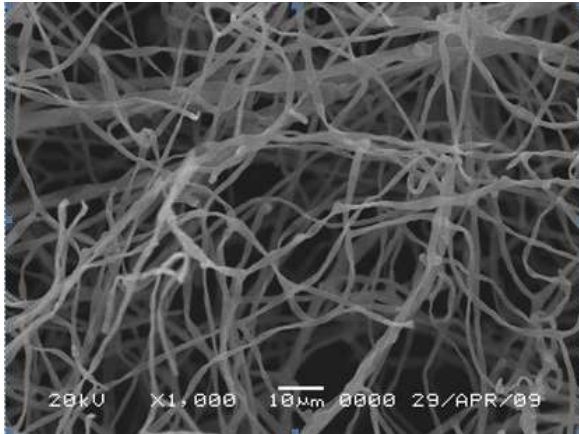


Figure 1: *Ganoderma lucidum* mycelium structure (Güler et al. 2011)

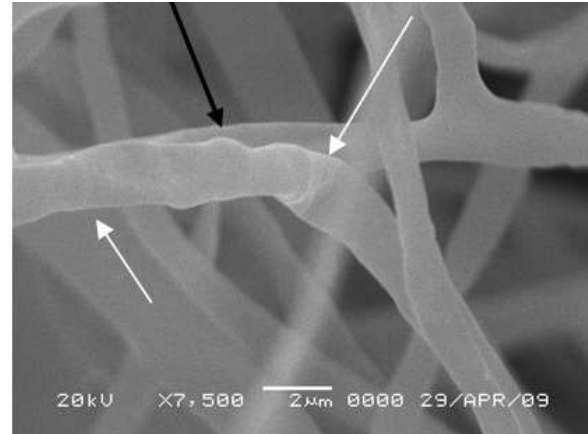


Figure 2: Black arrow: hyphae; White arrows: septa (Güler et al. 2011)



Figure 3: Spawn jar with *Ganoderma lucidum* mycelium growing on wheat grains (Author's image)

Mycelium comes in many sizes from very tiny to as large as a forest. A mycelium network that has been discovered in Oregon's Blue Mountains occupies almost 10 km<sup>2</sup> makes it the biggest living organism on earth (Hawksworth 2001).

Decomposing organic compounds is one of the primary existential purposes of fungi in the ecosystem. From dead plants, fungi recycle carbon, hydrogen, nitrogen, phosphorus, and minerals into nutrients for living plants, insects, and other organisms sharing that habitat (Stamets 2005). Without decomposer fungi, life on earth would probably cease after a few decades because carbon and mineral nutrients would be locked up in dead tissues and unavailable to autotrophs for continued primary production (Watkinson et al. 2016).



One should understand what a fungus is first in order to understand mycelium better. Fungi are heterotrophic eukaryotes which means they are not able to produce their own food like plants and some protists (McGraw-Hill 2016). Naturally, fungi have an asexual way of reproduction by spore release. Released spores are capable of turning into mycelium. Those mycelium created by spores are asexual until they join with another mycelium in order to constitute a dikaryotic mycelium. Fruiting bodies known as mushrooms are created by that mycelium.

Even though it may not be found easy to accept these notorious life forms are our kinsfolk. Incredibly, fungi are way far away than being plants in contrast to their look. Instead, they are closer to animals, to us (Montalti 2010).

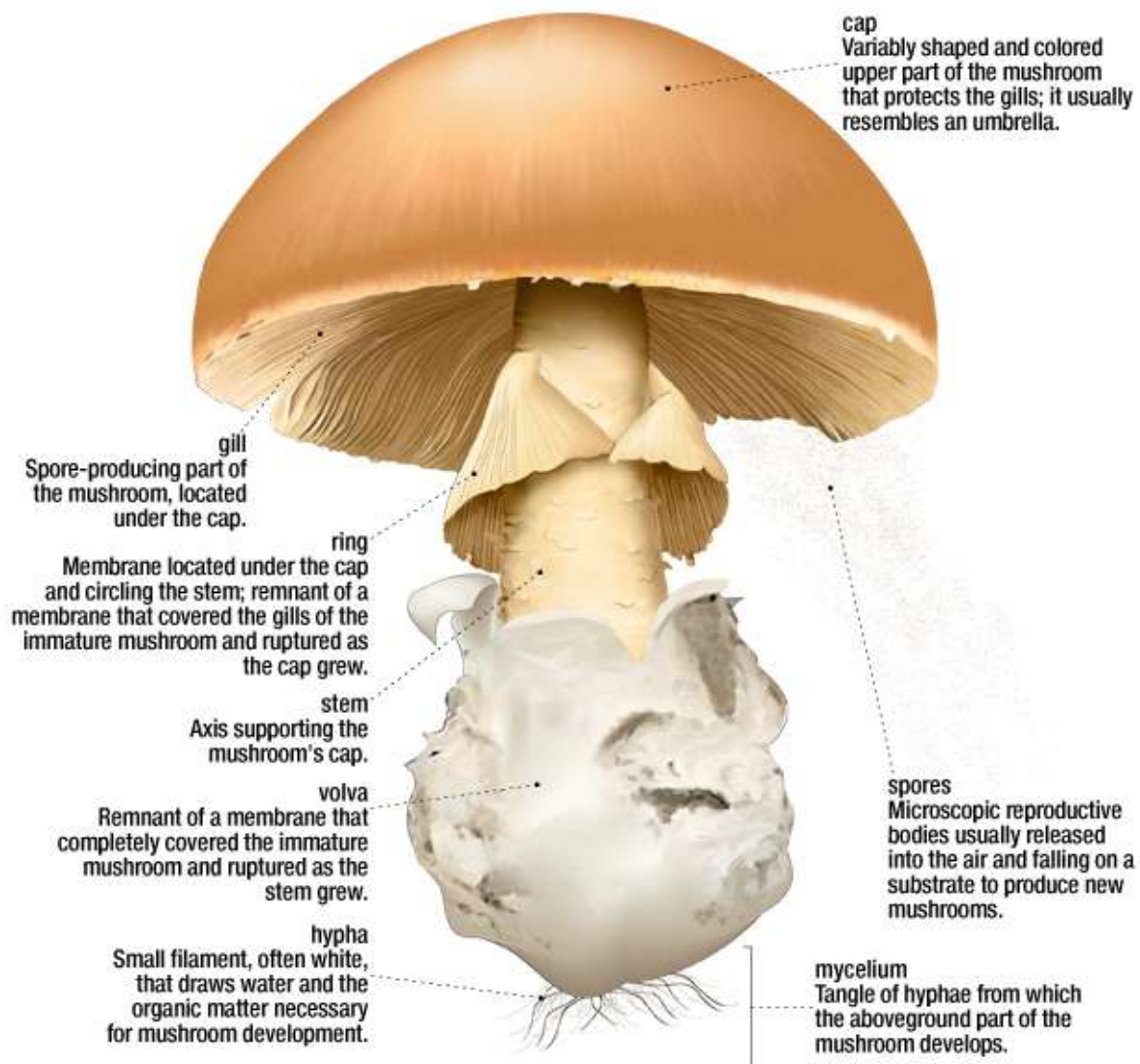


Figure 4: Parts of mushroom and their functions (Visual Dictionary Online, Structure of a mushroom 2018)

## 2.1 A literature review of mycelium and mycelium-based materials

Mycelium features a really wide range of potential in terms of the variety of applications and usage from daily usage products to medicine and more. Thus, in order to make a clear view of the real potential of mycelium not only in architectural applications but many

more fields, existing and potential applications and usages of mycelium and mycelium-based materials are covered in this section.

### 2.1.1 Medical applications

Development of biomaterials in medical sciences has been an area of research owing to increasing importance and awareness of biomaterials in medical applications. In 1996, researchers developed a “wovenable” skin substitute (Sacchachitin) made from the residue of the fruiting body of *Ganoderma tsugae* (Su *et al.* 1997) in order to be used in wound healing.

### 2.1.2 Biotechnological applications

Besides their importance in the food industry with unique flavors and rich protein values, some genus of edible mushrooms has a different aspect of usage in the biotechnology industry. Especially the ones with ligninolytic properties, ability to decompose lignin which is a complex non-carbohydrate polymer in wood, have various applications related to the use of their ligninolytic system on a variety of applications, such as the bioconversion of agricultural wastes into valuable products for animal feed and other food products and the use of their ligninolytic enzymes for the biodegradation of organo-pollutants, xenobiotics and industrial contaminants (Cohen *et al.* 2002).

### 2.1.3 Transportation industry

In 2011, some inventors applied for a patent in cooperation with Ford Global Technologies for a new method of making molded mycelium car parts. The system is based on forming a liquid aggregate which is inoculated with mycelium by inserting it into a mold. Various mycelium components and methods of production examined to provide strong parts adapted for use in vehicles, both in aesthetic and structural capacities (Kalisz and Rocco 2011).

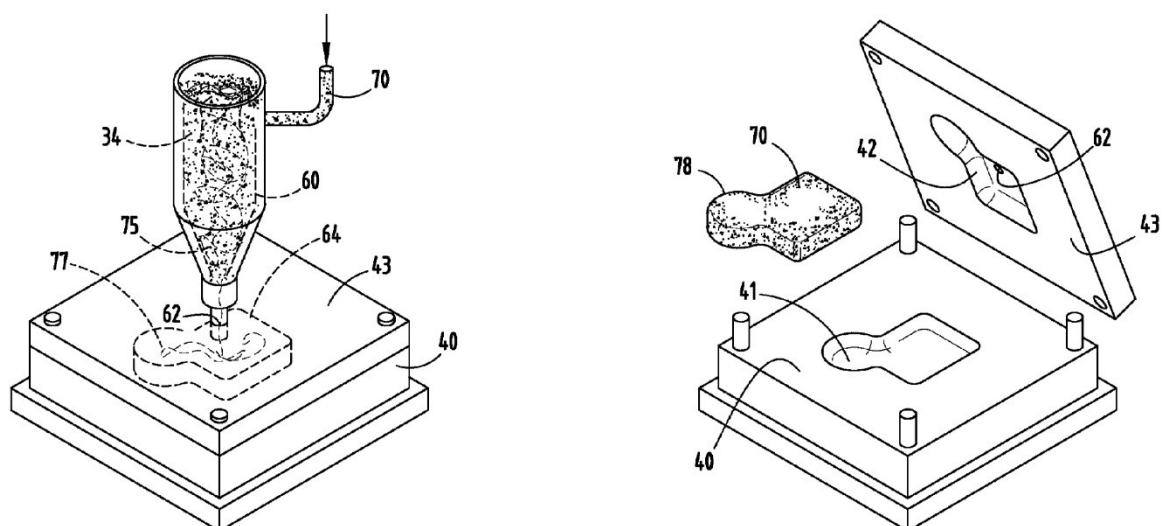


Figure 5: Mycelium material injection molding system to produce vehicle pieces by Kalisz and Rocco (2011)

### 2.1.4 Packing

Since 2007, US-based material science and technology company *Ecovative Design*, founded by Eben Bayer and Gavin McIntyre, has been developing alternatives to polystyrene

and plastic packaging by growing mycelium in agricultural waste (Parks 2017) like seed husks and corn stalks.



Figure 6: MycoFoam tile and MycoFoam single bottle wine shipper by Ecovative Design (Ecovative Design, MycoFoam 2018)

The table below shows the material properties of mycelium material named MycoFoam which is developed by *Ecovative Design*.

Metric	Standard	Testing Lab	MycoFoam
Density (kg/m <sup>3</sup> )	ASTM C303	Ecovative	122
Compressive Strength (kPa)	ASTM C165	Ecovative	124.11
Compressive Elastic Modulus (kPa)	ASTM C165	Ecovative	1137.63
Flexure Strength (kPa)	ASTM C203	Ecovative	234.42
Composability (days)	ASTM D6400	NSF International	30
Flame Spread	ASTM E84	QAI	20
Smoke Emission	ASTM E84	QAI	50
Thermal Conductivity, at 10 °C (W/mK)	ASTM C518	Oak Ridge National Lab.	0.039
Water Vapor Permeation (dry cup)	ASTM E96	Oak Ridge National Lab.	30
Moisture Storage at 53.5% RH (%)	ASTM C1498	Oak Ridge National Lab.	8
Moisture Storage at 75% RH (%)	ASTM C1498	Oak Ridge National Lab.	12

Table 5: Ecovative Design's MycoFoam material properties (Ecovative Design, MycoFoam 2018)

### 2.1.5 Building materials

An insulation material is also developed by the company *Ecovative Design* named *Greensulate* with the same method. Compared with traditional insulation material expanded polystyrene (EPS) panel, Ecovative Design's *Greensulate* panel is only 15% thicker with equal insulation performance.

*"At the same output level, Greensulate consumes one-tenth of the energy and produces one-eighth of the carbon-dioxide emissions as EPS (taking into account to the material transport phase). In fact, if EPS panels were replaced by Greensulate, CO2 emissions would be cut by 25,000,000 kg in two years"* (Diez et al. 2013).



Figure 7: Greensulate mycelium-based insulation material (Ecovative Design, Greensulate 2013)



Figure 8: Section of Greensulate by Ecovative Design (Ecovative Design, Greensulate 2013)

### 2.1.6 Furniture

Philip Ross, the co-founder and CTO of San Francisco based company *MycoWorks* that grow and investigate bioproducts and furniture based on mycelium, has been experimenting the possibilities of mycelium. During the experiments, he developed furnitures like stools, chairs, and lamps. Carbon-based agricultural waste mixed with mycelium tissue, obtained from *Ganoderma lucidum* mushroom, grows at room temperature over a couple of weeks and forms a chair (Jacewicz 2018).



Figure 9: Mycelium chair by Philip Ross (Workshop Residence, Yamanaka McQueen 2018)



Figure 10: Mycelium lamp by Jonas Edward (Edvard 2013)



The Netherlands based designer Eric Klarenbeek who combined digital fabrication and mycelium and experimented with various organic forms. He used a 3D printer to print a mold with an organic shape in order to create a chair and filled it with natural fiber mixture substrate and inoculated with mycelium.



Figure 11: 3D printed mold, filled with mycelium inoculated biomass by Eric Klarenbeek (Klarenbeek 2018)

#### 2.1.7 Textile

One of the most recent discoveries about the potential of mushroom mycelium is about textile formation. Researchers under *MycoWorks* developed a way to produce an “animal-free” leather as they like to refer. Besides the fact that it is more durable and stronger than regular leather, mycelium-based leather can be grown any kind of texture and nearly any size and shape (MycoWorks 2017).



Figure 12: Leather-like mycelium textile development by MycoWorks (MycoWorks 2017)

### 2.1.8 Architecture

In 2014, the project named *Hy-Fi* by the company *The Living* has been awarded the Young Architect Award at MoMA PS1. The design was made of more than 10.000 mycelium bricks of *Ecovative Design, LLC*. By using the computational techniques, *ARUP* engineered the statics of the design and many laboratory tests have been applied by the researchers at the laboratories of Colombia University.

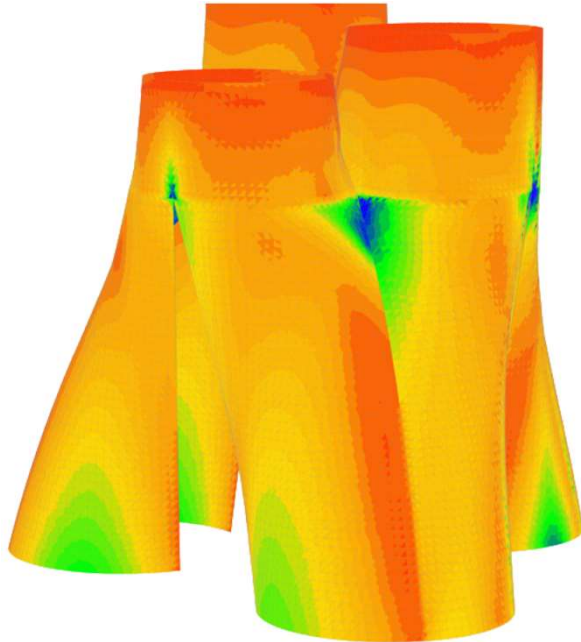


Figure 13: *Hy-fi mycelium tower FEA by ARUP* (Clark and Saporta 2014)



Figure 14: *Hy-fi mycelium bricks tower by The Living* (Stott 2014)

## 2.2 Potential usages of mycelium and advantages of mycelium-based materials

Even though the main focus of this thesis work is about mycelium-based materials, in order to have a clear and deeper understanding of the potential of mycelium, it is found really important to mention other possible applications and benefits of mycelium in different fields. Thus, in this section, some of the selected applications in various specific fields and the advantages of mycelium-based materials are listed below.

### 2.2.1 Using mycelium to clean oil spills

A team of biologists “plant” mushroom to clean the Amazonian oil spills which have been intoxicating the soil, water, vegetation, and people for more than last twenty years. Certain enzymes, produced by specific species like the *Pleurotus ostreatus* (Oyster mushroom) or new species that have been discovered by scientist that eats polyurethane plastic (Stone 2018), are able to break down the tough hydrocarbons found in petroleum.

### 2.2.2 Purification of urban streams, lake, and rivers

In Oregon, a nonprofit ecological restoration organization *Ocean Blue Project* used mushroom spawn filter, grown on waste coffee grounds and straw, to purify and filter the urban stream which ends up in natural water sources. Polluted urban stream filters through the

mycelium spawn bags which are replaced in storm drain substructure. Pollutants like oil, pesticides, and E.coli are broken down by mycelium (Bergado 2018) before polluted urban stream merges with natural water sources.

### 2.2.3 Fuel production

By using mycelium as an intermediate agent, Paul Stamets believes that it is possible to produce fungal sugars, econol in other words, which means more efficient and eco-friendly fuel production than cellulolytic ethanol.

### 2.2.4 Reforestation

Owing to mycelium's nutrient restoring capability, it could accelerate reforestation treatments.

*“A modified method has been developed for laboratory preparation of granulated mycorrhizal inoculum. Mycelia of ectomycorrhizal fungi are immobilized in alginate gel in a mixture with a silicate carrier-perlite. This inoculum is applied at sowing in forest nurseries to obtain resistant plants for afforestation of areas exposed to man-made stresses” (Kropáček et al. 1990).*

Despite the discovery of mycelium is not new, applications in material science and other fields are relatively recent. Thus, it might not be seen as sufficient in order to have a solid experience within the long-term results of mycelium-based materials, their applications and benefits. Nevertheless, mycelium-based materials have many inherent advantages related with the production techniques, raw materials, prime costs, carbon cycle, material properties and possible varieties etc. In addition to these, owing to its inimitable structure and composition large amounts of mycelium-based material production and developments are projected (Haneef et al. 2017).

Some of the most important advantages of mycelium-based materials are listed below based on various applications.

### 2.2.5 Locality

Locality is one of the really important key factors within the sustainable construction methods. As a dramatic example of the effect of locality, a reduction by 215% in the building energy was possible only with the use of local materials in the construction of some houses in France (Morel et al. 2001).

Mycelium-based materials have the best potential in order to be sufficient in the locality. As mycelium breaks up carbon-rich matters to use as food, mycelium-based materials mainly utilize agricultural waste as the raw material for mycelium filaments to grow on. In order to reduce the transportation costs and, increase the efficiency in the local production cycle, local agricultural wastes are the best preferences as a choice of raw material.

### 2.2.6 Close-loop cycle

The carbon cycle of nature brings the most efficient system in order to recycle matter and energy where there is no real waste. This cycle can be referred to as a closed-loop cycle



which is extremely sustainable. However, traditional construction techniques follow a linear approach which is prominently unsustainable (Nagy *et al.* 2015).

Usage of agricultural waste is once again the key factor of the closed loop cycle. Usage of natural and ecological resources provides decomposable and biodegradable properties.

*“Besides producing a completely organic and compostable material, this process also taps into an existing agricultural waste stream with little or no inherent value”* (Nagy *et al.* 2015).

In addition to this, since mycelium-based materials take form within a natural process, the energy required for the production is almost zero as well as the carbon emission.

#### 2.2.7 Fire resistance

Mycelium-based materials perform really well fire resistance. More specifically, the insulation panel *Greensulate* developed by *Ecovative Design* has a significantly lower flammability and it resists longer compared to Expanded Polystyrene (EPS) against fire (González and Diez 2015). Additionally, mycelium-based materials are not emitting poisonous gases if burned.



Figure 15: Fire test on mycelium-based insulation material *Greensulate* by *Ecovative Design* (Ecovative Design, Press Kit 2018)



## 2.3 A literature review of physical and mechanical properties of mycelium-based materials

Mycelium-based materials are natural composite materials with two or more constituent materials. Thus, there are various factors that affect the mechanical and physical properties of the final product. Besides environmental conditions like temperature, relative humidity and, light intensity, there are other factors related to the techniques and growing conditions of the mycelium that have different effects on the result. Those factors include the type of additional nutrition like wheat bran, oat bran etc. or amount of water in the substrate. However, there are two main factors that affect the results most. Mushroom species where mycelium obtained from and the type of natural fibers obtained from agricultural waste or any biological source.

In order to understand the systems that contribute to the properties of the resulting product, it is found crucial to have an understanding of the structure of mycelium and natural fibers.

### 2.3.1 Morphology and mechanical aspects of mycelium

Mycelium has a characteristic spongelike structure consisting of the tubular filamentous *hypha*. Generally, *hyphae* diameters vary depending on the species and environmental conditions between 1-30  $\mu\text{m}$  (Islam *et al.* 2017). In addition to hyphae dimension, the topological organization of the filaments and behavior of individual hypha filaments controls the mechanics of mycelium and mycelium-based biocomposite materials.

As a biopolymer composite, mycelium consists of various natural polymers called chitin, cellulose, proteins, etc. (Haneef *et al.* 2017) on hyphae cell wall. Providing mechanical strength is one of the main roles of the cell wall. Different species under different growing conditions may have different chitin properties and hyphae thicknesses which creates different mechanical behaviors. The figure below illustrates the physiology of mycelium at different scales.

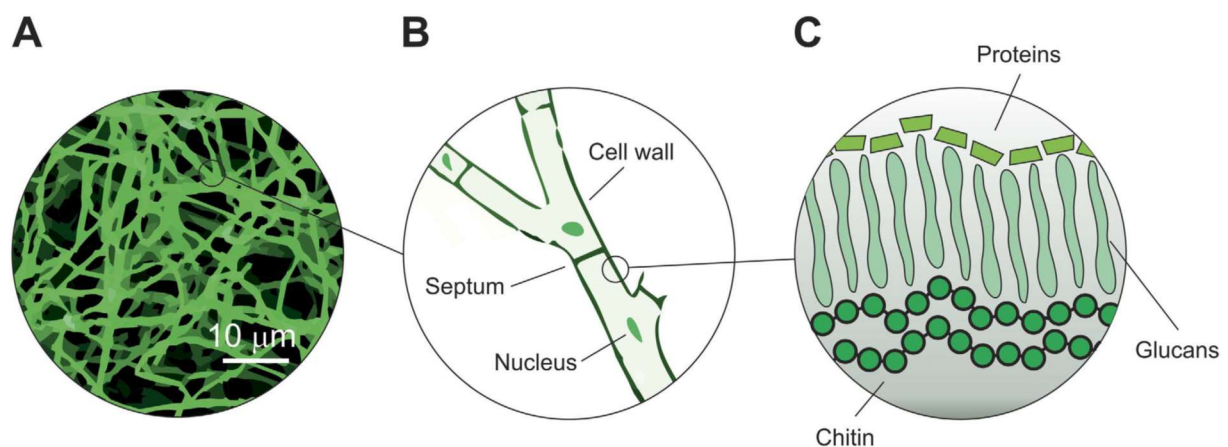


Figure 16: Schematic representation of mycelium physiology at different scales.(A) Branching network of hyphae, (B) Physiology of hypha, (C) Cell wall constituents (by Vega and Kalkum (2012), Haneef et al. (2017))

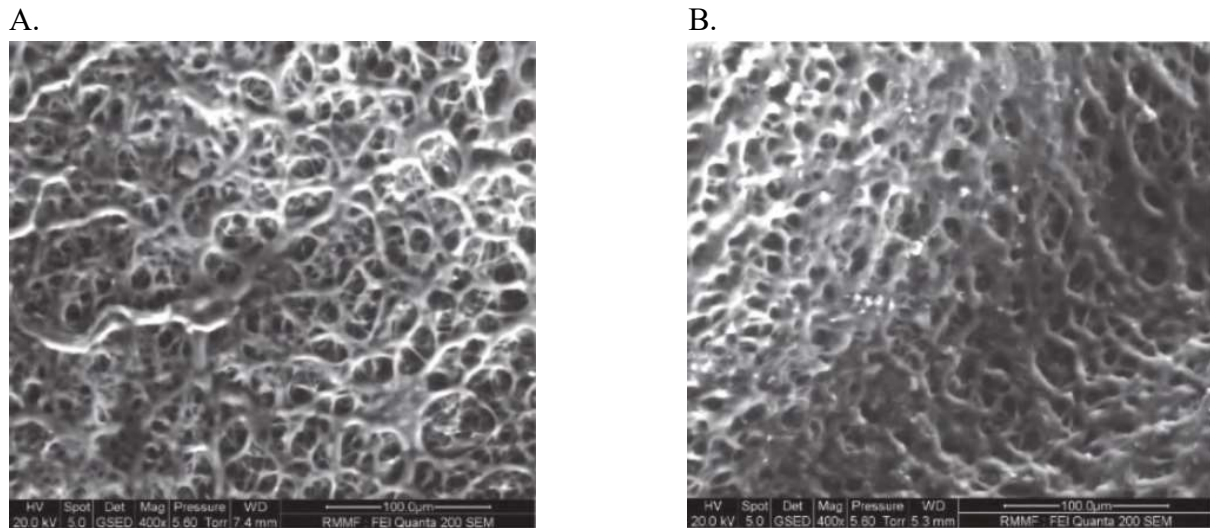


Figure 17: Micrographs of strongly branched hyphal networks of (A) *Pleurotus eryngii* (monomitic) and (B) *Ganoderma* sp. (trimitic) grown on wheat grain. Produced at the RMIT microscopy and microanalysis facilities using environmental scanning electron microscopy (Jones *et al.* 2017)

Besides the type of natural fibers in mycelium materials, the hyphal structure might affect the mechanical performance based on some conditional evidence (Bayer and McIntyre 2012, Lelivelt 2015) which indicate some relation between the hyphal structure of mycelium and its effect on the mechanical behavior of mycelium material. The architecture of hyphal structure may vary depending on environmental conditions like temperature, relative humidity, light intensity; chemical nutrition conditions, the water content of the substrate, pH value of the substrate etc. For instance, the density of the hyphal network is closely related with chemical nutritional content (Jones *et al.* 2017). If carbon concentration of the nutrition increases branching of hyphal growth increases while hyphal extension rate decreases (Trinici and Collinge 1975). On the other hand, if the concentration of nitrogen and sulfur results in an increase in numbers of branches per millimeter of hypha (Larpent 1966).

Like the density of hypha, the composition of cell walls of the mycelium has a potential effect on the mechanical properties of mycelium materials because it creates the cellular strength and form of fungi (Jones *et al.* 2017). The cell wall of the hypha consists of different polysaccharides like chitin, chitosan, cellulose, glucans etc. as a fibrous network. Chitin is one of the most crucial components of the cell walls which is also found as the main component for exoskeleton of most insects (Rinaudo 2007). As a linear polymer of N-acetylglucosamine amino sugar which is significantly strong and has a greater tensile strength compared to many synthetic materials like carbon fibers and steel owing to its hydrogen bonding (Webster and Weber 2007, Jones *et al.* 2017).

### 2.3.2 Natural fibers

Natural fibers are raw materials which are obtained from animals, plants or mineral sources consisted of agglomerated cells with insignificant diameters compared to their lengths. In order to create mycelium-based biocomposite materials, since plant fibers are the most suitable ones for mycelium to grow rather than animal fibers, this section focuses on plant fibers. Under natural fibers, plant fibers can be further categorized as bast, leaf, and seed, fruit, wood, stalk, and grass etc. The table below shows the classification of fibers.

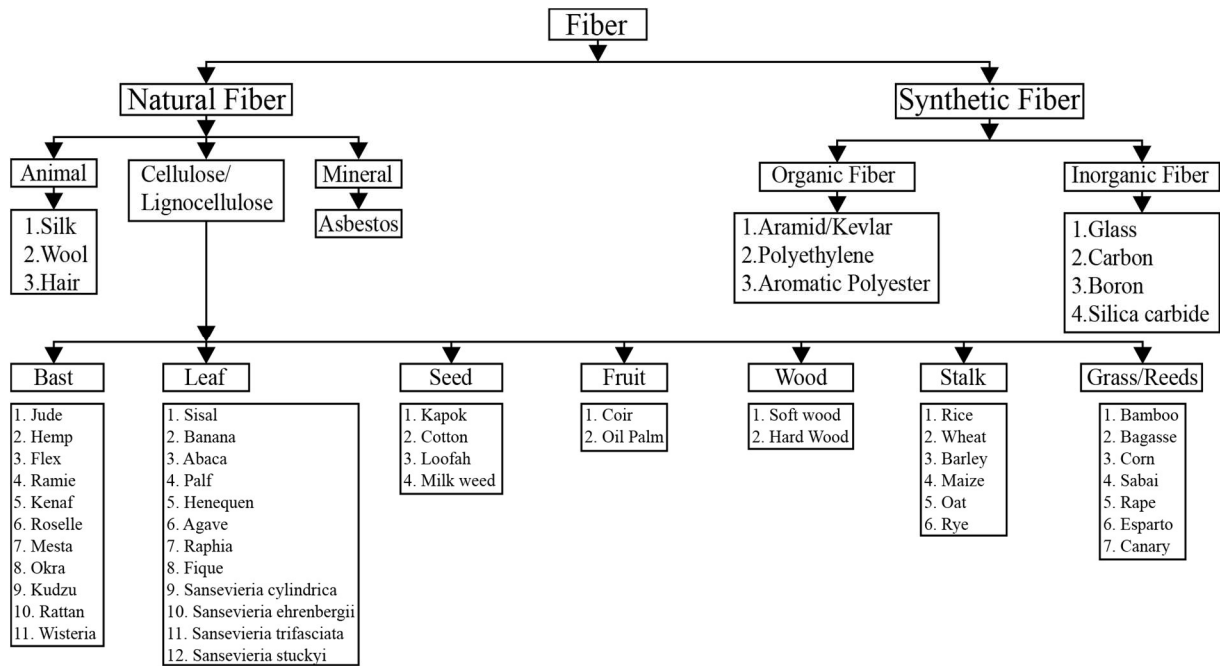


Table 6: Natural and synthetic fiber classification (Sathishkumar et al. 2014)

Plant-based fibers have a common structural hierarchy in their gradually increasing diameter of tubular fibers. A study of this hierarchical difference made by Bos *et al.* (2006) clearly presents the level differences of bundles of flax fibers in Figure 18. Due to their concentric tubular structures, natural fibers perform high strength in the axial directions besides being relatively lightweight according to their performance.

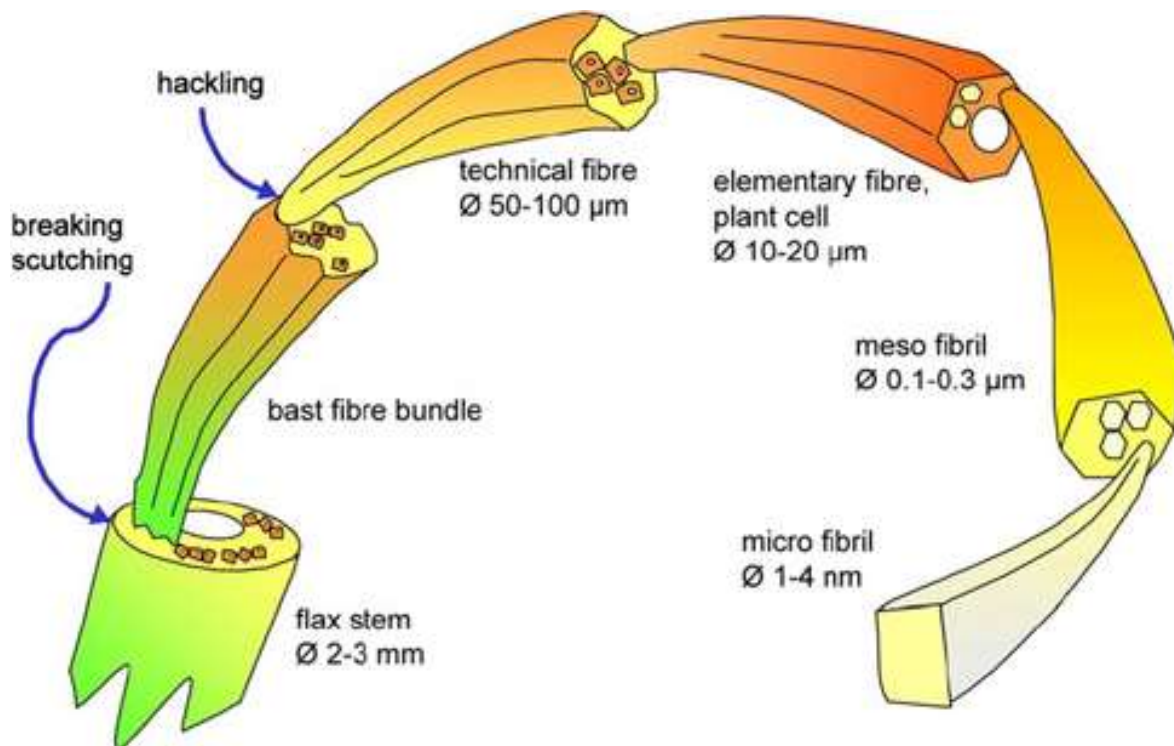


Figure 18: Hierarchy of flax bundles by Bos *et al.* (2006)

After the invention of synthetic fibers like glass fiber, polyethylene, and Kevlar, natural fibers have lost their part in industrial applications. However, the table below shows the comparison between natural fibers and fiberglass which clearly describes the recently increasing interest in natural fibers.

	Natural fibers	Glass fibers
Density	Low	Twice that of natural fibers
Cost	Low	Low, but higher than natural fibers
Renewability	Yes	No
Recyclability	Yes	No
Energy consumption	Low	High
Distribution	Wide	Wide
CO <sub>2</sub> neutral	Yes	No
Abrasion to machines	No	Yes
Health risk when inhaled	No	Yes
Disposal	Biodegradable	Not biodegradable

Table 7: Comparison between natural and glass fibers (Wambua *et al.* 2003)

Besides the listed properties of natural fibers in Table 7 above (Wambua *et al.* 2003), natural fibers have relatively equal or better mechanical performance. There is a wide range of studies and experiments on natural fibers in order to determine their mechanical behaviors and performances. Some of those results obtained from different sources and studies are represented in Table 8.

Fiber	Tensile Strength (MPa)	Tensile strain to failure (%)	Young's Modulus (GPa)	Density (g/cm <sup>3</sup> )	Source
Bagasse	222	1,1	17,9-27,1	-	a
Banana	700-800	2,5-3,7	27-32	-	a
Bamboo	500-575	1,9-3,2	27-40	-	b
Flax	780-1500	1,2-2,4	60-80	-	a
	800-1500	1,2-1,6	60-80	1,40	c
Kenaf	930	1,6	53	-	d
Jute	400-800	1,5-1,8	10-30	-	a
	400-800	1,8	10-30	1,46	c
Hemp	690	1,6	70	-	d
	550-900	-	24±8,5	1,48	c
	660±83	-	-	-	e
Ramie	500-870	1,2	44	-	a
	500	2	44	1,50	c
Abaca	400	3-10	12	-	d
Sisal	530-630	3,64-5,12	17-22	-	a
	600-700	2-3	38	1,33	c
Cotton	400	-	12	-	a
	400	3-10	12	1,51	c
Coir	220	23,9-51,4	6	-	a
	220	15-25	6	1,25	c
Oil Palm	248	3,2	25	-	d
Pineapple	180	3,2	82	-	a
Curaua	87-310	4-4,9	34-96	-	a
E-glass	2400	3	73	2,55	c

Table 8: Mechanical properties of natural fibers (a: Wambua *et al.* 2003, b: Satyanarayana *et al.* 2009, c: Symington *et al.* 2009, d: Faruk *et al.* 2012, e: Khalil *et al.* 2012, adapted from Lelivelt 2015)

Although natural fibers are advantageous in many senses, natural fibers also have some questionable drawbacks. First of all, because of their biological nature performance of natural fibers may vary in a significantly wide range over different harvests (Lelivelt 2015). Secondly,

natural fibers are meant to hold water due to their hydrophilic natures which makes them remarkably sensitive to moisture. If natural fibers are used as the reinforcement for composite structures with a polymer matrix, the contradiction between natural fibers' hydrophilic and polymer matrix's hydrophobic behavior causes a weakness in bonding between fiber and matrix (Symington *et al.* 2009, Lelivelt 2015).

### 2.3.3 Known properties of mycelium-based materials

Composite materials, including mycelium-based biocomposite materials, contain two or more stages which are continuous and dispersed levels (Jones *et al.* 2017), which means they are divided by an interface in the microscopic scale (Matthews and Rawlings n.d.).

The matrix is the *continuous stage* which is the primary load-bearing modules while the *dispersed stage* envelopes the fibrous material binding them together stable and acts like a load transmitter between the stages (Jones *et al.* 2017). On the other hand, fiber in the composite acts like a reinforcement in order to increase mechanical properties or stands as a volumetric filler to increase the material volume (Thakur and Singha 2013). This load transfer of the matrix to the fibers through shear stress at the interface requires well-bonded structure between the polymeric matrix and the fibers (Wambua *et al.* 2003).

Mycelium-based biocomposites have a wide range of compressive strength primarily depending on their constituents. Two samples of mycelium biocomposites using the species called *Ganoderma* has shown a remarkable difference in their results of compressive strengths regarding different natural fibers as their substrate materials (Jones *et al.* 2017). While the mycelium biocomposite with a cotton plant-based substrate achieved a result of compressive strength ranging between 1 to 72 kPa (Holt *et al.* 2012), the other mycelium biocomposite with red oak based substrate achieved 490 kPa (Travaglini *et al.* 2013). Substrate natural fibers as growth medium have a significant effect on the compressive performance of the composite as well as the hyphal structure of the mycelium which varies according to the species of the fungi.

Experiments showed that selected two species which are members of same white rot fungi group, *Ganoderma lucidum* and *Pleurotus ostreatus*, shows a higher Young's modulus ranges between 12-28 MPa vs. 4-17 MPa and lower elongation in ranges between 4-17% vs. 9-33%, when the growth medium is cellulose as opposed to potato dextrose, while the results for tensile strength was similar for both ranging between 0.7-1.1 MPa (Haneef *et al.* 2017, Jones *et al.* 2017) of thread-like mycelium filaments which were grown on Petri dishes.

Travaglini *et al.* (2013) conducted serious of tests to investigate the elastic and strength properties of mycelium-based materials. Travaglini *et al.* (2013) conducted more tests in order to investigate the flexural properties of mycelium-based materials by using four-point bending test methodology. Furthermore, Travaglini *et al.* (2014) showed the potential of mycelium-based materials in replacement of current insulation materials by conducting tests on the maximum use temperature, odor emission, and R-value.

Yang *et al.* (2017) examined physical and mechanical properties of mycelium-based biocomposite materials including dry density, thermal conductivity, and unconfined



compressive strength and, Young's and shear modulus. Different mixing, incubating, packing methods have been applied in order to find the best combinations of systems and processes.

Islam *et al.* (2017) investigated the morphology and mechanics of mycelium while they were developing a network-based model for mycelium. They applied tension and compression tests as well as microscopic imaging.

Material	Modulus, E (kPa)	Density (kg/m <sup>3</sup> )	Yield Strength (kPa)	Ultimate Strength (kPa)
Ganoderma lucidum	1300	318	47,5	490
Starch based foam	183000	260	1180	1090
Polystyrene foam	5700	41.2	-	179
Polyvinylchloride foam	3000	50	-	45000
Aluminum Foam	347000	255	1690	-

Table 9: Comparative material properties of mycelium material (by Travaglini *et al.* (2013))

### 2.3.3.1 Compressive strength

Compressive strength is the maximum amount of compressive load a material can bear before fractural failure divided by the cross-sectional area. The compressive strength of the mycelium-based biocomposite materials varies in a really wide range depending on their constituents (Jones *et al.* 2017) like natural fibers, fungi species, nutritional supplements etc. In this section, results of different researches and experiments conducted by various researches by using different species and substrates are collected together in order to represent the variety of the compressive strength of mycelium-based biocomposite materials.

According to the laboratory tests by Travaglini *et al.* (2013), the mycelium-based biocomposite material represented a yield point of 47.5 kPa while an ultimate strength of 490 kPa which can be seen in the graph below;

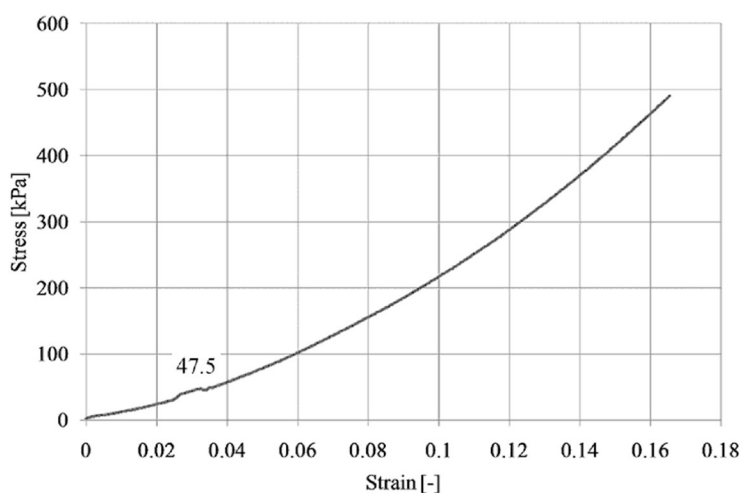


Table 10: Compressive stress-strain response (Travaglini *et al.* 2013)

Yang *et al.* (2017) achieved different results of compressive strength with different sample groups created with different methods on live and dried samples with various densities, as well as different incubation times as which are two and six weeks. As an average, mycelium-based composite material represented a value of 350-570 kPa. Observations showed that as incubation time increases in all different test groups so the compressive strength as well over 60%. Also, densely packed and longer incubated samples represented highest compressive strength.

Following table shows the different compressive strength results from different studies with various species and substrate combinations.

Specie	Substrate	Compressive strength (kPa)	Source
Ganoderma lucidum	Cotton plant	1.1-72	a
Ganoderma lucidum	Red oak wood chips	490	b
Pleurotus sp.	Cotton seed hulls + %5 SBR*	177-422.1	c
Pleurotus sp.	Triticum sp. (wheat, rye etc.)	35-42	d
An endemic to Alaska	Alaska birch sawdust	350-570	e
Trametes versicolor	Hemp mat	24-93	f

Table 11: Collection of different values for compressive strength of different mycelium-based materials (a: Holt et al. (2012), b: Travaglini et al. (2013), c: He et al. (2014), d: López Nava et al. (2016), e: Yang et al. (2017), f: Lelivelt et al. (2015), \*SBR=Carboxylated styrene butadiene rubber latex and silane coupling agent as an adhesive)

### 2.3.3.2 Tensile strength

Tensile strength is the maximum amount of load that a material can take before fractural failure when being stretched, divided by the original cross-sectional area of the material. This section contains a collection of tensile strength values of mycelium-based biocomposite materials obtained from different studies conducted by various researchers with different species of fungi and substrate combinations.

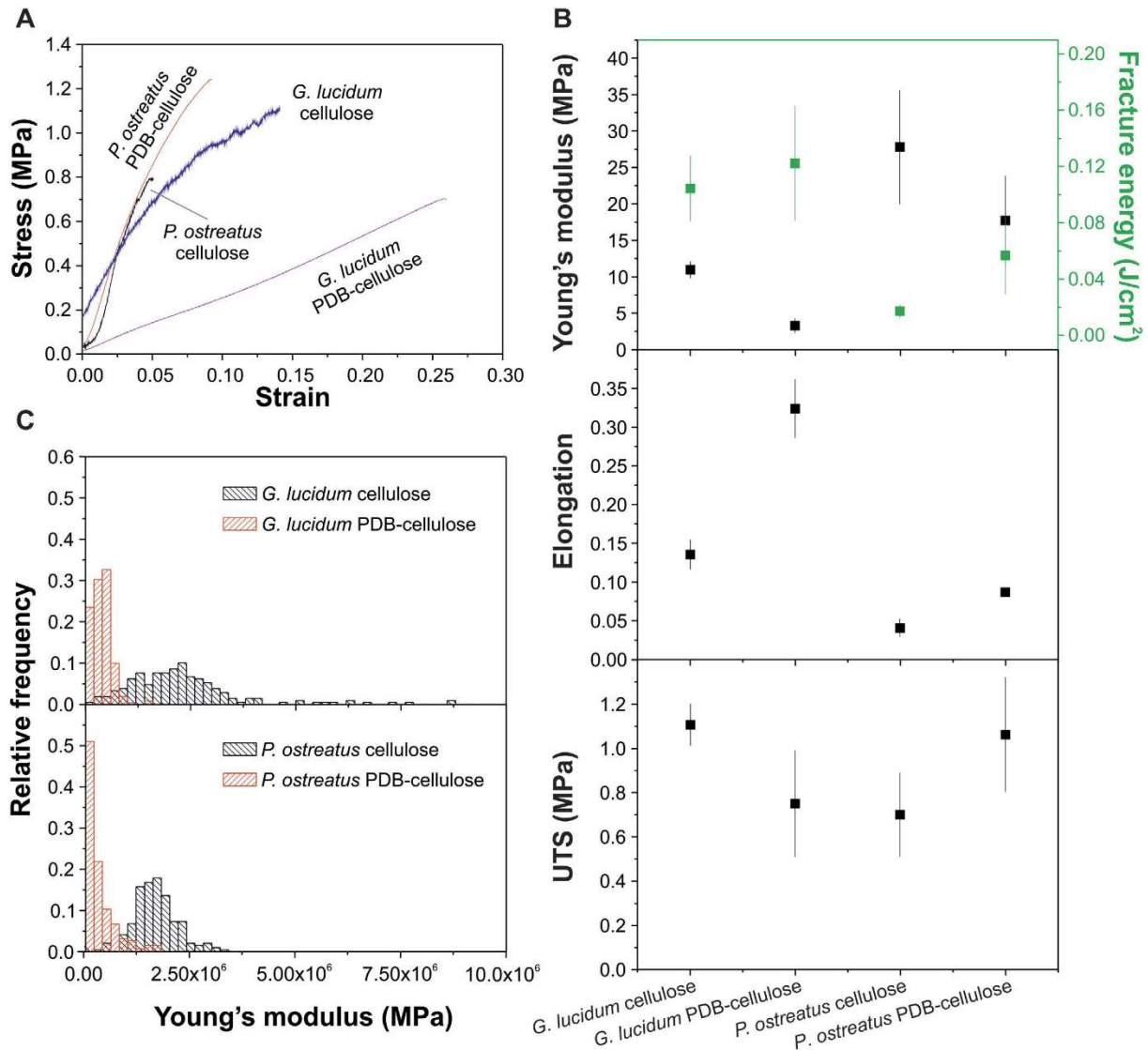


Table 12: Mechanical characterization. (A) typical stress-strain curves of 20-days old mycelium films. (B) Young's modulus, elongation and strength of the different samples. (C) Histograms of measurements of Young's modulus calculated by AFM indentation on 2-days old samples by Haneef et al. (2017)

Haneef *et al.* (2017) conducted a series of tests on mycelium obtained from *Ganoderma lucidum* and *Pleurotus ostreatus* which have been grown on different substrate mediums, in order to define the tensile strength value of fibrous mycelium in hyphal scale. Two substrate groups were pure cellulose and cellulose-potato dextrose (PDB) based on the facts that cellulose is the most abundant while PDB is rich in terms of simple sugar which is easy to break for mycelium and increases the fungal growth (Haneef *et al.* 2017). The research has demonstrated that the relation between the substrate type and the species results with different hyphal thicknesses as well as different mycelial density. The set of graphs above in Table 12 show the results of the achievements of the tests by Haneef *et al.* (2017).

According to the laboratory tests by, Travaglini *et al.* (2013), the mycelium-based biocomposite material represented a relatively low tensile strength of 15 kPa and a tensile modulus of 1300 kPa.

Islam *et al.* (2017), achieved the tensile strength with a range of values between 100-300 kPa while the yield strength varies between 40-80 kPa as a result of the tests applied on the samples obtained from Ecovative Design, LLC.

Following table shows the different tensile strength results from different studies with various species and substrate combinations.

Specie	Substrate	Tensile strength (kPa)	Source
<i>Ganoderma lucidum</i> *	Cellulose	700-1100	a
<i>Pleurotus ostreatus</i> *	PDB-cellulose		
<i>Ganoderma lucidum</i>	Wood chips	15	b
-No data-	Crushed corn stalks & hemp**	100-300	c
<i>Pleurotus</i> sp.	Corp residues ( <i>Triticum</i> sp.)	29,90-79,90	d

Table 13: Collection of different values for tensile strength of different mycelium-based materials (a: (Haneef *et al.* 2017), b: (Travaglini *et al.* 2013), c: (Islam *et al.* 2017), d: (López Nava *et al.* 2016) ,\*Examined in hyphal scale,\*\*Obtained from Ecovative Design, LLC)

### 2.3.3.3 Elastic modulus and shear modulus

According to Yang *et al.* (2017), mycelium-based biocomposite material has an average of Young's modulus between 50000 to 30000 kPa while the shear modulus 19000 to 11000 kPa.

For the elastic modulus, Islam *et al.* (2017), achieved the results with a significant difference between 600 kPa and 2000 kPa.

### 2.3.3.4 Poisson's ratio

Yang *et al.* (2017) investigated the Poisson's ratio for different test groups and recorded the results varying between 0.15 and 0.5. For some of the samples, there was a clear difference between the horizontal and vertical directions.

### 2.3.3.5 Density

The density of mycelium materials is in correlation with the fungi species, type of the natural fiber as the substrate, additional nutritional elements, the water content of the substrate, drying conditions etc. Also, it is found important to understand the difference between the



density of a pure mycelium sample and a composite mycelium material. This section contains a collection of density values for both pure mycelium samples and composite mycelium materials constituted of mycelium and natural fibers, obtained from different studies conducted by various researchers.

Islam *et al.* (2017) performed tests on the pure mycelium samples which were obtained from *Ecovative Design*. Those samples used to reproduce the vegetative mycelium tissue under sufficient nutritional conditions including calcium and carbohydrate and achieved samples densities in the range from 30 kg/m<sup>3</sup> to 50 kg/m<sup>3</sup>.

Holt *et al.* (2012) conducted various performance tests on mycelium materials in order to compare the mechanical performance of polystyrene boards and mycelium biocomposite materials with cotton byproducts. The density of the samples that have been created during the tests ranged between 66.5 kg/m<sup>3</sup> to 224 kg/m<sup>3</sup>. There was a notable difference in the densities of the samples between grain inoculated and liquid inoculated. Because of the higher mass of grain-based inoculum medium contrary to liquid-based inoculum medium, grain inoculated samples showed higher densities.

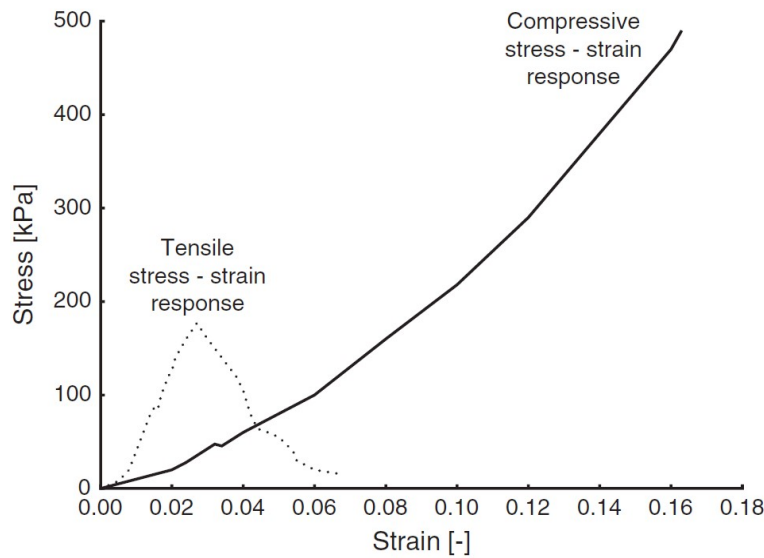
Yang *et al.* (2017) examined physical and mechanical properties of mycelium-based materials due to various tests on different sample groups. Those sample groups were categorized according to the packing method (loosely or densely), incubation time and dried or live test status. According to that, the densities of the densely packed and dried samples were in a range of 240-265 kg/m<sup>3</sup> and 230-280 kg/m<sup>3</sup>. On the other hand, the densities of the loosely packed and dried samples were in a range of 165-195 kg/m<sup>3</sup> and 160-280 kg/m<sup>3</sup>.

#### 2.3.4 Comparison of tensile strength and compressive strength values

In this chapter, a collection of values based on literature review represented in order to compare the tensile strength values and compressive strength values of mycelium-based biocomposite materials.

Tensile strength (kPa)	Compressive strength (kPa)	Source
-	1.1 – 72.2	a
176	490	b
100-300	40-85	c
29,90 – 79,90	35-42	d
-	24 – 93	e
700 – 1100**	-	f
-	350-570	g
-	177 – 422.1*	h
215	124,11	i

Table 14: Comparison of tensile strength and compressive strength values of mycelium-based materials (a: Holt *et al.* (2012) b: Travaglini *et al.* (2013) c: Islam *et al.* (2017) d: López Nava *et al.* (2016) e: Lelivelt *et al.* (2015) f: Haneef *et al.* (2017) g: Yang *et al.* (2017) h: He *et al.* (2014) i: Ecovative Design, MycoFoam (2018)) (\*SBR=Carboxylated styrene-butadiene rubber latex and silane coupling agent as an adhesive, \*\*Hyphal tensile strength)



The graph on the left is based on the research by Travaglini *et al.* (2013) shows the stress-strain response graphs of both under tension and compression of mycelium-based material with *Ganoderma sp.* Mycelium grew on Red Oak woodchips substrate. This show that compressive strengths of the mycelium-based material are greater than the tensile strength of the mycelium-based biocomposite material.

Figure 19: Tensile and compressive stress-strain comparison of mycelium-based material (Travaglini *et al.* 2013, Jones *et al.* 2017)

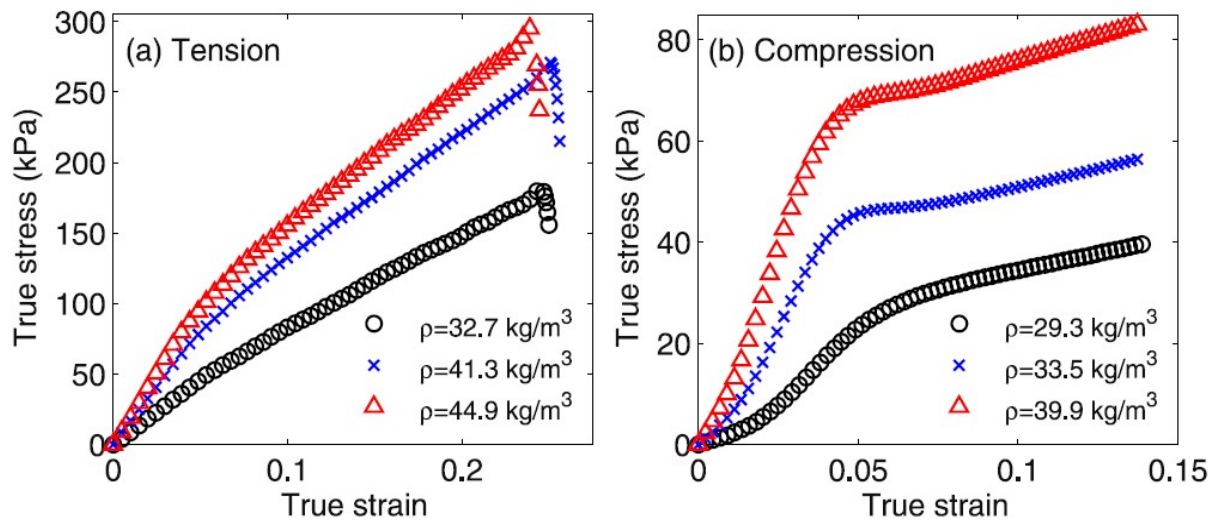


Figure 20: The effect of different densities on the stress-strain response both under tension (a) and compression (b) (Islam *et al.* 2017)

The set of graphs above represents the results of the research conducted by Islam *et al.* (2017) where the effect of different densities of mycelium-based materials on the stress-strain responses both in tension and compression. Although it is not a direct comparison of the tensile and compression strengths of the same mycelium-based material samples, it has been found important to bring a wider perspective. The graphs “a” and “b” above shows the tensile strengths of the mycelium-based material are greater than the compressive strengths.

Depending on the mushroom mycelium species as well as the type of the substrate and its fibril behavior, moisture content, orientation of the natural fibers in the geometry of the mycelium-based material etc. the values for tensile and compressive strengths may vary in a really wide range.

### 3. How to grow mycelium and mycelium-based materials?

Fungi can be seen existing in nature individually however, they usually associate with other lifeforms like plants to exist (Jones *et al.* 2017). By using specific mediums and techniques it is possible to provide the necessary conditions artificially in order to grow mycelium. Those techniques and growth mediums differ depending on the mushroom species due to different species require different environmental conditions. As Jones *et al.* (2017) stated, classification systems of fungi to describe the relevance between the growth and certain environmental conditions are significantly important in order to optimize the growth of mycelium for commercial production of mycelium-based biomaterials.

In order to grow mycelium under a controlled environment, the first mycelium sample to be cloned needs to be obtained. Mycelium can be obtained from a mushroom tissue, mushroom spore or a cultivated liquid culture. As well as the different environmental conditions depending on the classification of fungi, the growth medium as the substrate differs like soil, coffee grounds, straw, sawdust, etc.

While cultivating mushroom, one of the biggest considerations is sterility due to the fact that the air we breathe is full of microscopic living organisms (Stamets and Chilton 1983). The atmosphere is the carrier for fungi, bacteria, viruses etc. to distribute their descendant in order to increase their chance to populate. Even if the flow of these organisms can be reduced or eliminated, there is always a possibility of contamination (Stamets and Chilton 1983).

As Stamets and Chilton (1983) states, there are five main sources of contamination;

1. *The immediate external environment*
2. *The culture medium*
3. *The culturing equipment*
4. *The cultivator and the clothes*
5. *The mushroom spores or the mycelium*

With creating a sterile environment, the chance of mushroom mycelium to compete for available nutrition against another living organism.

In this chapter, the methodology which is used in this study to produce mycelium and mycelium-based materials have been described. The listed steps of growing mycelium and mycelium-based materials on the left side have been renamed as they are listed on the right side in the tables below, in order to make it easier to classify the steps;

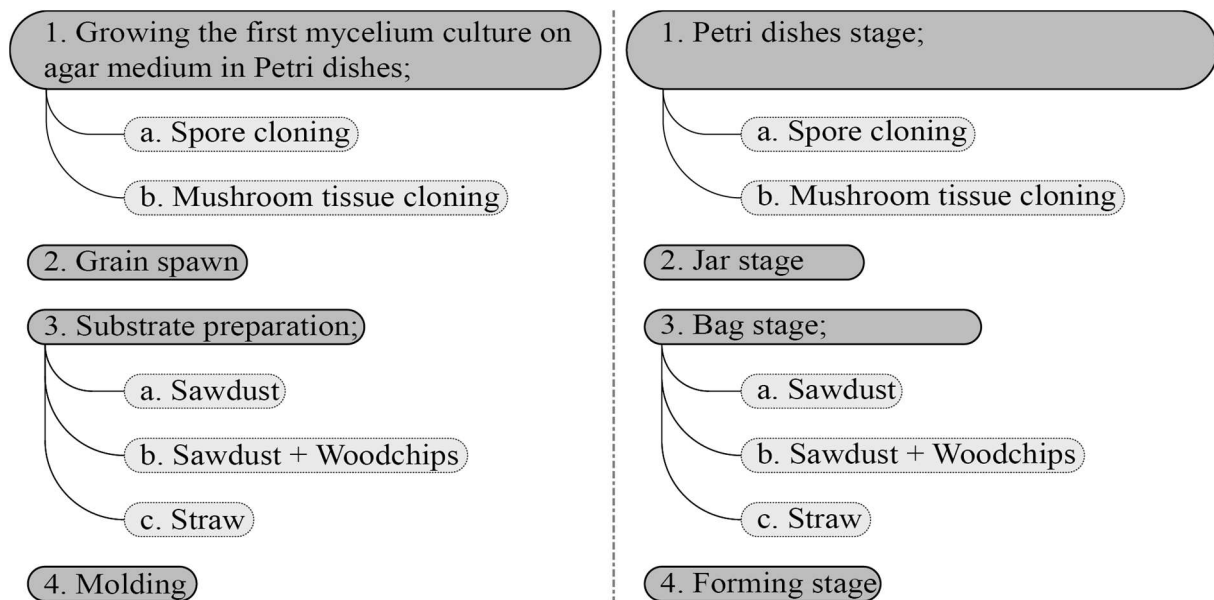


Table 15: Steps of the methodology to create mycelium-based material (Author's image)

### 3.1 Petri dish stage

Using agar medium mixture on Petri dishes is one of the most preferred ways to generate and grow mycelium. While there are many different recipes for nutrition-rich agar medium mixtures, Potato Dextrose Agar (PDA) and Malt Extract Agar (MEA) are the main ingredients for the supplemented agar mixtures where yeast is often included as nutritional supplementary (Stamets and Chilton 1983). The following recipe is convenient for most mushroom species known as cultivable. For 1 L of agar medium mixture (Stamets and Chilton 1983);

#### **Recipe:**

- 24 gr agar-agar
- 20 gr malt extract
- 2 gr nutritional dry yeast
- 1 L drinking water

#### **Tools:**

- Jar, glass bottle or Erlenmeyer flask
- Glass or disposable sterilized Petri dishes (Approx. 35 Petri dish for every 1 L of mixture)
- Scale
- Polyester pillow stuffing
- Parafilm
- Latex gloves
- Facemask and hairnet
- 99,99 % isopropyl alcohol
- Sterile working area: Glove Bag/Glove Box or sterile air flow (HEPA-filter, laminar flow hood)
- Pressure cooker/canner

Pour all the ingredients into the jar with warm water and shake it well until the ingredients dissolve in the water completely. Also, in order to dissolve the mixture better in the water, it can be heated up in a pot but it is important to note that mixture should not start to solidify. The size of the jar should be suitable according to the amount of the desired mixture considering the maximum limit of filling the jar which is the two third of the volume (Stamets and Chilton 1983). Make a hole to the lid of the jar with an approximate diameter of 4-5 mm to put the polyester pillow stuffing as the filter. Pass the polyester filter through the hole, close the lid and wrap the lid with an aluminum foil to prevent any water getting into the jar and change the humidity conditions which may cause molds.



Figure 21: Ingredients for malt extract agar medium (Author's image)



Figure 22: Malt extract agar medium mixture (Author's image)

Once the medium mixture is thoroughly mixed and dissolved, sterilize the medium in a pressure cooker/canner for 30-45 minutes at 15 Psi. Place the pressure cooker/canner on a stove and seal the lid. Let it heat till the ample steam starts to release and keep it steaming for 4-5 minutes. Once the pressure cooker reaches 15 Psi reduce the heating level to half and start counting down.

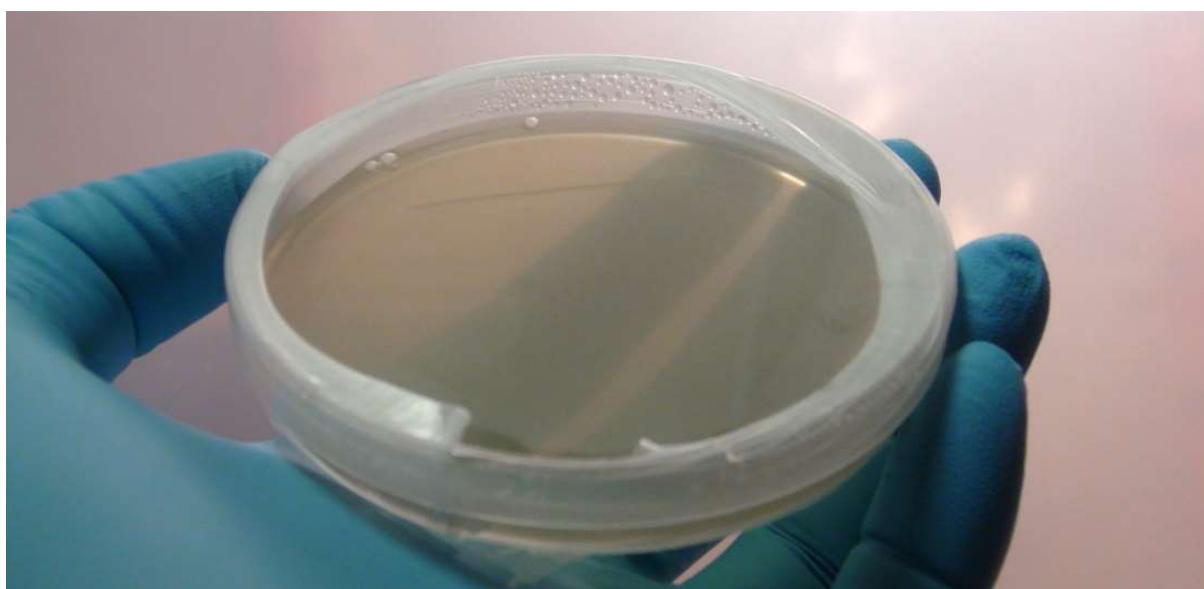


Figure 23: Petri dish with agar medium (Shields 2018)

After sterilization, let the pressure cooker/canner in front of a HEPA-filter or in a sterilized place to return to 1 Psi before opening. In the absence of HEPA-filter, placing a sanitized, isopropyl alcohol soaked cloth over the cover of the pressure cooker/canner works as a filter against the air sucked in during the pressure equalization process.

Pour the warm MEA mixture into the Petri dishes in front of a HEPA-filter or in a glovebox to reduce the contamination and let them cool down. Agar medium hardens while getting cooler. Once cool enough, they are ready to inoculate. Once the Petri dishes are ready with agar medium, two sources of mycelium to start a culture can be used; mushroom spores and mushroom tissue. In the following two sections, the methods to obtain those cultures will be explained.

### 3.1.1 Spore print culture

In order to obtain spores, choose a fresh mushroom and clean it well. Cut off the cap from the stem and place it on a disinfected carrier material like a piece of aluminum foil or a clean glass surface with gills facing down. After 12 to 24 hours, the spores should have been released and create a print-like mark on the carrier material. Those spores will be used to inoculate the agar mixture in the Petri dishes.

#### ***Tools:***

- *Aluminum foil, paper (as large that you can place a mushroom cap on it)*
- *99,99 % isopropyl alcohol or a strong workspace disinfect*
- *Latex gloves, facemask, and hairnet*
- *Scalpel and Parafilm to seal the Petri dishes*
- *Zip-Lock bags to pack the prints*
- *Sterile working area: Glove Bag/Glove Box or sterile air flow (HEPA-filter, laminar flow hood)*
- *One-way inoculation loop or needle holder with an inoculation loop*

Once spore print is obtained on the carrier material, to begin with mycelium culture, use gloves and disinfect your hands as well as the working space. Then, place the Petri dishes that have been prepared in the previous step in front of a laminar flow hood, HEPA-filter or in a glove box. Get the spore print and inoculation loop carefully and rub the inoculation loop until it collects enough spores. Slightly open the petri dish and apply the inoculation loop to the surface of the agar medium by drawing an “S” to import the spores. During the inoculation with spores, do not remove the lid of the petri dish completely and work fast in order to reduce the risk of contamination. Once the transmission of spores is done, close the lid and use Parafilm to seal it all around the petri dish.



Figure 24: Spore print of a mushroom cap  
(Tyroler, Glückspilze, Making of spore prints 2018)



Figure 25: Inoculation of an agar medium in a Petri dish  
(Tyroler, Glückspilze, Making of spore prints 2018)



### 3.1.2 Mushroom tissue culture

Opposite to spore culture, preservation of the same genetic characteristics of the medium mushroom sample is assured by tissue culture method. While multispore culture generates new strains of mycelium, tissue culture clones the same genetics of a living specimen (Stamets and Chilton 1983).

#### ***Tools:***

- *Hairnet and face mask*
- *99,99 % isopropyl alcohol or a strong workspace disinfect*
- *Latex gloves*
- *Scalpel*
- *Spiritus lamp (Alcohol burner)*
- *Sterile working area: Glove Bag/Glove Box or sterile air flow (HEPA-filter, laminar flow hood)*
- *Parafilm to seal the Petri dishes*

Mushroom, in other words, the fruit of mycelium, is actually consisted of compressed mycelia. Thus, any part of the mushroom body is suitable to obtain a culture. In order to obtain a clean tissue interior part of the cap, the upper part of the stem or the joint point between the gill surfaces can be advised.

Clean and sterilize the working space, put on a hairnet, face mask, and gloves. Disinfect your hands with alcohol and break the selected part of the mushroom fruit body into two in order to reach the interior hyphae. Use the spirit lamp to sterilize the scalpel by flaming it until the scalpel becomes red-hot. Cool the scalpel down by making a cut line in an agar media from a petri dish before cutting the tissue. Proceed with cutting the flesh from the selected part and remove a small tissue sample around 3x3 mm. Quickly import the tissue sample to the center of the agar medium filled petri dish. Once the transmission of the mushroom tissue is done, close the lid and use Parafilm to seal it all around the petri dish.



Figure 26: Tissue extraction from a mushroom section (Tyroler, Glückspilze, Mushroom cloning 2018)



Figure 27: Tissue transformation into an agar Petri dish (Tyroler, Glückspilze, Mushroom cloning 2018)

### 3.1.3 Mycelium growth

Spawn run of the mycelium is the development and growth of the mycelium on the agar medium. During this process, Petri dishes should be stored in a dark and sterilized place.

Environmental conditions like humidity, temperature and light density depend on the genus of the sample mushroom species. Likewise, depending on the species, fibrous mycelium filaments will be visible after 3-5 days.

### 3.2 Jar stage

Once mycelium spawn is healthily grown and colonized in Petri dishes either from spore or mushroom tissue culture, it can be used to inoculate a carrier medium to enlarge the mycelium mass from agar mediums. According to the mushroom species that has been cultivated, the carrier material varies although most spawn makers prefer to use rye grain (Stamets and Chilton 1983). In this study, rye and wheat grain substrates have been used which work equally well.

#### *Tools:*

- *Rye grain*
- *Gypsum*
- *Container for mixing*
- *Pressure cooker*
- *Sieve*
- *Jar and polyester pillow stuffing as a filter*

In order to proceed, grains need to be soaked in water mixed with gypsum and coffee. Gypsum will prevent the grains from sticking to each other and coffee will increase the strength. Put the rye into a container, add warm water around 75 °C at a level to be 4-5 cm higher than the rye level. Pure a cup of warm coffee and cover the container with a stretch wrap or an aluminum foil. Let the rye soak between 18-24 hours. Once the rye is soaked, simmer the mixture for about 10-15 minutes to increase the moisture content inside the grains. Then, drain the water for about 15 minutes using a sieve in order to get rid of the extra water on the surface of grains. Give it a control by hand to feel how moist the grains are and if it does not feel too sticky, then fill the jars with the rye grains for the sterilization process.



Figure 28: Ingredients to soak the rye grain (Author's image)



Figure 29: Simmering the soaked rye grain (Author's image)

Similar to the sterilization process of the agar medium mixture, a pressure cooker/canner is used. Jars filled with rye grains closed with the polyester filter applied lids.



Once the ample steam started to release which shows the pressure cooker/canner reached 15 Psi, the countdown started at 1.5 hours.



Figure 30: Simmered rye grains in the jars (Author's image) Figure 31: Polyester filter on the lid of the jars (Author's image)

When the pressure cooker/canner fully depressurized, open the lid and carefully remove the jars using latex gloves. Jars should cool down to room temperature in a sterile place like in a glove box or in front of a laminar flow hood.

Once the jars cooled down below 30 °C, it is ready to proceed with the inoculation process by using the mycelium spawn grown on agar medium.

#### ***Tools:***

- *Petri dish (at least 3/4 colonized, not mutated)*
- *Sterilized rye substrate*
- *Scalpel with a sterile blade*
- *Bag sealer or strong adhesive tape*
- *Face mask, hairnet and latex gloves*
- *Disinfectants for workspace and hands*
- *Sterile working area: Glove Bag/Glove Box or*
- *Sterile air flow (HEPA-filter, laminar flow hood)*

In order to be as sterile as possible to reduce the risk of contamination, proceed carefully and use hairnet, face mask, gloves and sanitize everything with 99.99% isopropyl alcohol.

Use one petri dish of mycelium spawn to inoculate one jar of sterilized rye grain which is equal about 350-400 grams. Do not use different Petri dishes to inoculate the same jar of sterilized rye grain. This could create a competition between two mycelium strains which may end up with a failure in germination of healthy mycelium.

Remove the Parafilm seal around the petri dish inside the glove box or in front of a HEPA-filter. Flame sterilize the scalpel until it is red-hot. Make a long cut on one side of the petri dish to cool down the scalpel and make a grid-like cuts on the other side of the petri dish. Collect the mycelium covered pieces of agar medium with the scalpel and carefully transfer them into the jar and close the lid. Distribute the pieces by shaking the jar in order to increase the speed and homogeneity of inoculation. Make sure that all the pieces are in contact with the rye

grain substrate. After few days, the mycelium will start to expand from the agar medium into the rye substrate. In order to accelerate the speed of inoculation, shake and distribute the colonized rye grain in the jar. With the appropriate conditions depending on the species, colonization process should be fully complete about 2-3 weeks after inoculation.



Figure 32: Inoculated jar of rye grain with mycelium on an agar medium (Author's image)

### 3.3 Bag stage

Different species of fungi require different substrates in order to give mushroom fruit bodies because of nutritional conditions. Straw, sawdust, coffee grounds, logs, compost, paper products, etc. are some examples of different substrates. However, in this study, it is not aimed to grow fruiting mushroom bodies. Mycelium itself as the biopolymer is used as the fibrous filament and binder element of the biocomposites that have been created in this study. Therefore, the growth of mycelium is terminated before it starts to fruit mushroom bodies, once it full colonizes and covers the natural fiber substrate. Type of the substrates will be examined according to its effect on the physical and mechanical properties of the mycelium-based material as well as the species.

In this study, mainly hardwood sawdust, sawdust-woodchips mixture, and straw have been used while creating the mycelium-based biocomposite materials. Thus, preparation of those substrates will be covered under this chapter.

#### 3.3.1 Sawdust, sawdust + woodchips

**Tools:**

- Wood chips
- Hard wood saw dust
- Rye bran
- Water
- Autoclave bags
- Scale
- Bag sealer or strong adhesive tape
- Sieve
- Container for mixing
- Pressure cooker
- Tyvek sleeves as filter

Soak the wood chips in cold water between 12-18 hours with an amount of water enough to make the wood chips floating. Drain the wood chips using a sieve around 15 minutes. On the other side, mix the hardwood sawdust pellets with water and let them expand. Make sure that water mixes through the pellets. Once the sawdust expended enough, mix it with woodchips and rye bran into a mixing container.



Figure 33: Woodchips (Author's image)



Figure 34: Woodchips soaked in water (Author's image)

In order to fill one autoclave bag with an approximate 2.5 kg substrate;

- 400 g wood chips
- 750 g hardwood sawdust
- 250 g rye bran
- 1 L of water

should be mixed. Once the bags are filled, clean the upper part of the bag from inside and remove all the particles of the mixture to reduce the risk of contamination. Use an appropriately sized piece of Tyvek Sleeve to use as a filter as wide as the opening of the bag. Slice it into the bag and fold the autoclave bag into two. Place the bag into the pressure cooker/canner and sterilize it about 3-4 hours at 15 Psi. Make sure that pressure cooker/canner does not run out of the water. Once the sterilization process is over, pressure cooker/canner should cool down in front of a HEPA-filter, laminar flow hood or a disinfected place. When the substrate has cooled down below 30 °C, it is ready for inoculation. To inoculate the substrate, grain spawn substrate will be used.



Figure 35: Oak sawdust pellets (Author's image)

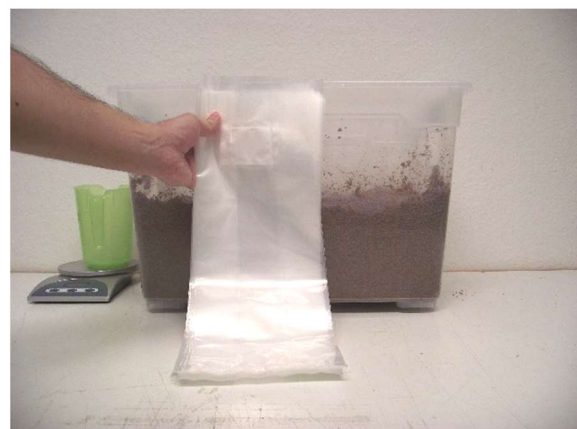


Figure 36: Autoclave bags (Author's image)



### 3.3.2 Straw

Most of the fungi species are suitable to grow on straw like most of the *Pleurotus* strain since it is easy to break into plant fibers. Like other substrate mediums, straw also needs to be sterilized before in order to provide suitable conditions for mycelium to be able to grow. However, unlikely hardwood sawdust or wood chips, the straw substrate does not need to be pressure sterilized rather pasteurized. There are different techniques to pasteurize the straw substrate. Down below, the technique that has been used in this experiment is explained.

#### **Tools:**

- Cereal straws (wheat, rye, and oat etc.)
- Water
- Autoclave bags
- Scale
- Pot
- Sieve



Figure 37: Straw substrate (Author's image)



Figure 38: Pasteurization of straw substrate (Author's image)

First, cut the straw in small pieces of 1-3 centimeters and place them into the pot. Fill the pot with water and place something heavy like a smaller lid or some plates on top of the straw. Make sure that all the straw pieces are under water. Heat it up to 65-85 °C and once the temperature reached, let it pasteurize for 1.5 hours. Once it is pasteurized, use a sieve to drain all the exceeding water on the straw. Then, spread the straw on an alcohol-sterilized wide surface like a table top in order to cool the straw down faster and reduce the risk of contamination since it is exposed. Once the pasteurized straw is cooled down to 30 °C, inoculate the substrate with grain spawn buy just simply and fill the alcohol sterilized molds.



Figure 39: Draining the pasteurized straw (Author's image)



Figure 40: Inoculation with mycelium spawn (Author's image)

In this study, three different proportions of sawdust and wood chips mixture and two different sawdust substrate with different moisture values have been used in order to see the contribution of different substrate composition on the physical properties of mycelium-based materials.

Sawdust and straw substrates have been inoculated with *Pleurotus eryngii* (King Oyster) while the sawdust and woodchips mixtures have been inoculated with *Ganoderma lucidum* (Lingzhi or Reishi).



Figure 41: Oak sawdust and woodchips substrate  
(Author's image)



Figure 42: Substrate mixtures with different ratios  
(Author's image)



Figure 43: Pressure cooker to sterilize the substrate mixtures  
(Author's image)



Figure 44: Sterilized substrate mixtures  
(Author's image)

### 3.4 Forming stage

Almost all commercial building materials are processed either chemically or physically in order to give a suitable shape that matches with their usage. Likewise, growing building materials with mycelium require a similar process in order to form the material.

There could be different ways to form the mycelium-based materials. Depending on the desired material form, the inoculated substrate can be pre-formed in a self and free-standing way and mycelium can grow directly onto the desired form. Similarly, mycelium material can be formed in molds basically filling them with the inoculated substrate and let the mycelium run through. A different method comes with machinability feature of the mycelium materials. So, the inoculated substrate can grow as a mass in an autoclave growth bag instead of molds. Once the mass is completely colonized and the growth process is terminated by drying the material with a different method which is explained in the following chapters, the mass can be

cut into a variety of shapes depending on the substrate type and the shape of the mass. Furthermore, the mass can be CNC (computer numerical control) shaped into more complex shapes.

In this study, a thermoforming machine has been used to create plastic molds in order to grow the mycelium-based materials in. Thus, the negative forms to use in the thermoforming machine have been created by using CNC out of MDF material.



Figure 45: Thermoforming machine  
(Author's image)



Figure 46: CNC processed MDF negative form and  
thermoformed plastic for acoustic panel samples (Author's image)

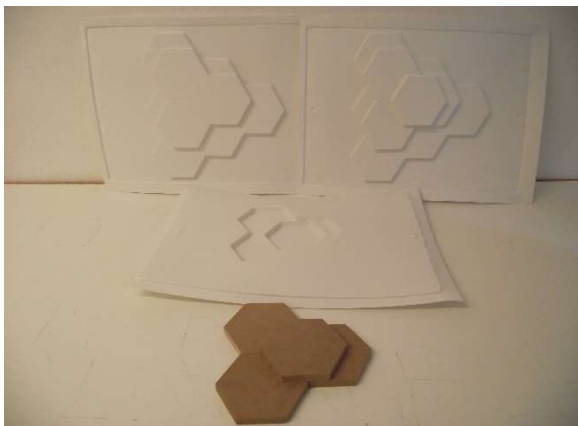


Figure 47: Thermoformed plastic and negative forms  
(Author's image)

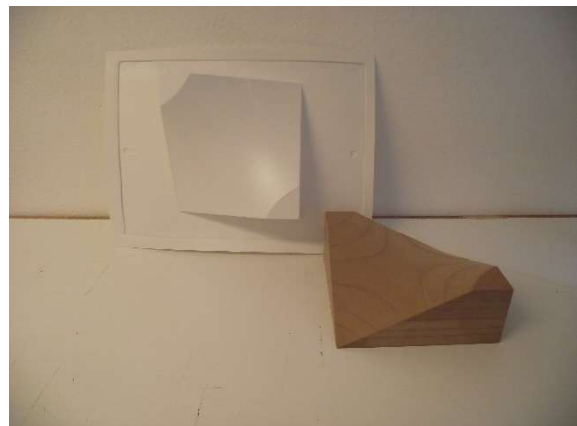


Figure 48: Negative form and thermoformed plastic of  
hyperbolic paraboloid brick (Author's image)

The hyperbolic paraboloid shaped bricks have been growing in the following molds which have been produced with the combination of two hyperbolic paraboloid surfaces held in a rectangular form out of cardboard as they are shown in the following pictures.

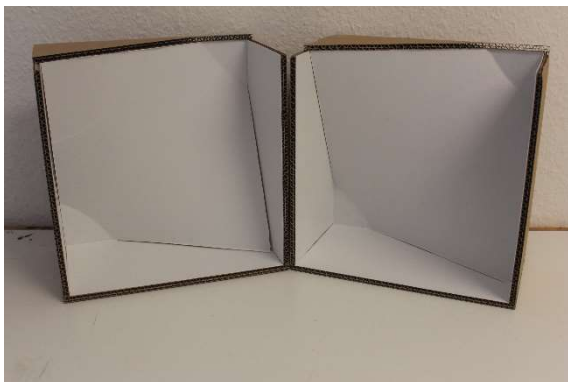


Figure 49: Section of the molds for hyperbolic paraboloid bricks  
(Author's image)



Figure 50: Hyperbolic paraboloid brick mold  
(Author's image)



### 3.5 Drying

Mycelium materials are literally living organisms with a high potential of fruiting mushroom fruit bodies under suitable environmental conditions. Hence, one last step is required to be able to use mycelium materials is to terminate the growth of mycelium. Therefore, all the moisture and water inside the mycelium material should be removed. Thus, this procedure is literally a drying process, however, there are different ways to dry the mycelium materials which potentially results with different mechanical properties.

One method to dry the mycelium material to determinate to growth is simply to take the material out of the mold and leave it in a preventing setting from contamination. Either under direct sunlight or in a well-ventilated environment, mycelium material loses all the moisture around one or two weeks depending on the moisture level. During the experiments, it has been observed that during the first few days mycelium continues to grow especially on the exterior of the material. This is an advantage in order to repair the damages and rehabilitate the continuity of the filamentous mycelium tissue which may happen during the removal from the molds.

Another method is to use an oven or a drying machine to speed up the process and completely remove the moisture from the mycelium material content. During their experiment, Arifin and Yusuf (2013), used a drying machine for 46 hours at 50 °C to terminate the mycelium growth while Holt *et al.* (2012) used a convection oven for 8 hours at 60 °C on a different experiment. In the instruction set of “*Grow it yourself*” toolkit from *Ecovative Design*, drying conditions are defined as 95 °C for 45 minutes in an oven. Those experiments show that drying time and temperature varies and it has an effect on the resulting mechanical properties and behavior of the mycelium material.

One other method is to apply heat and pressure at the same time to the mycelium material. This removes all the exceeding water from the mycelium material content and increases the binding feature of the filamentous mycelium while increasing the mechanical behavior and reducing the thickness. Thus, the final shape of the mycelium material can be given with the heat pressure process which may bring an advantage in terms of having a simple plane-like preform mold for different geometries.

In this study, some samples have been dried in a conventional oven at 95 °C for a period of time ranging between 3 hours and 6 hours. More the moisture content released, the samples became more rigid and lighter. For instance, the sawdust block in Figure 51 which have been inoculated with *Pleurotus eryngii* mycelium have lost 192 grams after 4 hours of drying in the oven at 95 °C. After drying process in the oven, the block has been left outside and after 2 weeks it has been observed that the block has lost 244 grams more. At the end, the block lost a total weight of 436 grams from 1572 grams to 1136 grams, which has been represented in the following images.



Figure 51: A sawdust mycelium block before oven drying (Author's image)

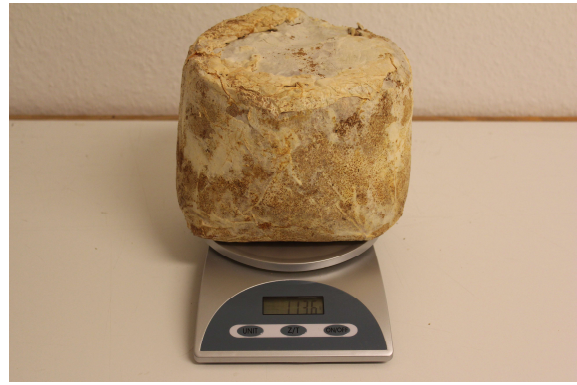


Figure 52: A sawdust mycelium block after oven drying (Author's image)



Figure 53: Mycelium bricks before oven drying (Author's image)



Figure 54: Mycelium bricks after oven drying (Author's image)

### 3.6 Experiences and deduces of mycelium growing process

During the experiments of growing mycelium and producing mycelium-based biocomposite materials, combined with the literature knowledge and researches, personal experiences, and observations involved in finding the direction to successful results.

Before starting the experiments with producing mycelium-based materials, it has been found critically necessary to understand the nature of mycelium and its growing behavior. Thus, a pre-study has been done with two different mushroom species, *Lentinula edodes* (Shiitake) and *Pleurotus eryngii* (King Oyster), in order to understand how the environmental conditions like light, relative humidity, and temperature affect the growth rate of mushroom mycelium.



Figure 55: *Lentinula edodes* (Shiitake) (Northwest Wild Foods 2018)



Figure 56: *Pleurotus eryngii* (King Oyster) (Thepinsta.com 2018)



Three different sample groups of mycelium in Petri dishes with malt extract agar have been placed in different environments with different light, relative humidity and temperature conditions and growth rates have been observed for 10 days.

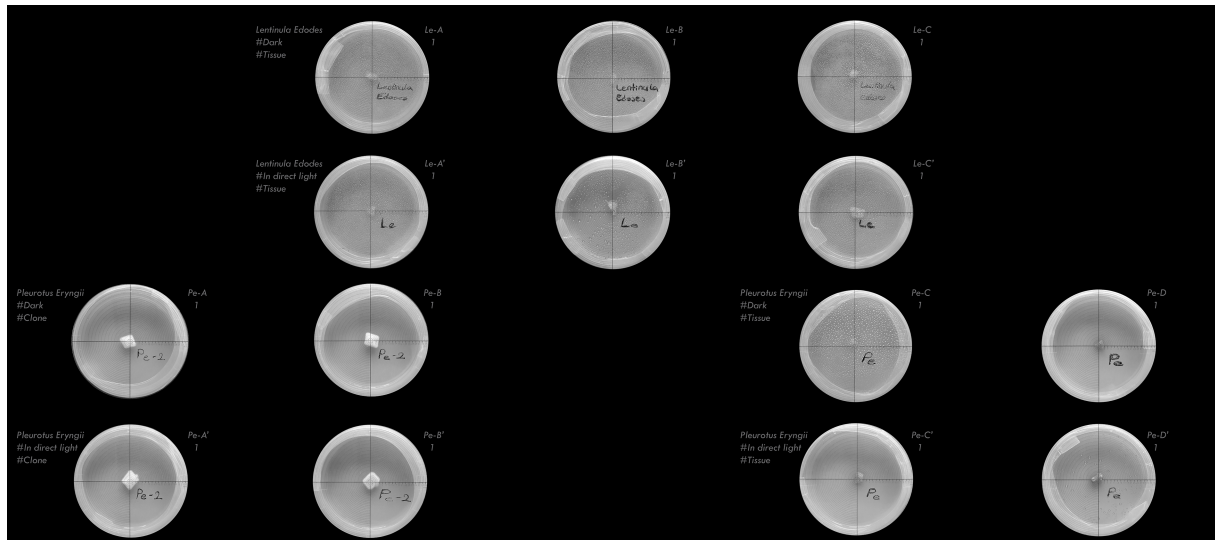


Figure 57: First day of the observation on the sample groups (Author's image)

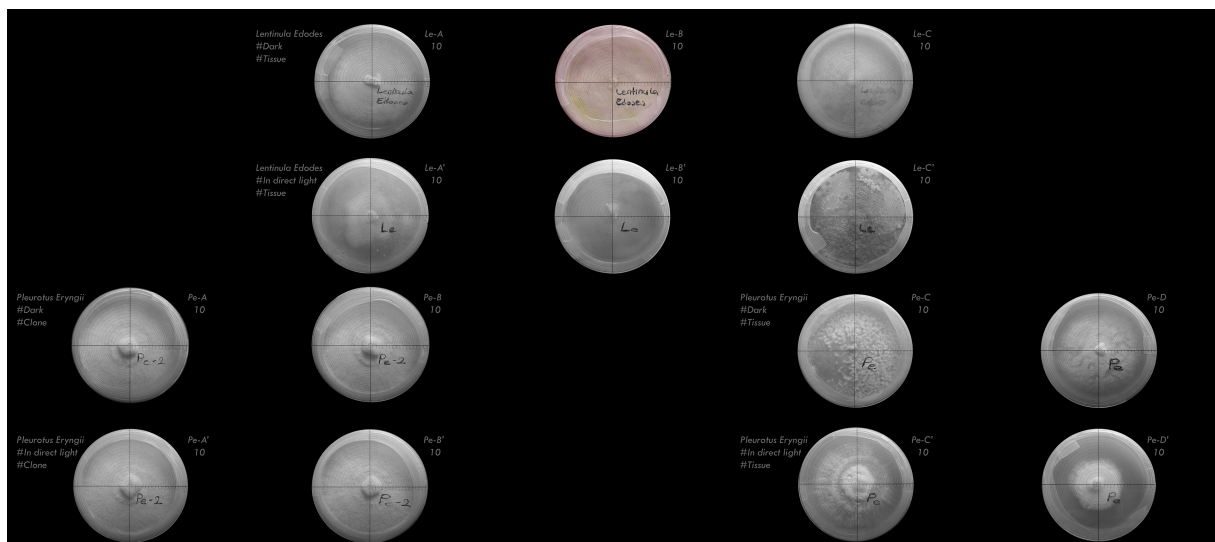


Figure 58: 10<sup>th</sup> day of the observation on the sample groups (Author's image)

It has been observed that the mycelium obtained from *Pleurotus eryngii* performed a faster growth rate against the species *Lentinula edodes*, which was a second generation clone from a previously generated mycelium sample on agar medium. Thus, it has been selected to be used in further experiments with mycelium-based biocomposite material production.

During the experiments on material production with sawdust substrates, sawdust pellets have been selected from two different species of trees; Maple and Oak. Between the two sawdust substrate samples, it has been observed that mycelium has grown slightly faster on Oak samples. However, the overall growth time was relatively long compared to the reported values in the literature. Also, the first mechanical tests on the first mycelium-based composite bar samples showed that the strength of the material is really low.

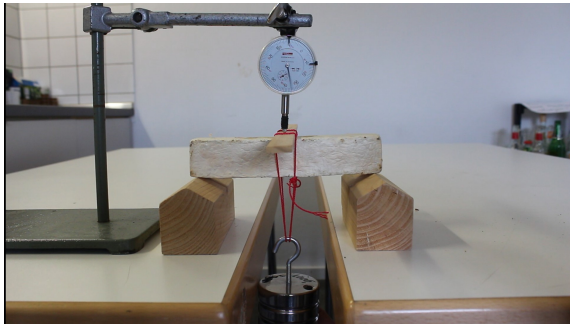


Figure 59: 3 point load mechanical tests (Author's image)

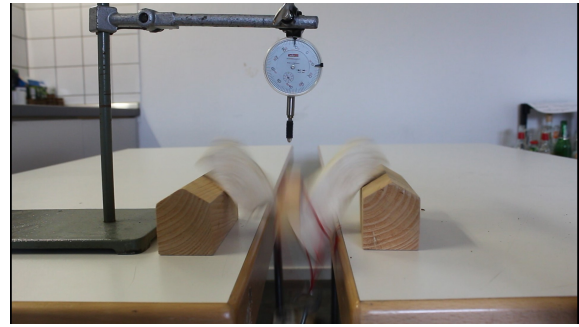


Figure 60: Failure of the first samples (Author's image)

Thus, it has been found important to experiment also with another fungi species and different substrate types. Based on the literature review, since it is commonly used in the field of mycelium-based biomaterials, it has been decided to work with the fungi species called *Ganoderma lucidum* (Lingzhi or Reishi).



Figure 61: *Ganoderma lucidum* mushroom fruiting on nutritional substrates (Pavòn 2018)

In the further experiments on mycelium-based biocomposite material production, Oak sawdust, beech woodchips, and straw have been used as the substrate. Straw substrates have been inoculating only with *Pleurotus eryngii* mycelium spawn. Mixtures of sawdust and woodchips in different ratios have been inoculated with both of the fungi species. It has been observed that the samples of *Ganoderma lucidum* colonize in the substrates remarkably faster than the samples of *Pleurotus eryngii*. The image below shows four different bags of substrates and the status of colonization of mycelium.

The bags A, B, and C in the image have been inoculated at the same time and the photo is taken at the first week of their inoculation while the bag D has been inoculated 10 weeks ago from the time that the photo was taken. The substrates and the mushroom mycelium species in each bag are like below;

- **A:** 2.5 L Oak sawdust and 2.5 L beech woodchips inoculated with *Ganoderma lucidum*
- **B:** Oak sawdust with higher moisture content inoculated with *Pleurotus eryngii*
- **C:** Oak sawdust with lower moisture content inoculated with *Pleurotus eryngii*
- **D:** Maple sawdust inoculated with *Pleurotus eryngii*



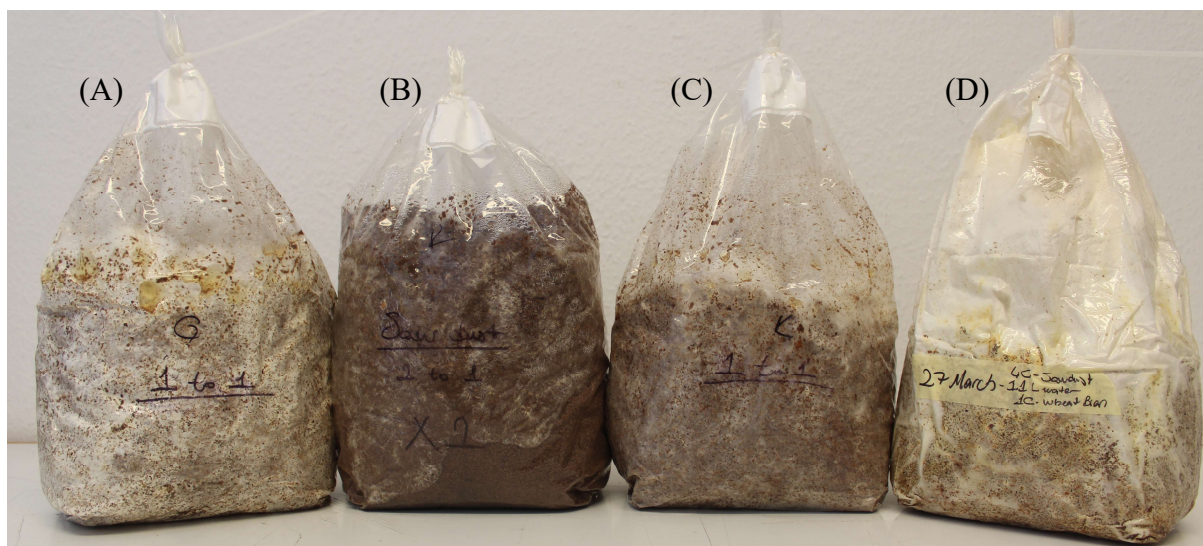


Figure 62: Comparison of different substrates inoculated with different species (Author's image)

However, the species *Pleurotus eryngii* has represented a quite faster growth and colonization speed on straw substrates instead of sawdust substrates. The image below shows two samples of substrates, A is sawdust and woodchips mixture and B is straw substrates both inoculated with *Pleurotus eryngii* spawn.

(A)



Figure 63: Mycelium growing on straw substrate (Author's image)

(B)

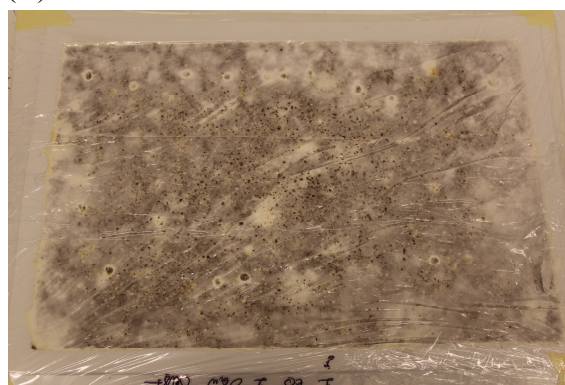


Figure 64: Mycelium growing on Oak sawdust substrate (Author's image)

The following photos show some samples of the inoculated different substrates in different molds.

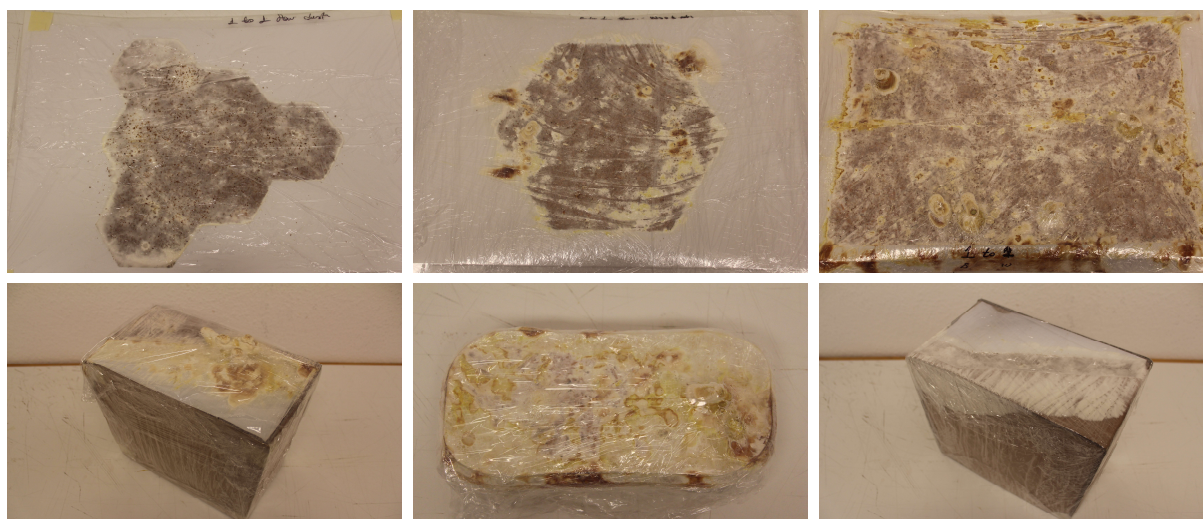


Figure 65: Samples growing in different molds (Author's image)

## 4. Biodegradable pavilion design

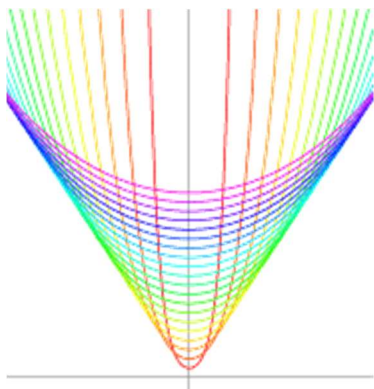
Among all the other unique features of mycelium-based biocomposite materials, obviously, biodegradability is the strongest. Considering this fact, it has been seen to design a temporary pavilion is one of the most suitable approaches to examine the potential applications of mycelium-based biocomposite materials. Based on the literature review and laboratory tests conducted by many researchers, it has been shown that mycelium-based biocomposite materials work better under compression due to their greater compression strengths than tension strengths. Thus, it has been chosen to work with a catenary curve which is a natural curve on a uniformly dense chain with both ends pinned at an equal height under uniform gravitational force (Weisstein 2008) in order to design a catenary vault pavilion.

During the design process, parametric design tools like *Grasshopper* for *Rhinoceros 5* from Robert McNeel & Associates and finite element analysis software *ANSYS* and its various interfaces like *SpaceClaim*, *Mechanical Enterprise* etc. have been used.

### 4.1 Catenary curve, arch, and vault

Both in geometry and physics, “catenary” is defined as a planar curve that represents the shape of an ideal hanging chain which is fixed at its ends and acted under uniform gravitational forces (Conversano *et al.* 2011).

Even though the term “catenary” was first mentioned by Dutch mathematician Christiaan Huygens (1629-1695) in a letter written to Gottfried Wilhelm Leibniz (1646-1716) on November 18, 1690, the word is originated from the Latin word *catēna* which means “chain”. Galileo Galilei (1564-1642), intelligent Italian astronomer, besides his radical ideas and discoveries about astronomy he also developed ideas about projectile motion which means the path of an object thrown into the air at an angle. He proved that the path of those objects is a parabola. Galileo also studied catenary curves for the first time however, he stated the curve as a parabola. German mathematician Joachim Jungius (1587-1657) proved that the catenary is not a parabola and published after his death in 1669. In 1691, the correct mathematical equation of catenary curve was described by Gottfried Wilhelm von Leibniz, Christiaan Huygens, and Johann Bernoulli. As it is described by Weisstein (2008);



“The parametric equations for the catenary are given by;

$$x(t) = t \quad (1)$$

$$y(t) = \frac{1}{2} a (e^{t/a} + e^{-t/a}) \quad (2)$$

$$= a \cosh\left(\frac{t}{a}\right), \quad (3)$$

where  $t = 0$  corresponds to the vertex and  $a$  is a parameter that determines how quickly the catenary “opens up.” Catenaries for values of  $a$  ranging from 0.05 to 1.00 by steps of 0.05 are illustrated on the graph left.”

Figure 66: Graph of different catenary curves (Weisstein 2008)





Figure 67: An almost catenary arch of Taq Kasra, 6<sup>th</sup> Century BC (Wikipedia, Taq Kasra 2018)

In pre-Greek and pre-Roman architecture, catenary was used in order to construct arches which later reversed to circular arches and semi-spherical vaults. Even though it was more used in Islamic Architecture, it was forgotten for a significant amount of time in Europe. In 1671, Hooke had achieved the solution of the optimal shape of an arch. During the rebuild of St Paul's Cathedral, Robert Hooke's (1635-1703) analogy between a hanging chain and an arch has been re-discovered by Giovanni Poleni (1683-1761).

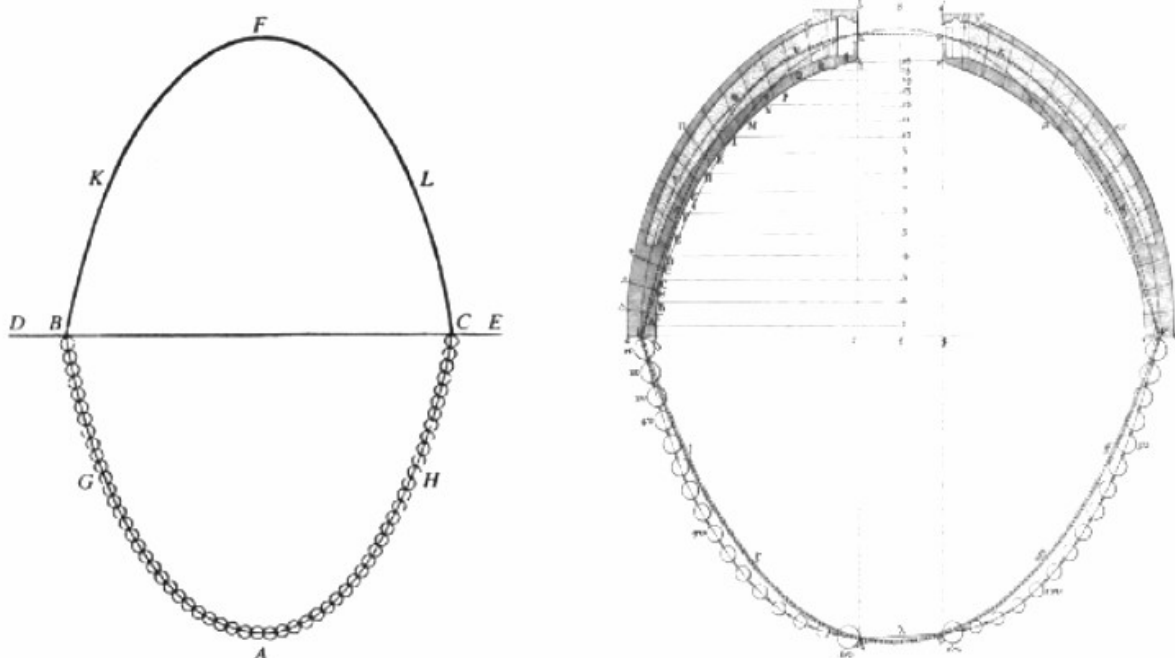


Figure 68: (A) Poleni's drawing of a hanging chain and an arch (B) the analysis of the dome of St-Peter's by Poleni (by (Block et al. 2006))

The relationship between a hanging chain which creates a catenary form in tension under its own weight and an arch, the form when the hanging chain is inverted which stands in compression supporting its own weight, is explained by Robert Hooke. Later he was going to state his discovery in one of his completely unrelated books "as hangs the flexible line, so but

*inverted will stand the rigid arch*” (Heyman 1998). The condition for the chain and the arch is an equilibrium of forces while the forces are basically reversed versions of corresponding ones. In other words, if a chain is hung with a set of loads, once fixated and reversed represents the path for the set of compressive forces of an arch structure which works safely under the identical set of loads (Block et al. 2006).

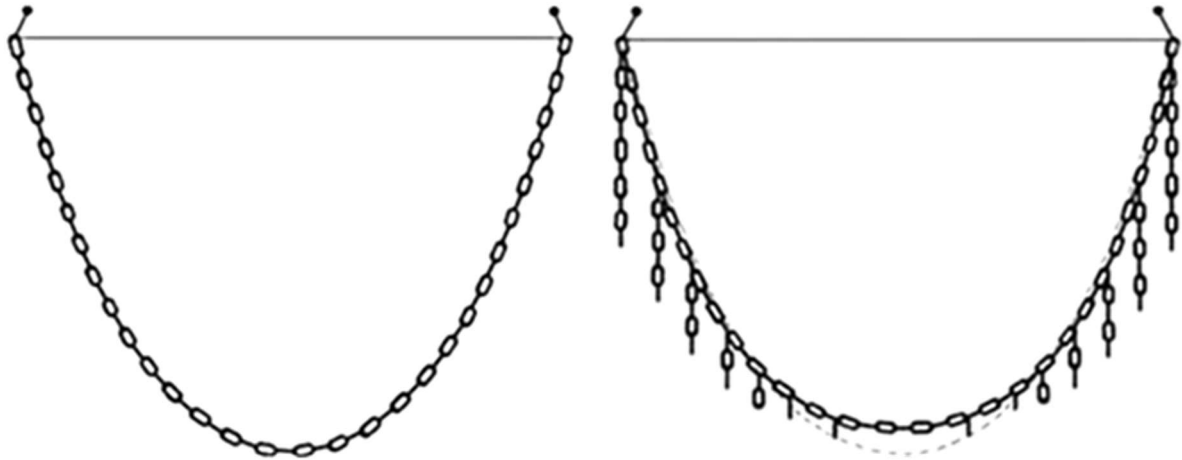


Figure 69: Hanging chain under only gravitational forces creating undistributed catenary form and chain loaded with different loads creating modified catenary (The Auroville Earth Institute, Stability calculations, Catenary Method 2018)

## 4.2 Parametric catenary vault design

In the design process of the catenary vault, graphical algorithm editing and parametric design plug-in named *Grasshopper* for *Rhinoceros 5* by McNeel & Associates have been used. A parametric design script has been developed to provide a broad control over the design of the catenary vault. This enables the designer to instantly change or update the design with numerical parameters to control the size of the catenary vault and the bricks, numbers of the bricks etc. In this section, the creation of the catenary vault through the Grasshopper script is explained.

### 4.2.1 Hanging chain model

The physical method of hanging chain model is simulated with the Grasshopper script. Following diagrams step by step explains the creation of the catenary vault. The related section of the complete Grasshopper script is also shown below.

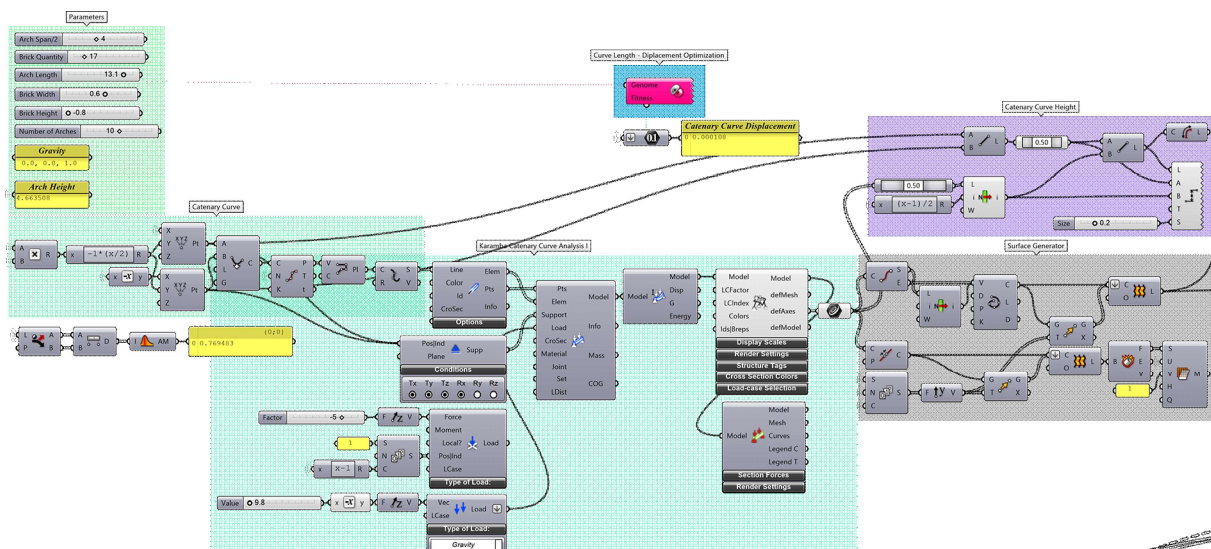
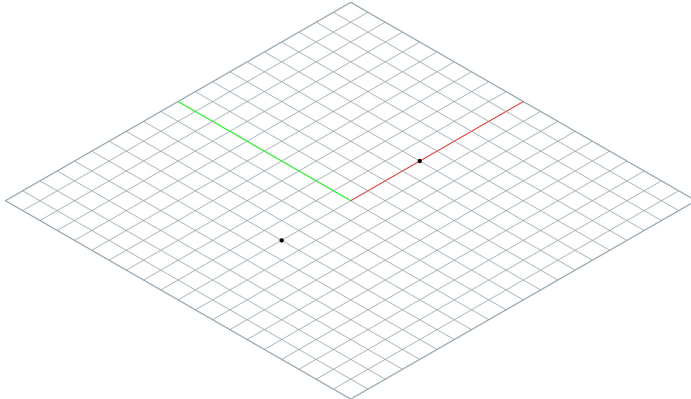


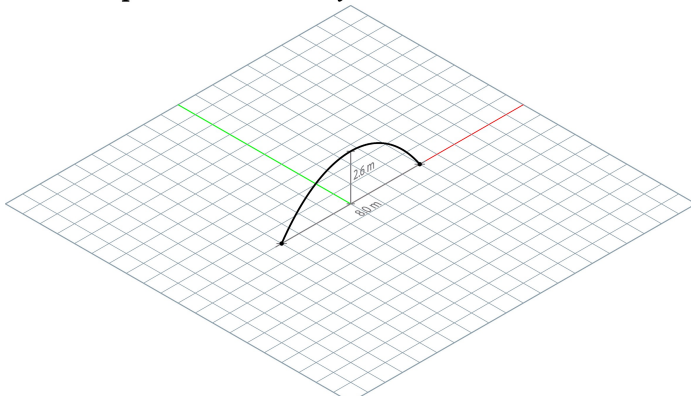
Figure 70: Related part of the Grasshopper definition to simulate the hanging chain model (Author's image)

### 1. Anchor points:



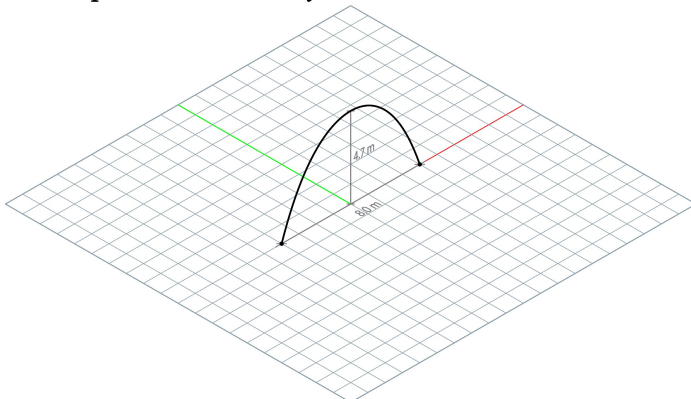
As the first step to create a hanging chain model, two anchor points have been defined where the “chain” will be hanged in between in order to create a catenary curve.

### 2. Unoptimized Catenary Curve:



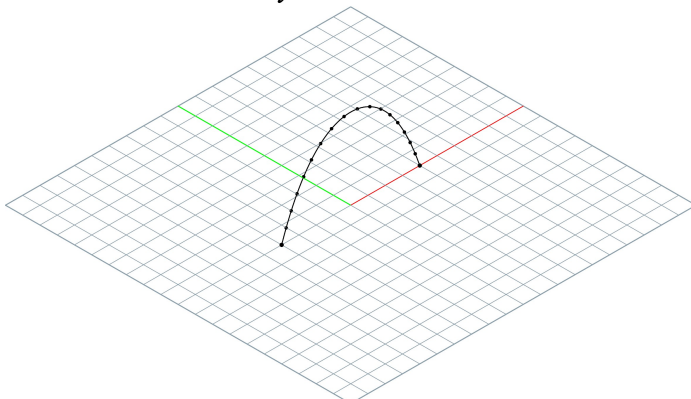
The *Catenary* component of Grasshopper enables to have a control on the length of the catenary curve. Together with that, the positions of anchor points and the direction of gravity force design the shape of the catenary curve. Thus, an arbitrary value for the length of the curve has been given at the beginning.

### 3. Optimized Catenary Curve:



Then, the built-in evolutionary solver component and optimization tool for Grasshopper called *Galapagos* and the plug-in named *Karamba3D* which a parametric engineering and structural analysis tool have been used. In order to find the minimum displacement on the catenary curve, the length of the curve has been optimized by the Grasshopper definition.

### 4. Divided Catenary Curve:

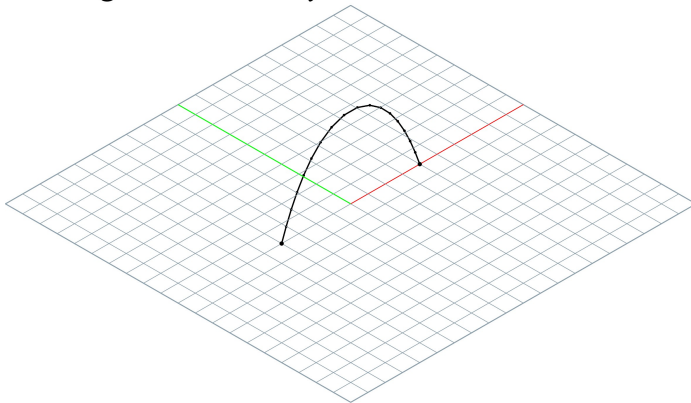


Once the catenary curve is optimized, in order to define the number of bricks in the catenary arch, the curve has been divided into points which later will be used as the segments for the bricks. This also gives a control on the length of the bricks.

Figure 71: Steps 1 to 4 to create the hanging chain model with Grasshopper script (Author's image)

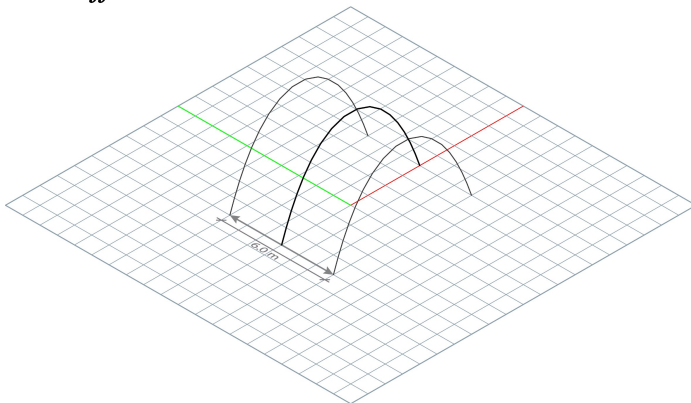


### 5. Segmental Catenary Arch:



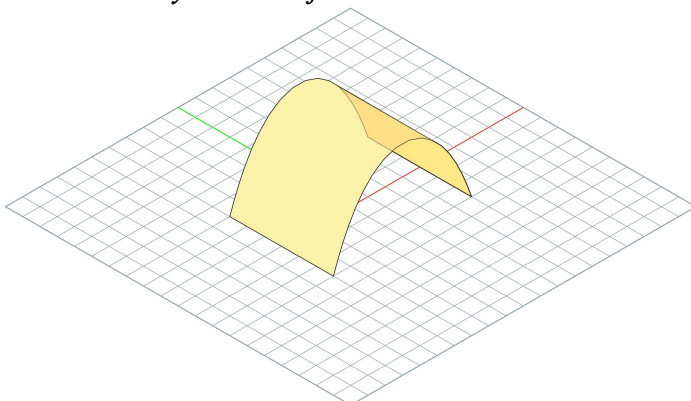
The points on the divided curve have been connected together simply by drawing lines in between to create the segmental catenary arch form.

### 6. Offset:



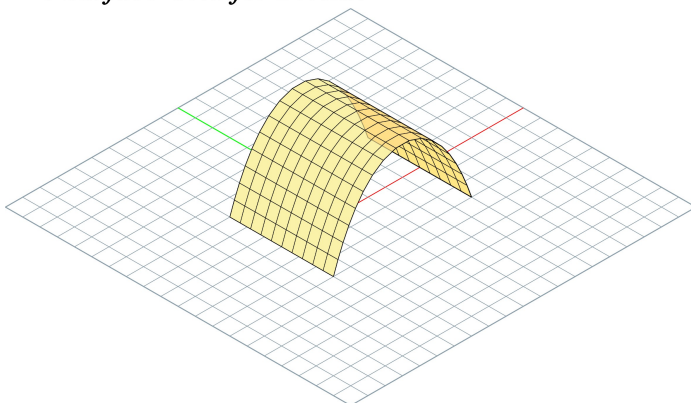
Then, the segmental catenary arch has been replicated on both negative and positive y directions in order to define the length of the catenary vault.

### 7. Catenary Vault Surface:



Once the boundary of the catenary vault is defined, a surface has been created between the two segmental catenary arches by using the *Loft* component of Grasshopper.

### 8 Surface Grid for Bricks:



After creating the catenary vault surface, a rectangular grid has been generated on the surface in order to define the number of catenary arches on the vault as well as the number of bricks. This also gives a control on the width of the bricks.

Figure 72: Steps 5 to 8 to create the catenary vault surface with Grasshopper script (Author's image)



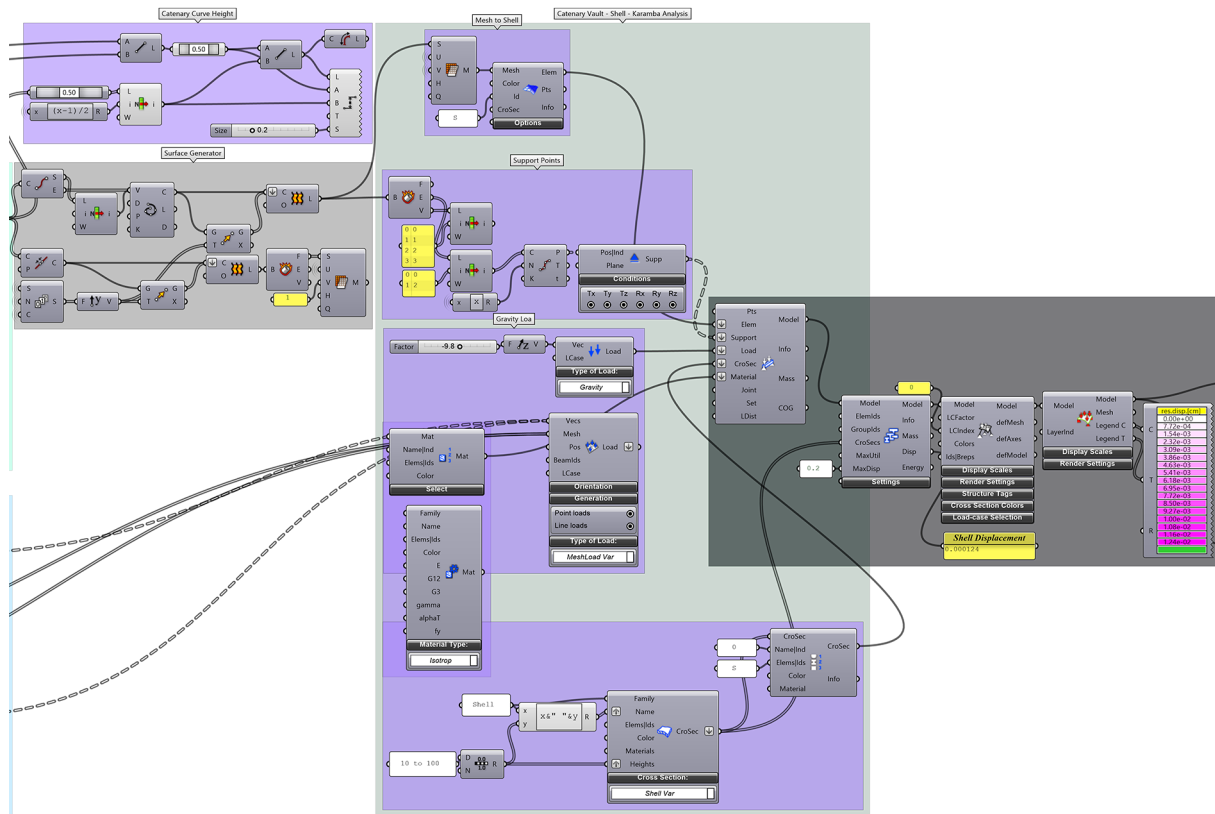
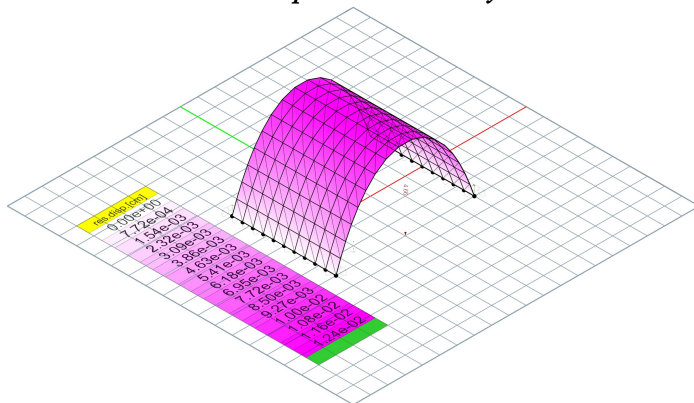


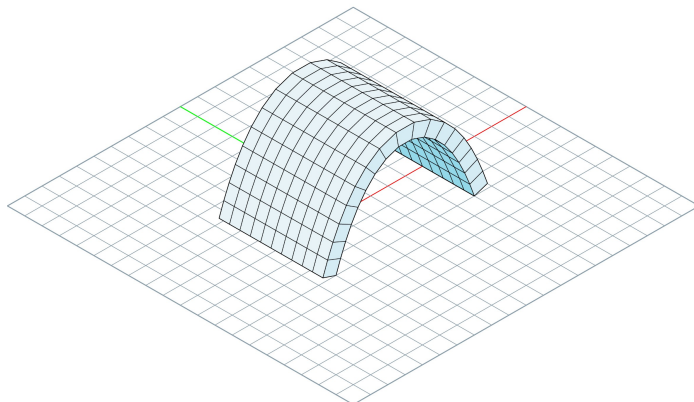
Figure 73: Karamba3D analysis of the catenary vault surface (Author's image)

## 10. Karamba3D Displacement Analysis:



Once the catenary vault surface is generated, a Karamba3D analysis has been applied to visualize the displacement on the catenary vault only under gravitational forces while being supported on each anchor point of each arch that creates the vault.

## 11. Brick Placement:



After the analysis, the grid is used to place the regular rectangular bricks to create the masonry catenary vault.

Figure 74: Steps 10 to 11 to analyze the displacement on the catenary vault and first brick generation (Author's image)

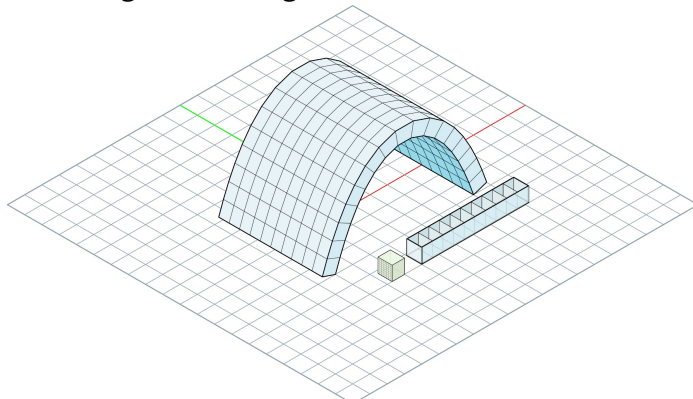
However, since the material to build the catenary vault is mycelium-based biocomposite materials, it has been noted that the regular rectangular bricks would require a

greater amount of biomass. Also, the design is prone to be affected by wind loads due to the greater surface area on the sides of the vault. Thus, the shape of the bricks has been optimized which is described how in the following section.

#### 4.2.2 Adaptive mold system and hyperbolic paraboloid bricks

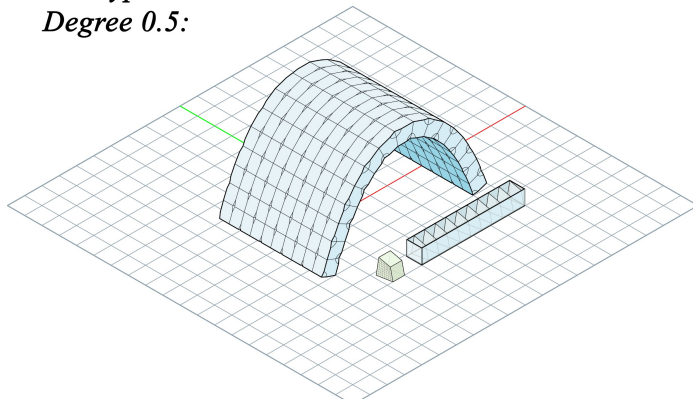
While creating a parametric Grasshopper definition for the catenary vault, a set of parameters have been also integrated which controls the design of the bricks. Once the brick shape changes, the whole design of the catenary vault is updated. Also, the definition creates a mold for 10 bricks simultaneously with the catenary vault. Likewise, once the brick shape changes, the mold is updated automatically. The relationship between the shape of the brick and the catenary vault design as well as the mold model is shown in the following diagrams below.

##### ***12. Regular Rectangular Bricks and Mold:***



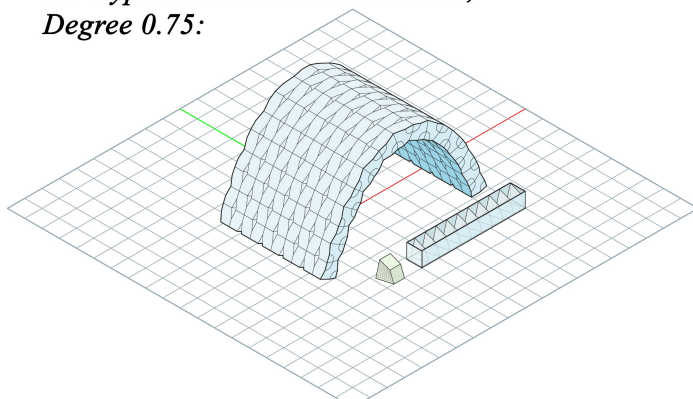
In case of using regular rectangular bricks to construct the catenary vault, dimensions of each brick are around 60 cm x 80 cm x 80 cm. As an example, in order to create 10 bricks out of a mold, the length of the mold model is around 6 meters.

##### ***12. Hyperbolic Paraboloid Bricks; Degree 0.5:***



Parametric Grasshopper definition enables the designer to control the degree of a hyperbolic paraboloid. In a range between 0.0 to 2.0 which controls the hyperbolic degree, the image on the left shows the hyperbolic paraboloid brick with 0.5 degrees. With the change of the brick shape, the mold already starts to become shorter.

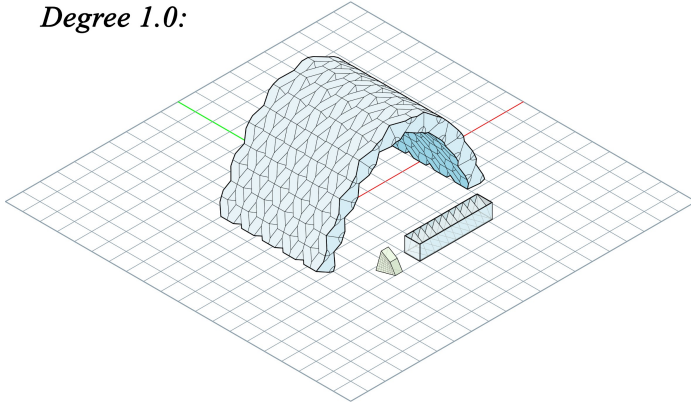
##### ***13. Hyperbolic Paraboloid Bricks; Degree 0.75:***



The image on left shows the hyperbolic paraboloid brick with 0.75 degrees. As the degree grows, the brick gets thinner.

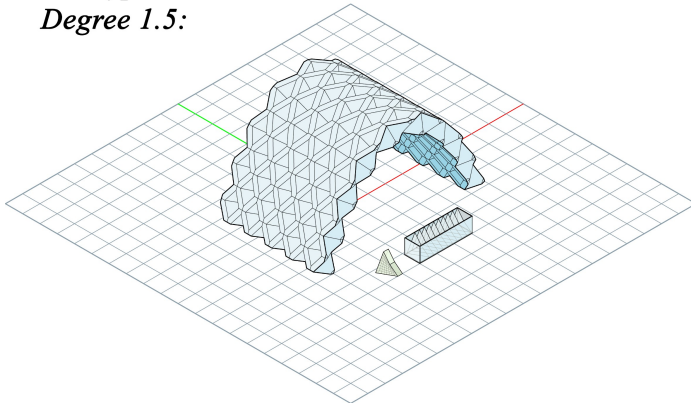
Figure 75: Steps 11 to 13 of the adaptive mold system and variations of the vault with each brick type (Author's image)

**14. Hyperbolic Paraboloid Bricks;  
Degree 1.0:**



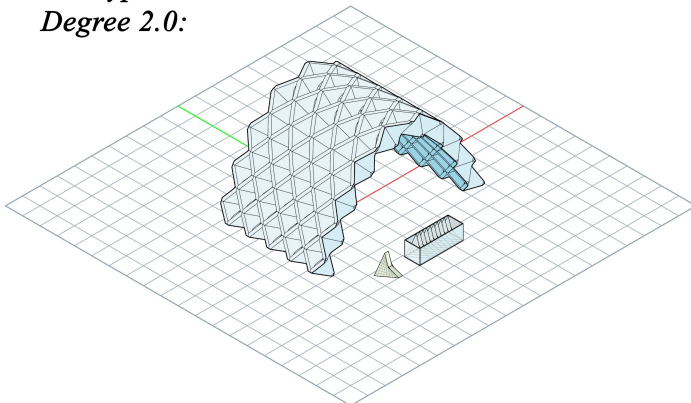
More the degree increases, due to the shape of the bricks, openings start to appear on the side of the catenary vault. Thus, the effect of the wind load on the catenary vault starts to reduce.

**15. Hyperbolic Paraboloid Bricks;  
Degree 1.5:**



Even though the “bounding box” volume of the bricks are the same with the regular rectangular bricks, since the real volume of the bricks becomes lower the weight of the overall structure reduces.

**16. Hyperbolic Paraboloid Bricks;  
Degree 2.0:**



The image on left shows the final design of the catenary vault with the 2.0 degree hyperbolic paraboloid bricks. Due to hyperbolic paraboloid transformation, the bricks turned into hyperbolic paraboloid shells instead of rectangular blocks.

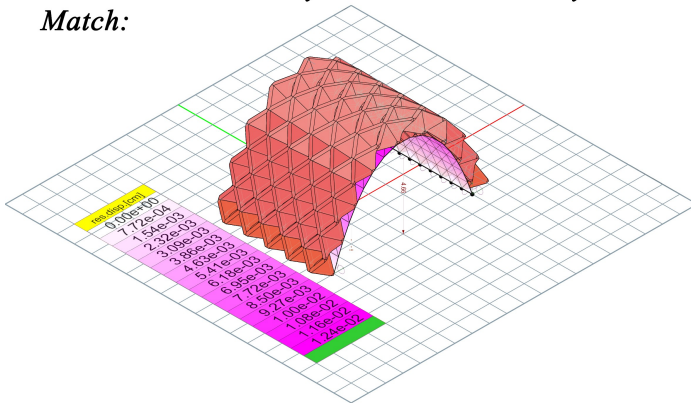
Figure 76: Steps 14 to 16 of the adaptive mold system and variations of the vault with each brick type (Author's image)

#### 4.2.3 Density matching with Karamba3D analysis

As it has been discussed in the previous chapters, mycelium materials have a wide range of density values depending on many factors like species of the mushroom mycelium, natural fibers as substrate and nutritional conditions etc. Thus, three different densities of bricks have been distributed in response to the displacement analysis of Karamaba3D as it is shown in the images below.

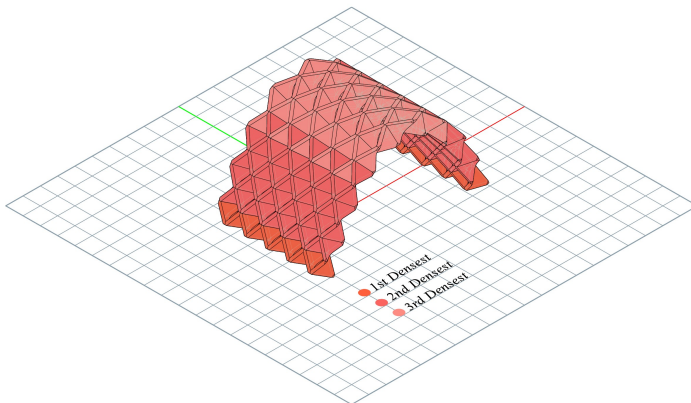


### 17. Karamba3D Analysis and Brick Density Match:



The result of the analysis from the plug-in Karamba3D has been matched to distribute the bricks with 3 different densities. The matching procedure is based on the average utilization of each element on the catenary vault and the displacement results. The values have been remaped in order to distribute the corresponding densities.

### 18. Brick Placement:



The result of this distribution and data matching is shown in the image on the left. The bricks which are in direct contact with supports has been matched with the densest bricks while the ones on the sides have been matched with the 2nd densest and the ones on the top part with the least dense bricks.

Figure 77: Steps 17 to 18 of the Karamba3D analysis and density matching (Author's image)

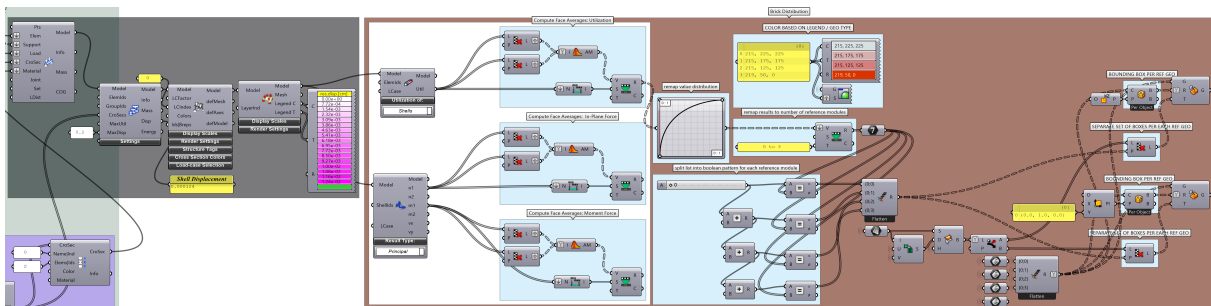


Figure 78: Related part of the Grasshopper script to match the densities and the Karamba3D analysis results (Author's image)

## 4.2.4 Structural analysis by ANSYS

During the structural analysis by ANSYS, different scenarios have been tested in order to have a clear understanding of how different material properties of mycelium-based materials can affect the behavior of the structure. Therefore, analyses have been applied to five different scenarios;

- Distributed bricks according to their densities
- Bricks based on the material properties data of *MycoFoam* obtained from *Ecovative Design*
- Bricks based on the material properties data obtained from Travaglini *et al.* (2013)
- Bricks based on the material properties data obtained from Yang *et al.* (2017)
- Catenary vault with regular rectangular shaped bricks based on the material properties data obtained from Yang *et al.* (2017)

which have been described in the following sections.

#### 4.2.4.1 Catenary vault with the hyperbolic paraboloid bricks with different densities

Once the distribution of bricks with different densities are complete, the 3D model from *Grasshopper* is “baked” to *Rhinoceros 5* software in order to create the data for finite element analysis. Following that, the data of the 3D model is imported into *ANSYS Workbench* through *SpaceClaim* modeling software from *ANSYS*.

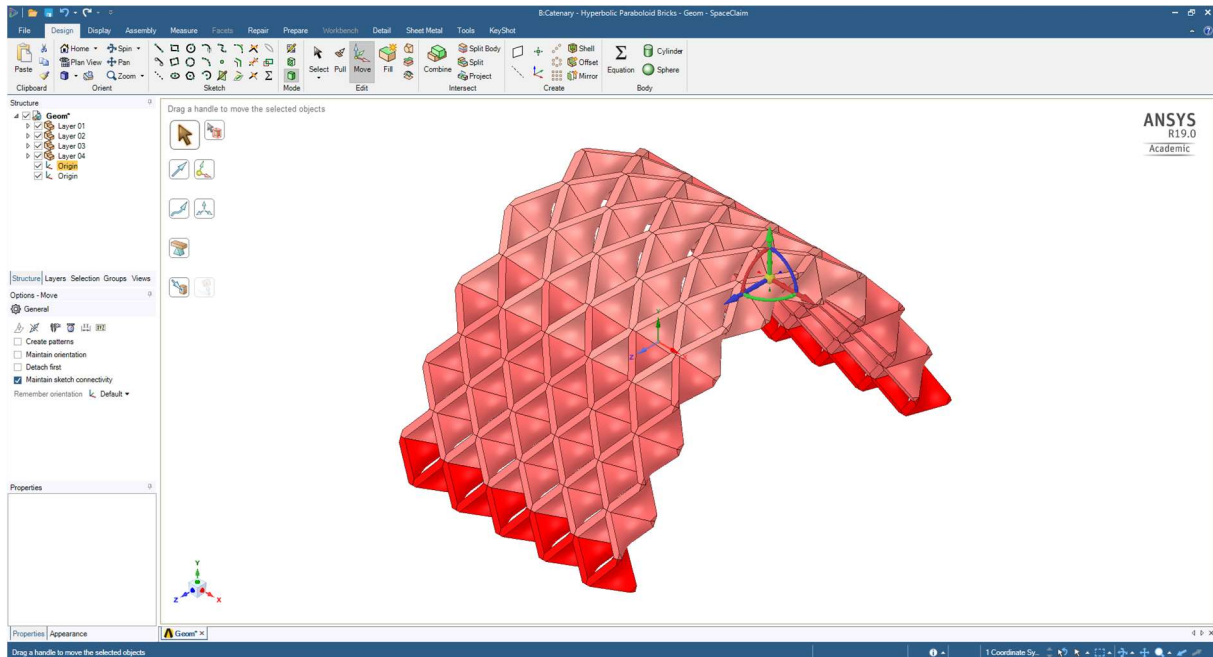


Figure 79: The interface of *SpaceClaim* where the *Rhinoceros 5* model has been imported and grouped according to the densities (Author's image)

While importing the 3D model, different densities have been distributed into different layers. Thus, it has been enabled to apply different material properties to the selected density groups.

After importing the 3D model data, a set of data in order to define the material properties of mycelium-based materials has been manually introduced to *ANSYS Workbench* since it is not in the built-in material library. In order to do that, the component called “*Engineering Data*” has been used. Three different data sets of material properties have been manually introduced, based on the collected data from the literature review. The interface of the engineering data editor enables to create custom materials with many different material properties and behaviors like linear elasticity properties including isotropic, orthotropic, anisotropic elasticity etc. strength values including tensile and compressive strength, Young's modulus, shear modulus and Poisson's ratio etc. Later, these different material properties are matched with the corresponding elements on the catenary vault structure and assigned as the material of the bricks. The image below shows the interface of the engineering data editor from *ANSYS Workbench*.

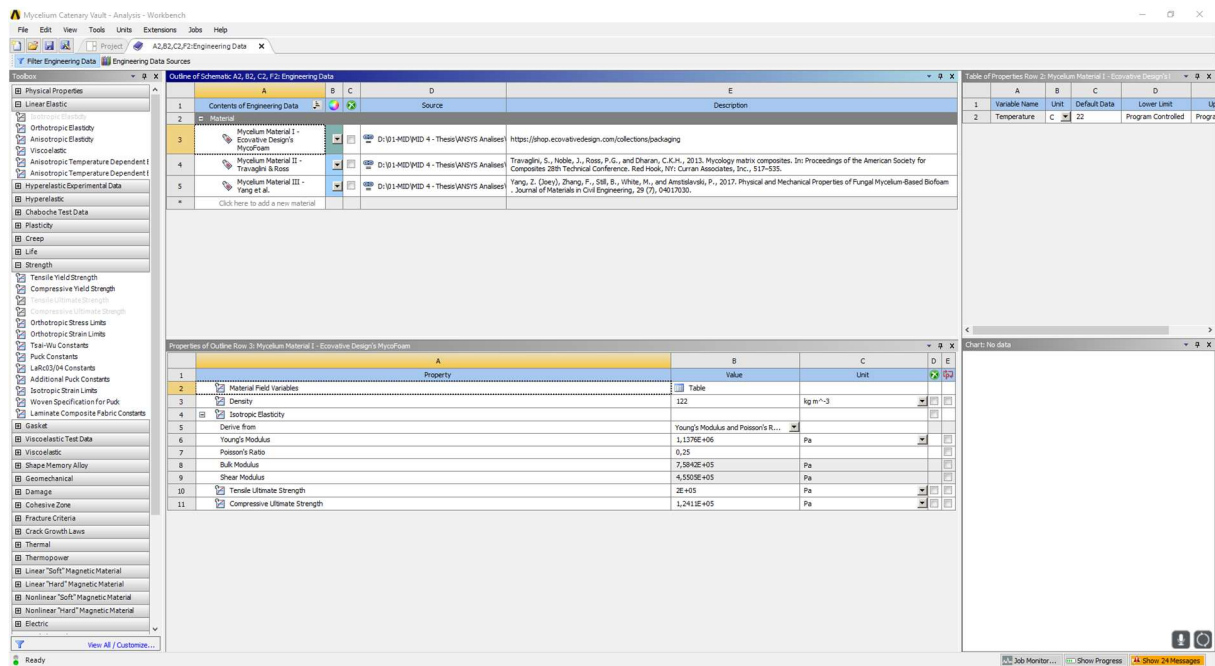


Figure 80: Interface of the “Engineering Data” component of ANSYS Workbench to define material properties (Author's image)

- Data of MycoFoam by Ecovative Design, LLC:

The first data set of material properties for mycelium-based materials is obtained from *Ecovative Design* for their product named *MycoFoam* is shown in the table below.

Property	Value	Unit
Density	122	kg/m <sup>3</sup>
Young's Modulus	1137.63	kPa
Poisson's Ratio	0,25	-
Shear Modulus	455,05	kPa
Tensile Ultimate Strength	215	kPa
Compressive Ultimate Strength	124,11	kPa

Table 16: Material properties of *MycoFoam* by *Ecovative Design, LLC* (Ecovative Design, MycoFoam 2018)

- Data of Travaglini *et al.* (2013):

Second data set of material properties for mycelium-based materials includes the values which have been derived from the research by Travaglini *et al.* (2013) which is published in *Proceedings of the American Society for Composites 28th Technical Conference*. The table below shows the values of the available material properties that have been used for the FEA analysis.

Property	Value	Unit
Density	318	kg/m <sup>3</sup>
Young's Modulus	1300	kPa
Poisson's Ratio	0,25	-
Shear Modulus	520	kPa
Compressive Yield Strength	47,5	kPa
Tensile Ultimate Strength	176	kPa
Compressive Ultimate Strength	490	kPa

Table 17: Material properties of the mycelium-based material by Travaglini *et al.* (2013)

- Data of Yang *et al.* (2017):

Third data set of material properties for mycelium-based materials includes the values which have been derived from the research by Yang *et al.* (2017). Among the test groups, the values for the sample which represented the biggest compressive strength have been used. The table below shows the values of the material properties of the selected material.

Property	Value	Unit
"Density	255	kg/m <sup>3</sup>
Young's Modulus	60000	kPa
Poisson's Ratio	0,25	-
Shear Modulus	24000	kPa
Compressive Ultimate Strength	570	kPa

Table 18: Material properties of the mycelium-based material by (Yang *et al.* 2017)

Once the 3D model and material properties are introduced, the project schematic has been created as it is shown in the image below.

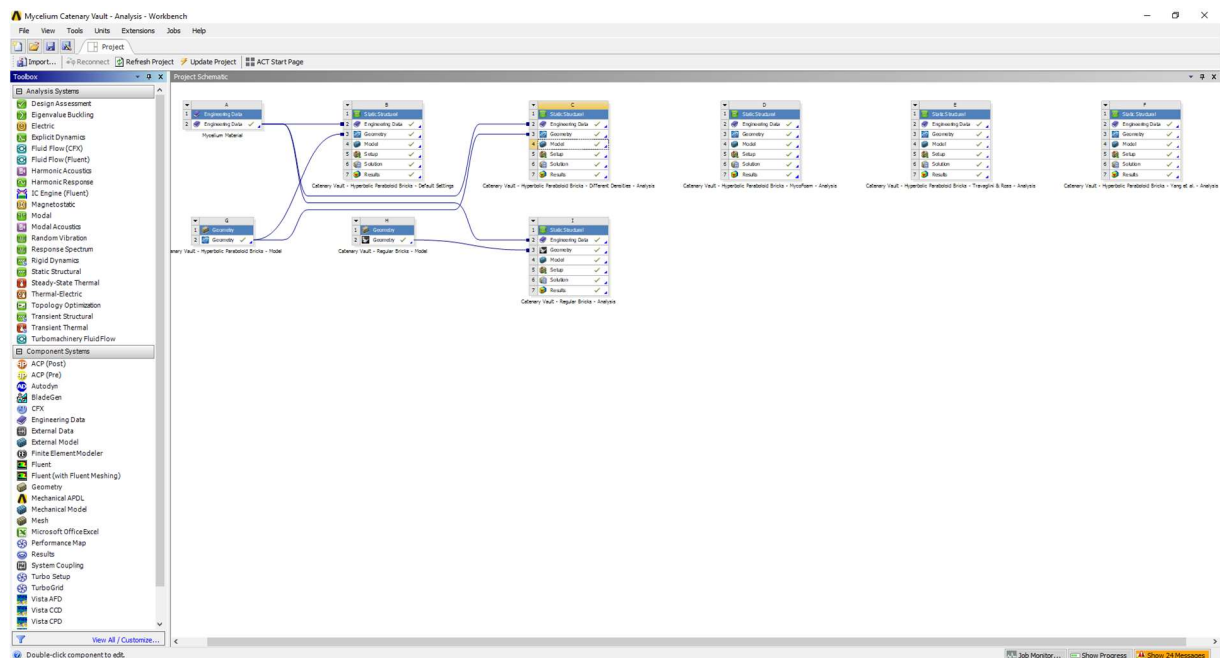


Figure 81: The schematic interface of ANSYS Workbench (Author's image)

ANSYS schematic working environment enables to have the same 3D model data in different sessions where the user can feed with different materials from one material library. Thus, the 3D models of catenary vaults with regular rectangular shaped bricks and the one with hyperbolic paraboloid shaped bricks from Rhinoceros are introduced once. Then, they are multiplied several times in order to feed them with the data of different material properties.

The built-in interface of ANSYS called *Mechanical Enterprise* enables to define all the physical and environmental factors as well as the analysis types and simulations. The image below shows the interface of Mechanical Enterprise.



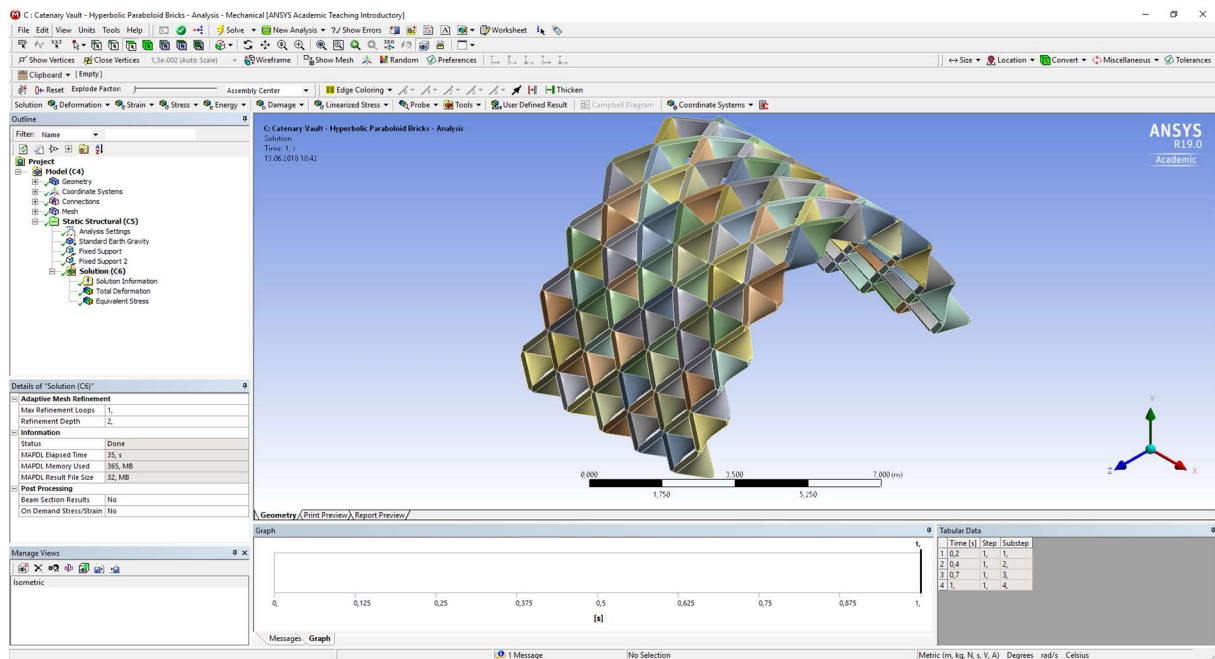


Figure 82: The interface of ANSYS Mechanical (Author's image)

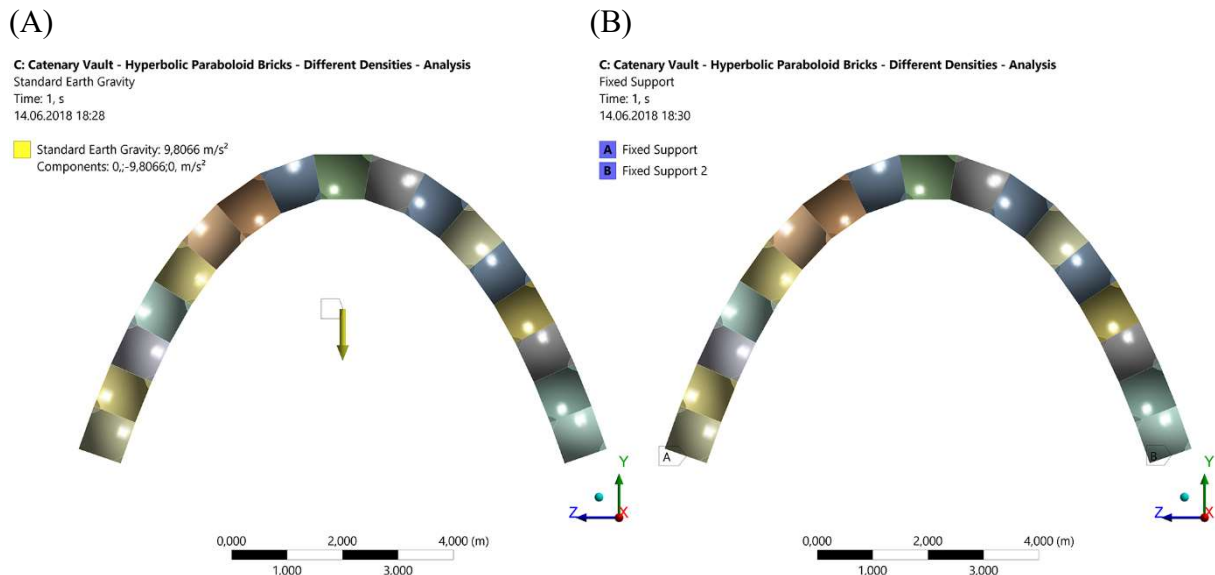


Figure 83: (A) Standard Earth Gravity force applied to the catenary vault, (B) Fixed supports of the catenary vault (Author's image)

Since the data sets of three different mycelium-based material properties from the engineering data interface are introduced, they have been assigned to the corresponding bricks on the catenary vault. Then, standard Earth gravity force has been introduced. The bottom faces of the bricks at the bottom of the catenary vault have been defined as the fixed supports.

Three different simulations have been done;

- *Total deformation*
- *Equivalent (von-Mises) stress*
- *Maximum Principal stress*

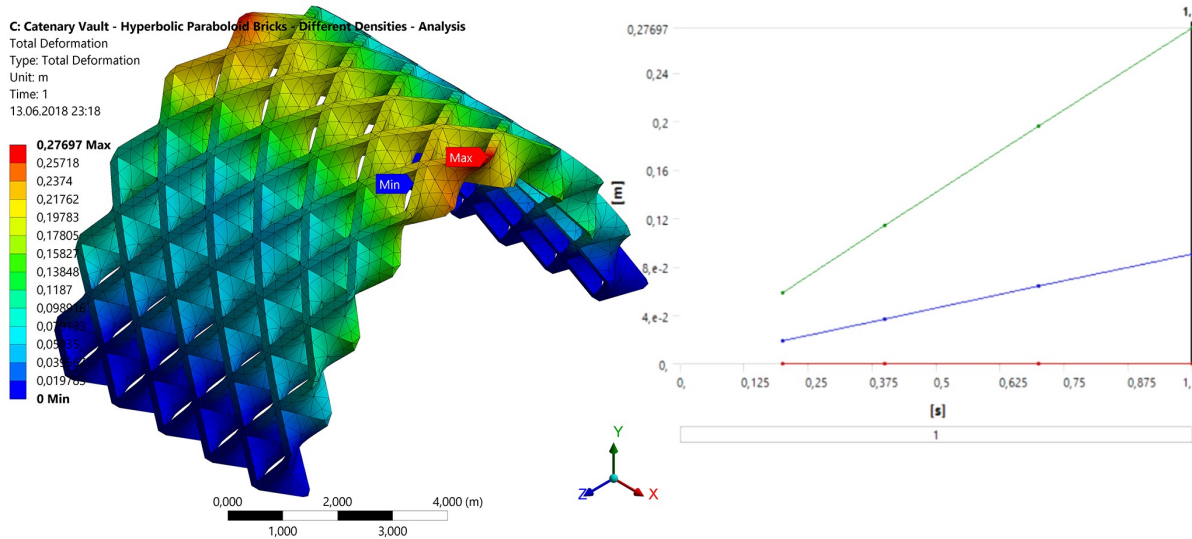


Figure 84: Total displacement analysis of the catenary vault with different density bricks (Author's image)

According to the analysis result, the total deformation of the catenary vault constituted with the bricks of different densities is 0.27697 meters which is 276.97 millimeters.

Time (s)	Minimum (m)	Maximum (m)	Average (m)
0,2	0	0,05819	0,018919
0,4		0,11398	0,037178
0,7		0,19582	0,064059
1		0,27697	0,090723

Table 19: Results of the total displacement analysis of the catenary vault with different density bricks

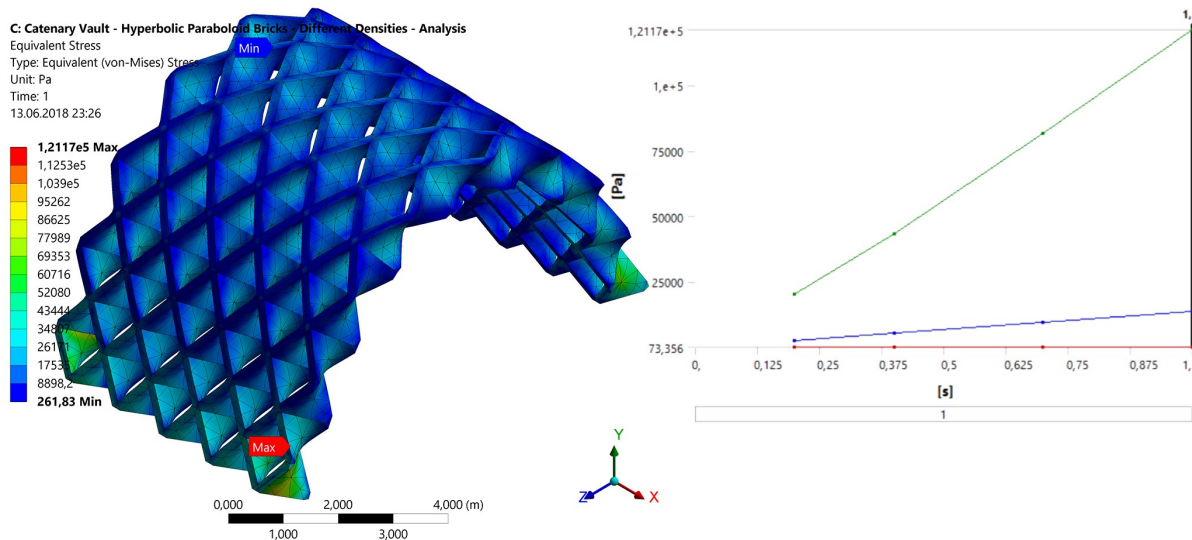


Figure 85: Equivalent (von-Mises) stress analysis of the catenary vault with different density bricks (Author's image)

According to the analysis result, the maximum equivalent (von-Mises) stress is 121170 Pa. The table below shows the values for different time periods in 1 second.

Time (s)	Minimum (Pa)	Maximum (Pa)	Average (Pa)
0,2	73,356	0,05819	2704,2
0,4	131,11	4320	5413,9
0,7	198,23	81551	9481,8
1	261,83	121170	13554

Table 20: Results of the Equivalent (von-Mises) stress analysis of the catenary vault with different density bricks

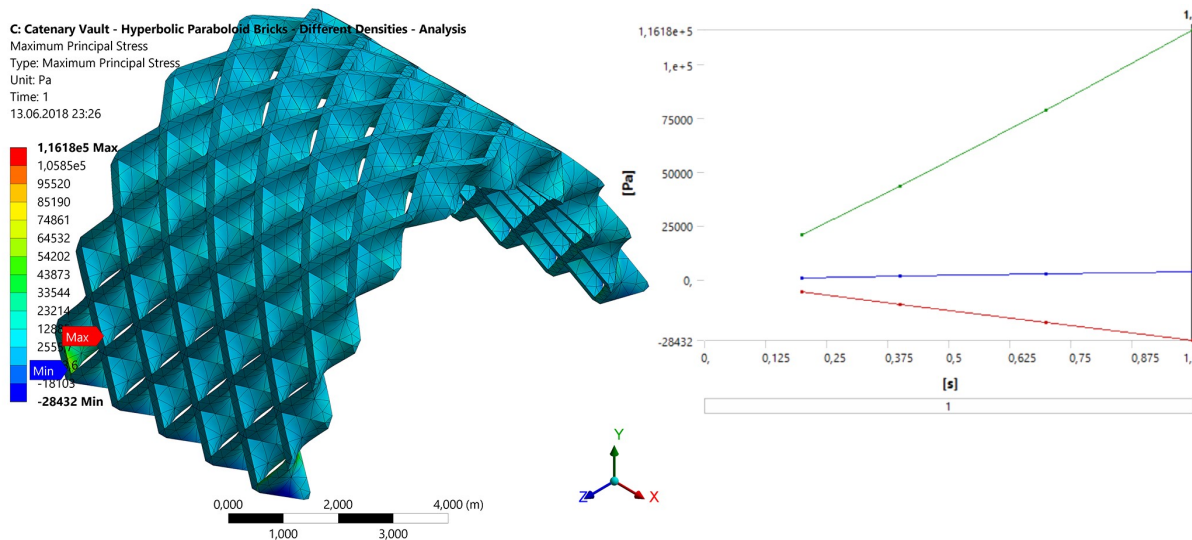


Figure 86: Maximum principal stress analysis of the catenary vault with different density bricks (Author's image)

According to the analysis result, the maximum principal stress is 116180 Pa. The table below shows the values for different time periods in 1 second.

Time (s)	Minimum (Pa)	Maximum (Pa)	Average (Pa)
0,2	-5836,3	20688	670,42
0,4	-11659	43138	1336,1
0,7	-20157	78939	2328
1	-28432	116180	3318

Table 21: Results of the maximum principal stress analysis of the catenary vault with different density bricks

The image below shows the difference between the original shape and deformed version of the catenary vault which have been overlapped onto each other.

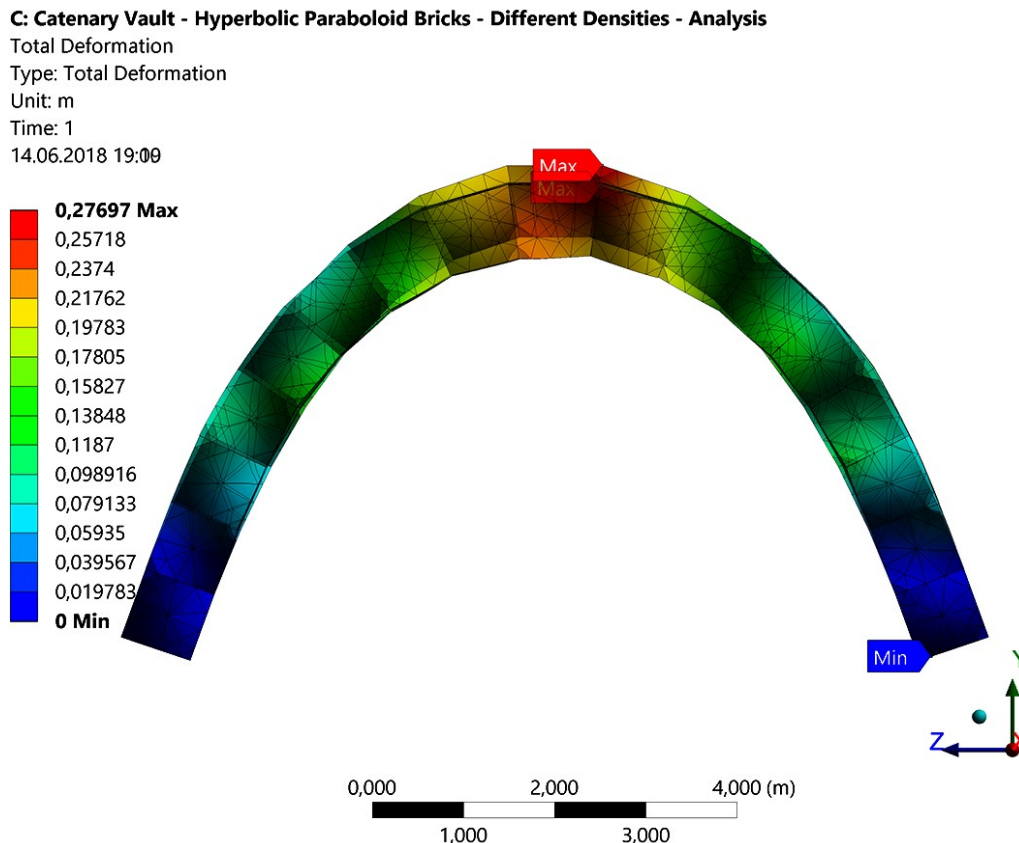


Figure 87: Comparison of the deformed and undeformed catenary vault with different density bricks (Author's image)

#### 4.2.4.2 Catenary vault with the hyperbolic paraboloid bricks based on the data of *MycoFoam*

In this scenario, all the material data of all the bricks of the catenary vault have been assigned from the data of *MycoFoam* by *Ecovative Design*.

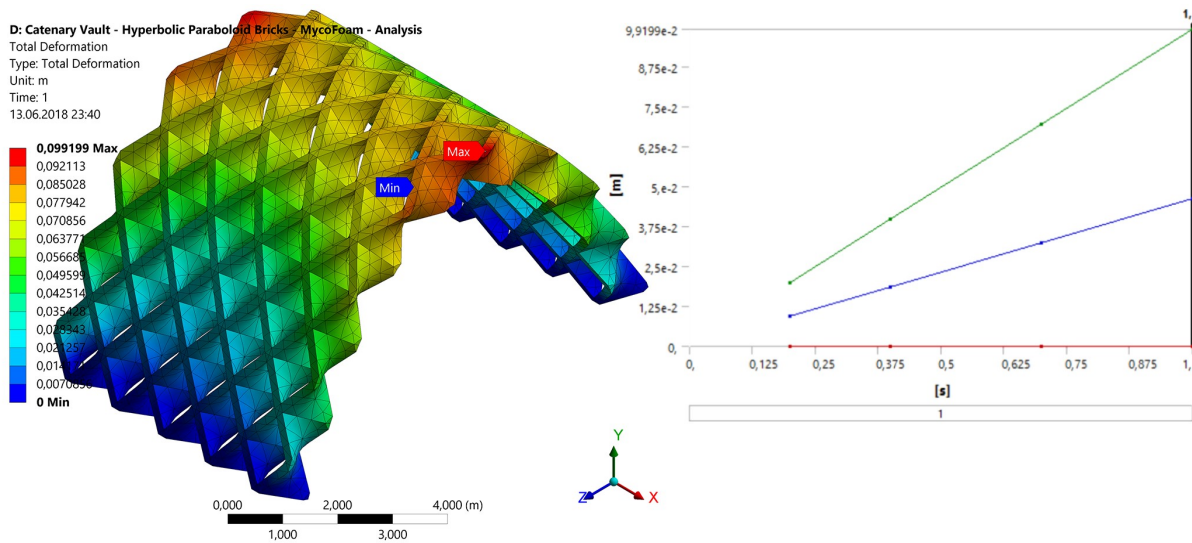


Figure 88: Total displacement analysis of the catenary vault with *MycoFoam* mycelium material (Author's image)

Time (s)	Minimum (m)	Maximum (m)	Average (m)
0,2	0	0,019943	0,0093587
0,4		0,039775	0,018632
0,7		0,069485	0,032449
1		0,099199	0,046217

Table 22: Results of the total displacement analysis of the catenary vault with *MycoFoam* mycelium material

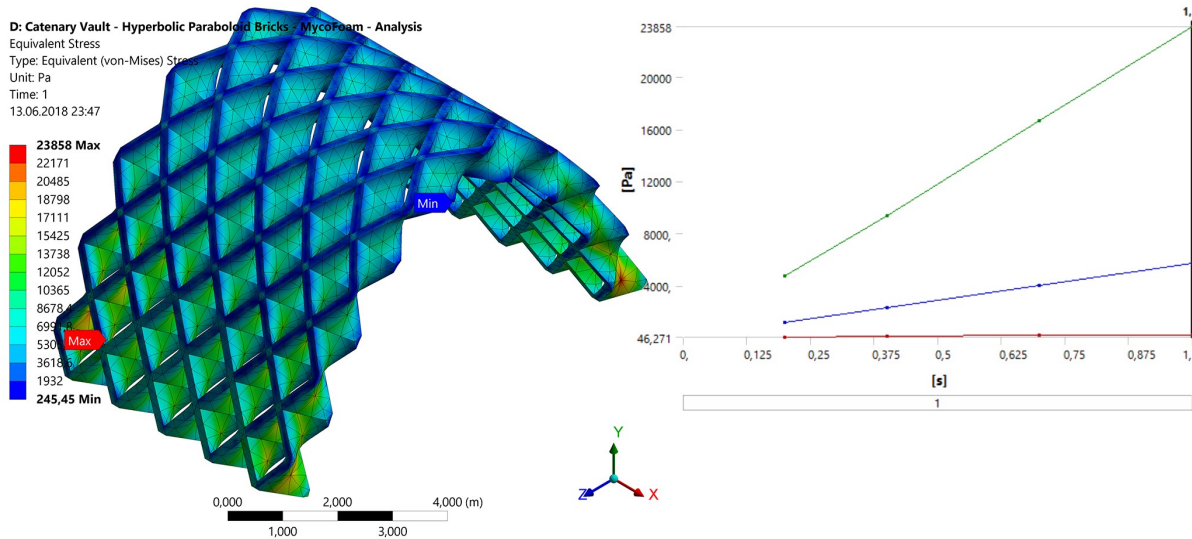


Figure 89: Equivalent (von-Mises) stress analysis of the catenary vault with *MycoFoam* mycelium material (Author's image)

Time (s)	Minimum (Pa)	Maximum (Pa)	Average (Pa)
0,2	46,271	4705	1140,5
0,4	94,329	9399,2	2285
0,7	169,02	16676	4003,6
1	245,45	23858	5722,6

Table 23: Results of the Equivalent (von-Mises) stress analysis of the catenary vault with *MycoFoam* mycelium material



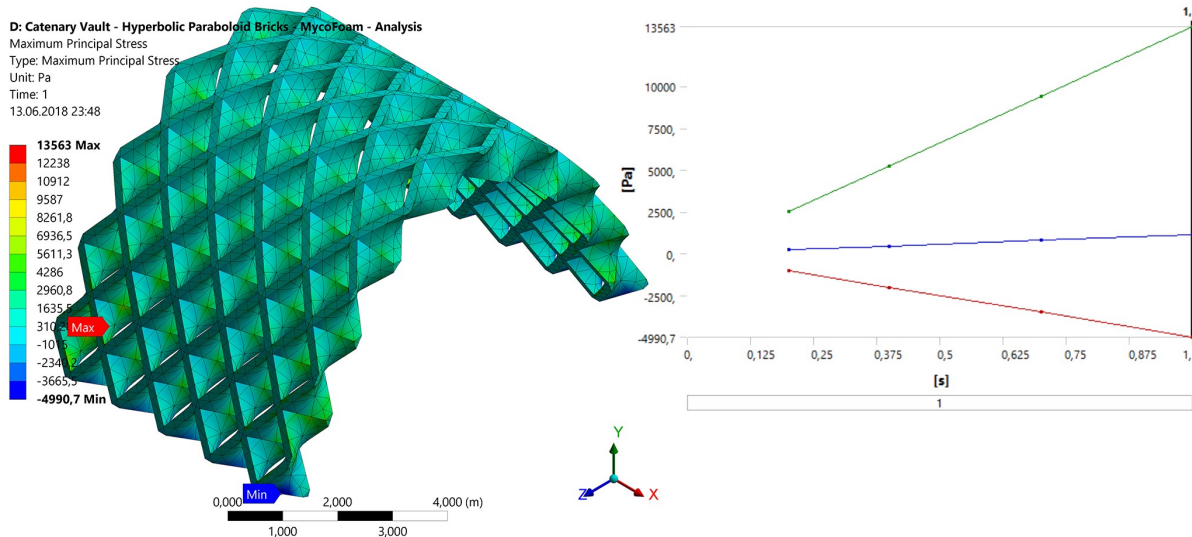


Figure 90: Maximum principal stress analysis of the catenary vault with MycoFoam mycelium material (Author's image)

Time (s)	Minimum (Pa)	Maximum (Pa)	Average (Pa)
0,2	-5836,3	20688	670,42
0,4	-11659	43138	1336,1
0,7	-20157	78939	2328
1	-28432	116180	3318

Table 24: Results of the maximum principal stress analysis of the catenary vault with MycoFoam mycelium material

#### D: Catenary Vault - Hyperbolic Paraboloid Bricks - MycoFoam - Analysis

Total Deformation

Type: Total Deformation

Unit: m

Time: 1

14.06.2018 20:30

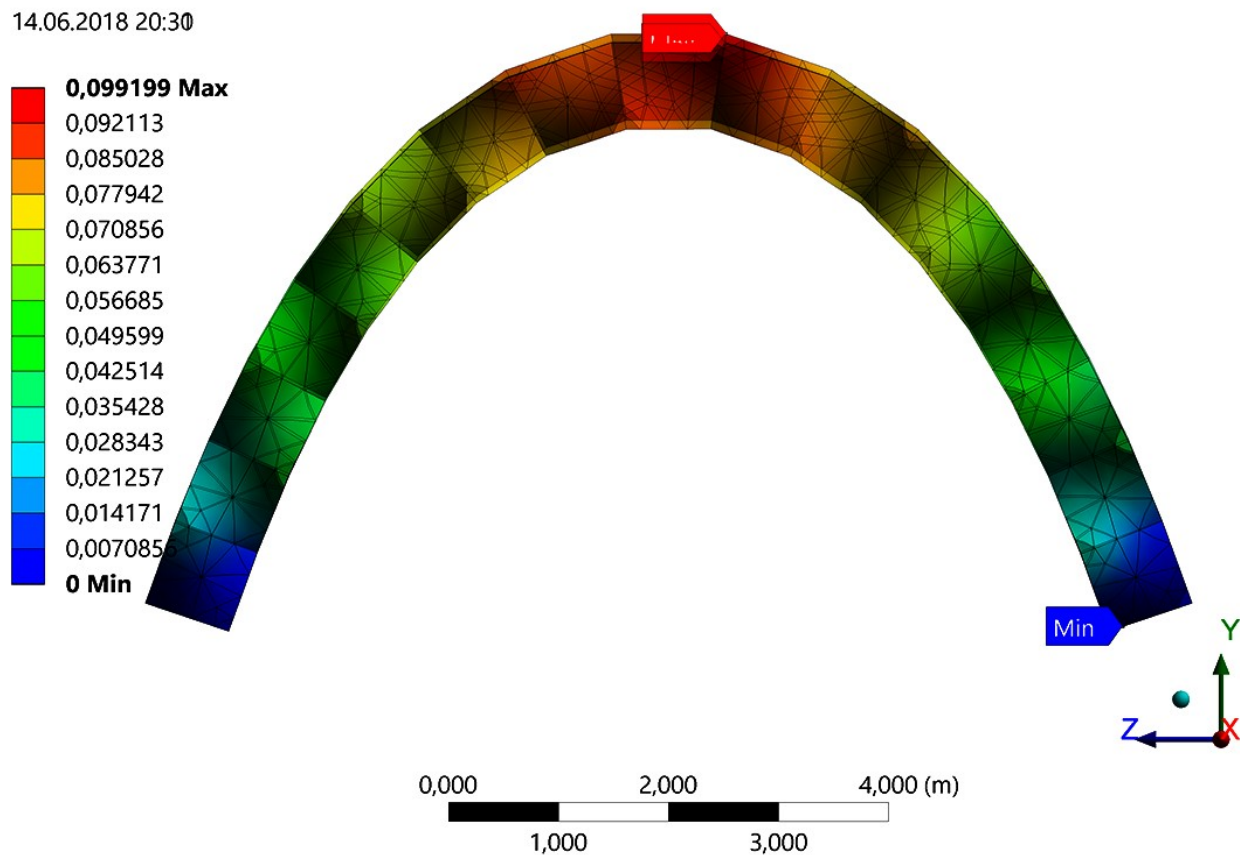


Figure 91: Comparison of the deformed and undeformed catenary vault with MycoFoam mycelium material (Author's image)

#### 4.2.4.3 Catenary vault with the hyperbolic paraboloid bricks based on the data of Travaglini *et al.* (2013)

In this scenario, all the material data of all the bricks of the catenary vault have been assigned from the data of mycelium composite materials which have been studied by Travaglini *et al.* (2013).

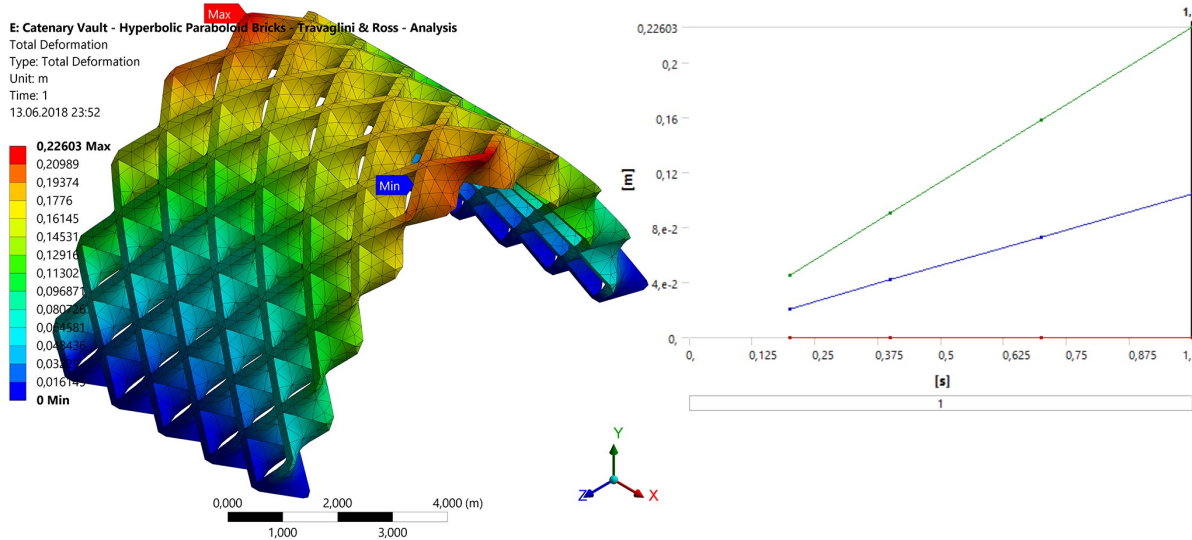


Figure 92: Total displacement analysis of the catenary vault with the data of Travaglini *et al.* (2013) (Author's image)

Time (s)	Minimum (m)	Maximum (m)	Average (m)
0,2	0	0,045239	0,021114
0,4		0,090398	0,042078
0,7		0,1582	0,073393
1		0,22603	0,10464

Table 25: Results of the total displacement analysis of the catenary vault with the data of Travaglini *et al.* (2013)

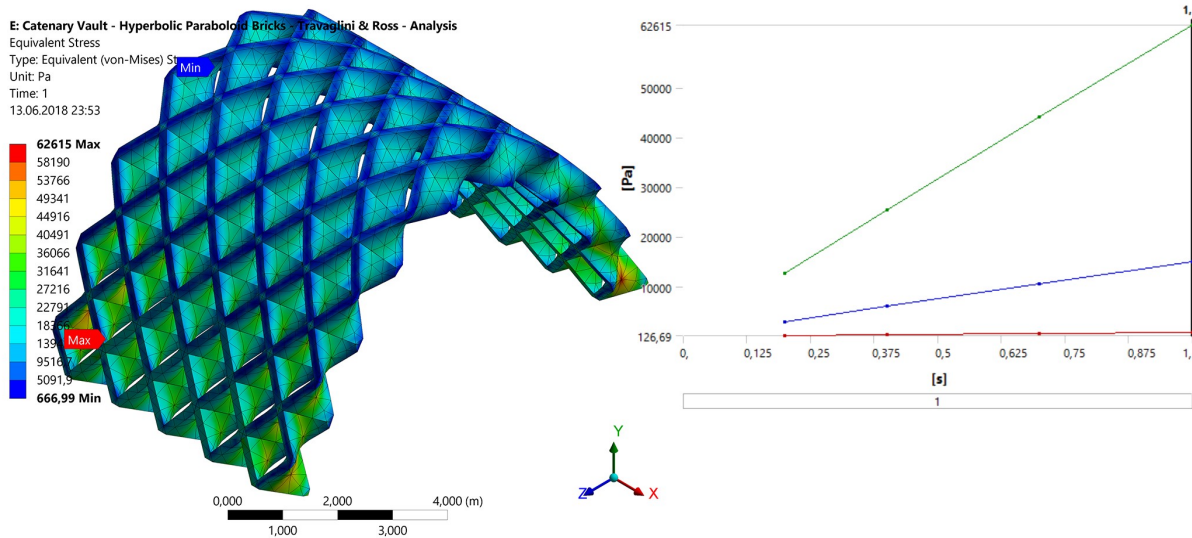


Figure 93: Equivalent (von-Mises) stress analysis of the catenary vault with the data of Travaglini *et al.* (2013) (Author's image)

Time (s)	Minimum (Pa)	Maximum (Pa)	Average (Pa)
0,2	126,69	12620	2985,1
0,4	285,5	25334	5974,6
0,7	461,76	44042	10460
1	666,99	62615	14946

Table 26: Results of the Equivalent (von-Mises) stress analysis of the catenary vault with the data of Travaglini *et al.* (2013)

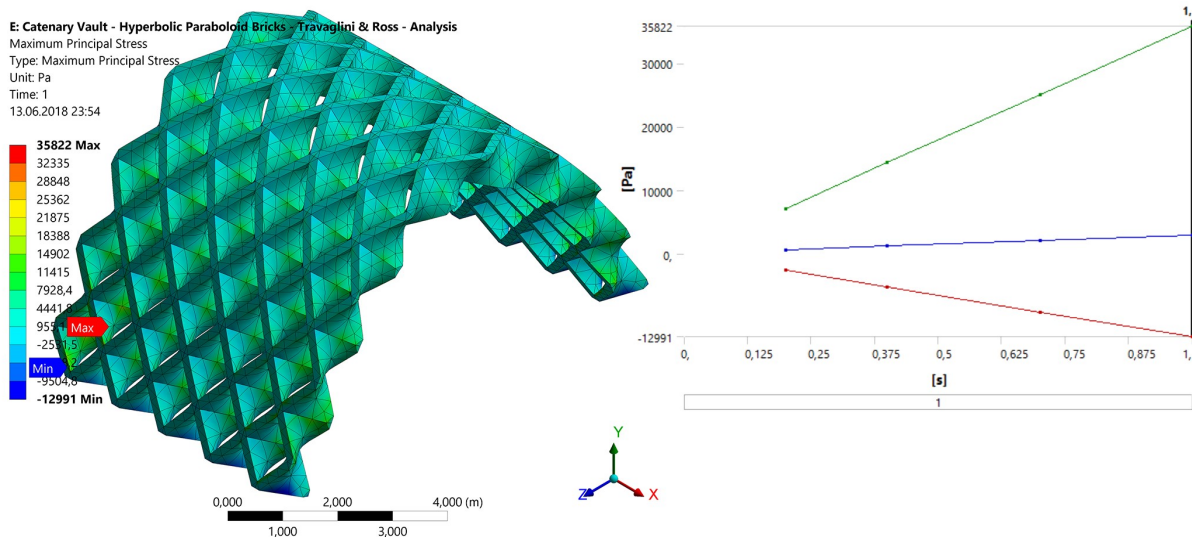


Figure 94: Results of the maximum principal stress analysis of the catenary vault with the data of Travaglini et al. (2013) (Author's image)

Time (s)	Minimum (Pa)	Maximum (Pa)	Average (Pa)
0,2	-2600,8	7076,	607,08
0,4	-5198,3	14344	1210,3
0,7	-9094,1	25092	2110,5
1	-12991	35822	3008,8

Table 27: Results of the maximum principal stress analysis of the catenary vault with the data of Travaglini et al. (2013)

### E: Catenary Vault - Hyperbolic Paraboloid Bricks - Travaglini & Ross - Analysis

Total Deformation

Type: Total Deformation

Unit: m

Time: 1

14.06.2018 21:13

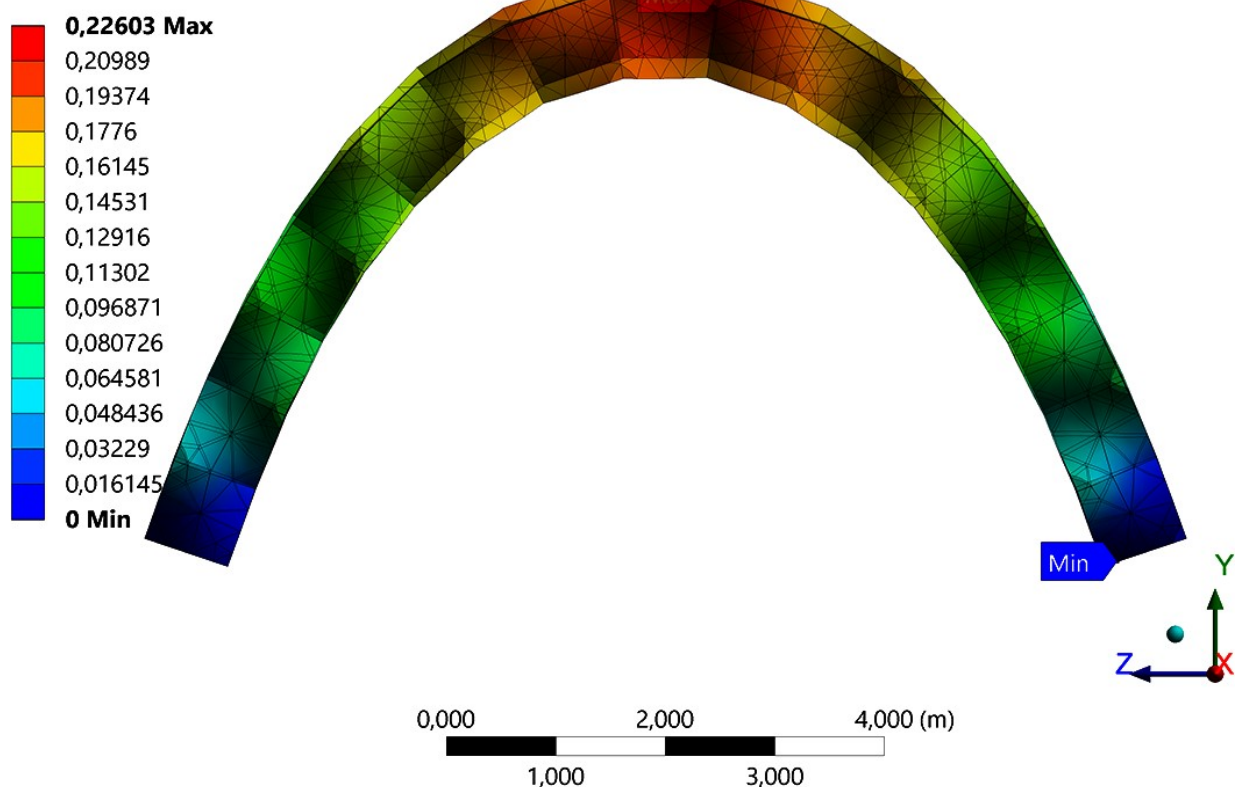


Figure 95: Comparison of the deformed and undeformed catenary vault with the data of Travaglini et al. (2013) (Author's image)



#### 4.2.4.4 Catenary vault with the hyperbolic paraboloid bricks based on the data of Yang *et al.* (2017)

In this scenario, all the material data of all the bricks of the catenary vault have been assigned from the data of mycelium composite materials which have been studied by Yang *et al.* (2017).

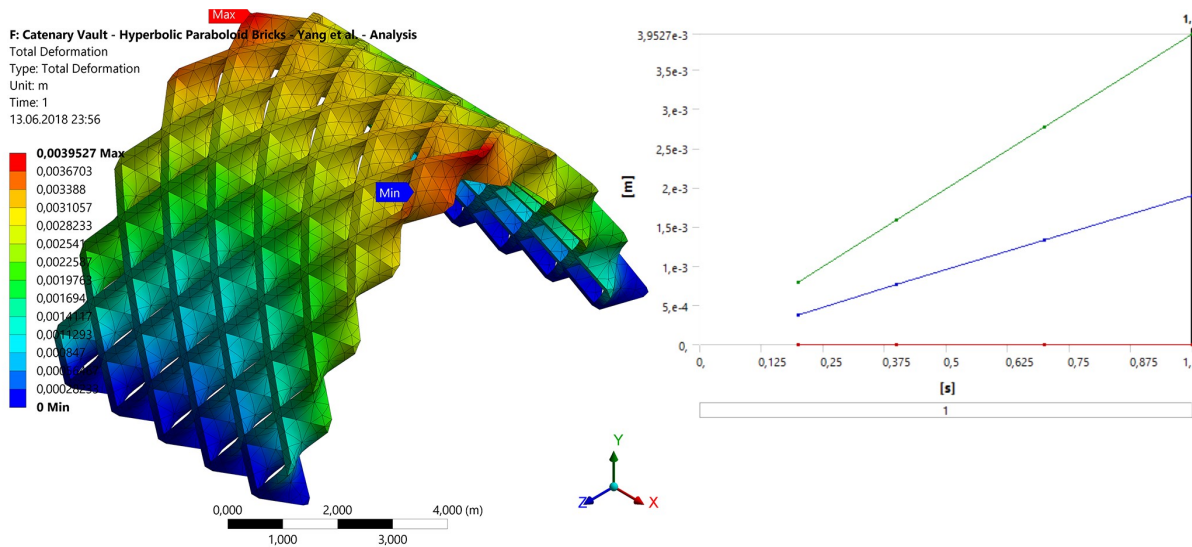


Figure 96: Total displacement analysis of the catenary vault with the data of Yang *et al.* (2017) (Author's image)

Time (s)	Minimum (m)	Maximum (m)	Average (m)
0,2	0	0,00079014	0,00037995
0,4		0,0015805	0,0007599
0,7		0,0027661	0,0013293
1		0,0039527	0,001872

Table 28: Results of the total displacement analysis of the catenary vault with the data of Yang *et al.* (2017)

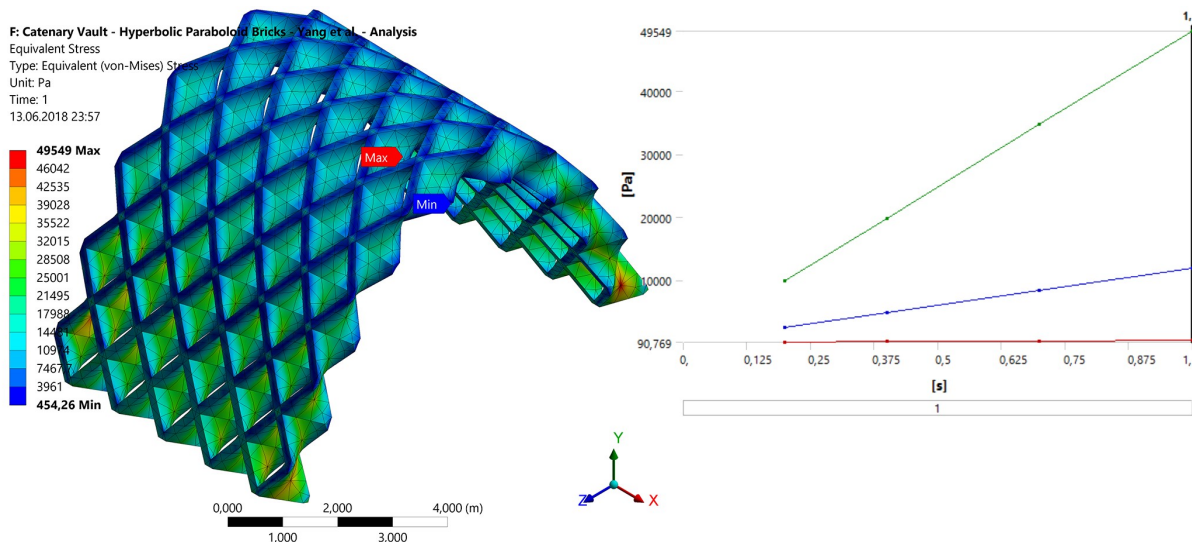


Figure 97: Equivalent (von-Mises) stress analysis of the catenary vault with the data of Yang *et al.* (2017) (Author's image)

Time (s)	Minimum (Pa)	Maximum (Pa)	Average (Pa)
0,2	90,769	9920,8	2363,9
0,4	181,56	19842	4727,9
0,7	317,81	34709	8273,6
1	454,26	49549	11821

Table 29: Results of the Equivalent (von-Mises) stress analysis of the catenary vault with the data of Yang *et al.* (2017)

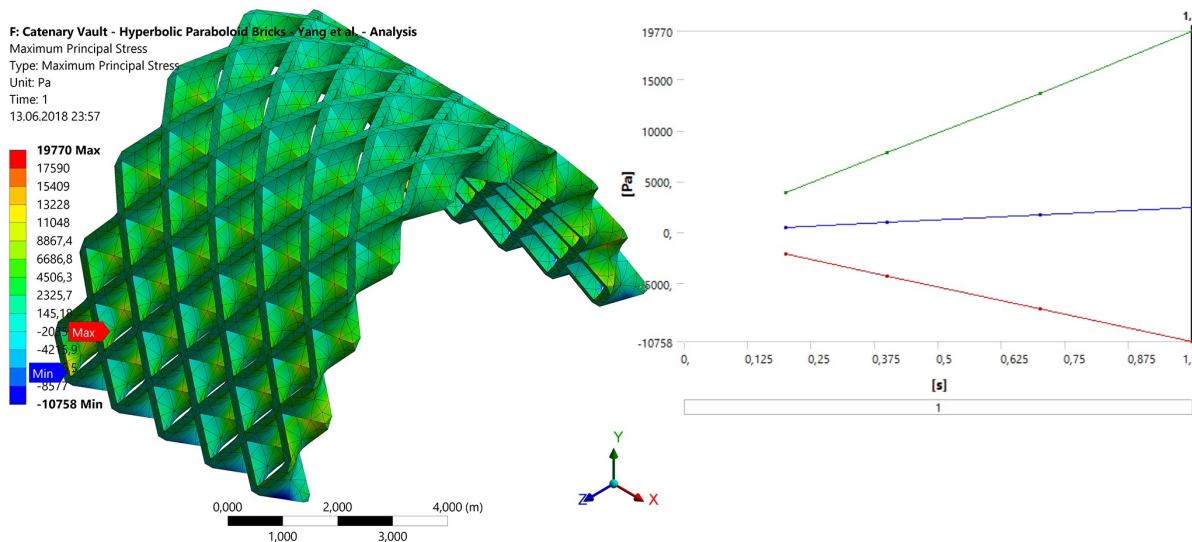


Figure 98: Results of the maximum principal stress analysis of the catenary vault with the data of Yang et al. (2017) (Author's image)

Time (s)	Minimum (Pa)	Maximum (Pa)	Average (Pa)
0,2	-2158,5	3900	493,09
0,4	-4317,1	7800,8	986,16
0,7	-7546	13597	1724,7
1	-10758	19770	2461,5

Table 30: Results of the maximum principal stress analysis of the catenary vault with the data of Yang et al. (2017)

#### F: Catenary Vault - Hyperbolic Paraboloid Bricks - Yang et al. - Analysis

Total Deformation

Type: Total Deformation

Unit: m

Time: 1

14.06.2018 22:09

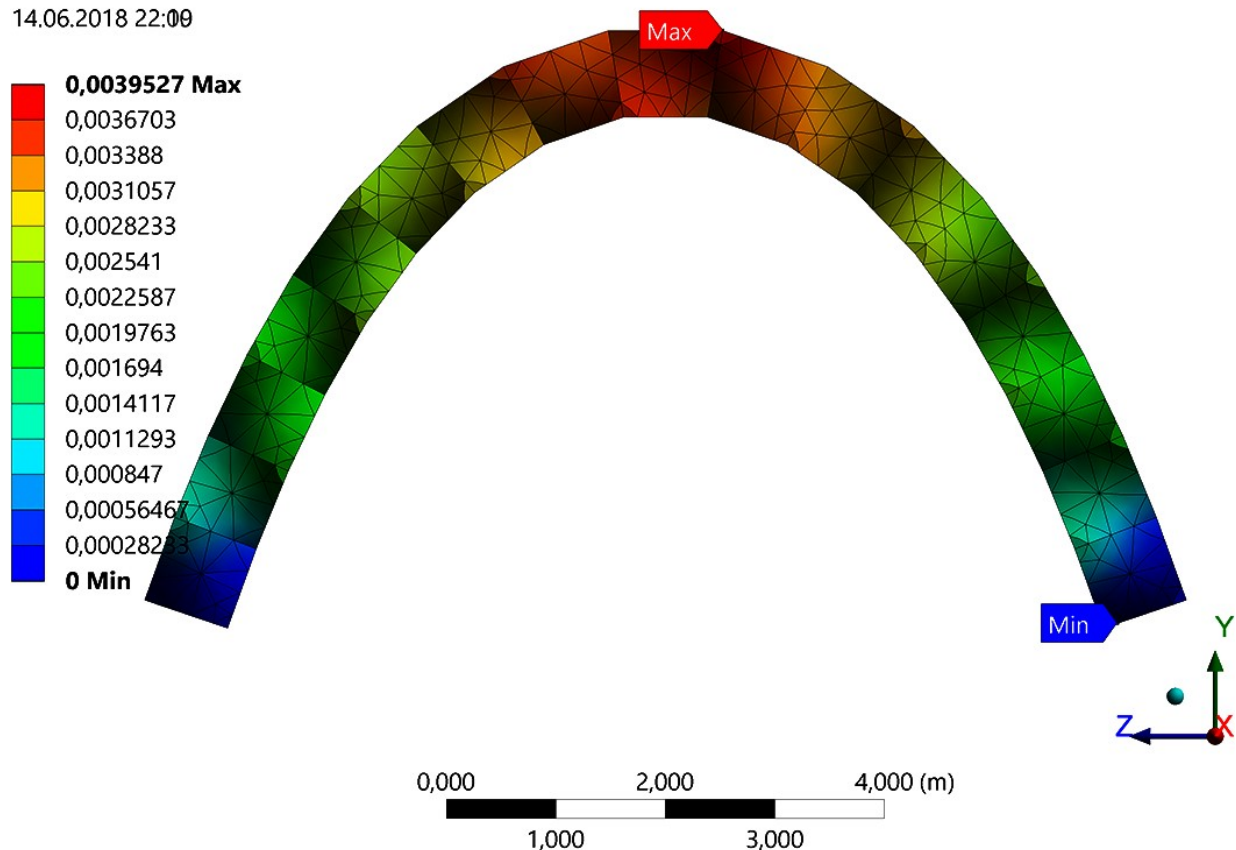


Figure 99: Comparison of the deformed and undeformed catenary vault with the data of Yang et al. (2017) (Author's image)

#### 4.2.4.5 Catenary vault with the rectangular shaped bricks based on the data of Yang *et al.* (2017)

In this scenario, all the material data of all the bricks of the catenary vault have been assigned from the data of mycelium composite materials which have been studied by Yang *et al.* (2017) and the bricks are regular rectangular shaped bricks.

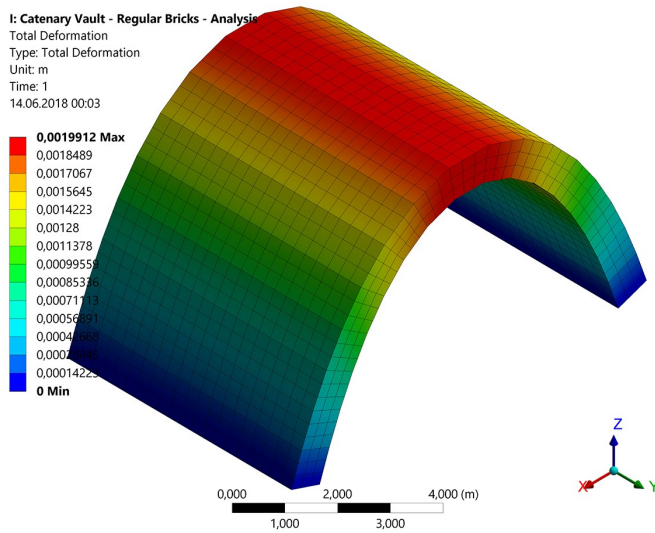


Figure 100: Total displacement analysis of the catenary vault with the regular rectangular shaped bricks based on the data of Yang *et al.* (2017) (Author's image)

Time (s)	Minimum (m)	Maximum (m)	Average (m)
1	0	0,0019912	0,001055

Table 31: Results of the total displacement analysis of the catenary vault with the regular rectangular shaped bricks based on the data of Yang *et al.* (2017)

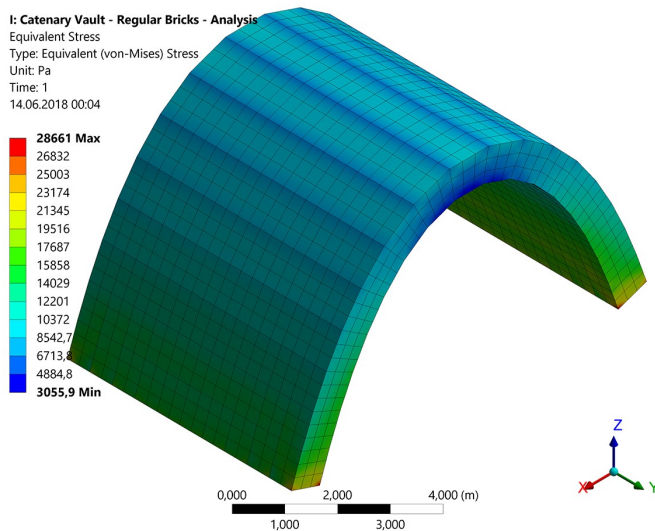


Figure 101: Equivalent (von-Mises) stress analysis of the catenary vault with the regular rectangular shaped bricks based on the data of Yang *et al.* (2017) (Author's image)

Time (s)	Minimum (Pa)	Maximum (Pa)	Average (Pa)
1	3055,9	28661	10092

Table 32: Results of the Equivalent (von-Mises) stress analysis of the catenary vault with the regular rectangular shaped bricks based on the data of Yang *et al.* (2017)

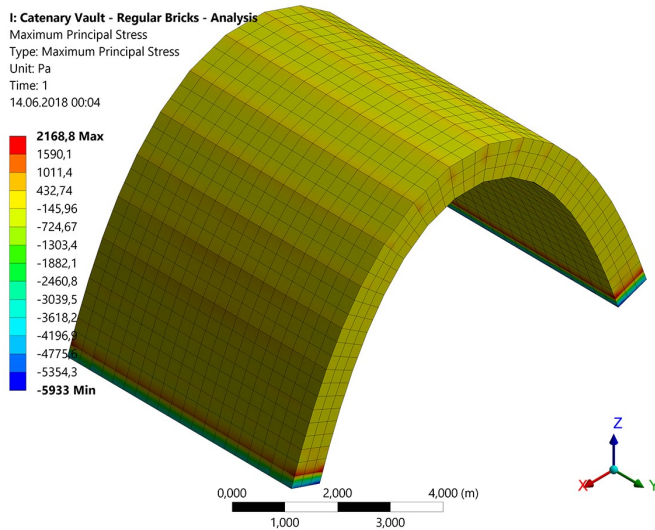


Figure 102: Results of the maximum principal stress analysis of the catenary vault with the regular rectangular shaped bricks based on the data of Yang et al. (2017) (Author's image)

Time (s)	Minimum (Pa)	Maximum (Pa)	Average (Pa)
1	-5933	2166,8	-48,448

Table 33: Results of the maximum principal analysis of the catenary vault with the regular rectangular shaped bricks based on the data of Yang et al. (2017) (Author's image)

In this scenario, the total deformation of the catenary vault is extremely small which is 0.0019912 meters and that is equal to 1.991200 millimeters. Thus, through the *ANSYS Mechanical*, it has been simulated with 310 times more deformation of the vault in order to have a better understanding of the stability and rigidity of the structure. Comparison between the simulations of deformations at different scales has been represented below.

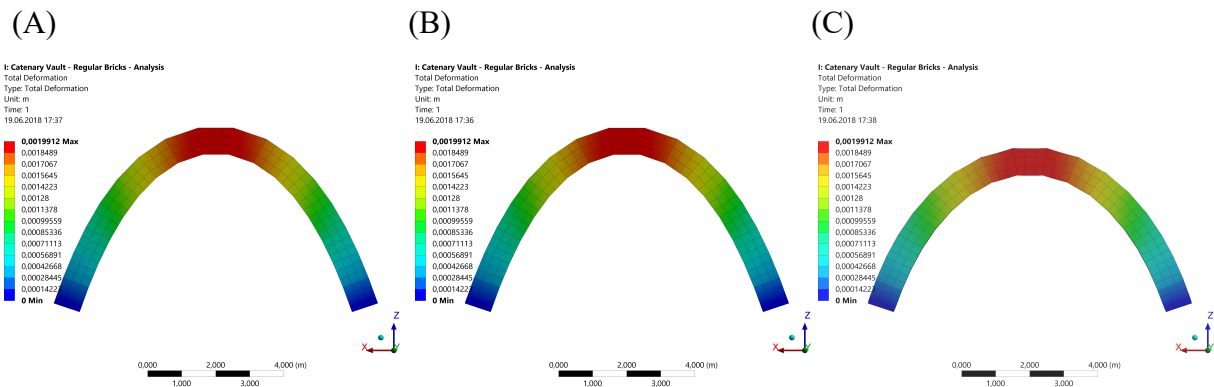


Figure 103: Comparison of the deformed and undeformed catenary vault with the regular rectangular shaped bricks based on the data of Yang et al. (2017) (Author's image) (A: Undeformed form, B: Deformed form at the true scale, C: 310 times more deformed form)

### 5. Conclusion

In this master thesis study, a wide range of experiments have been experienced with mycelium and mycelium-based materials. It has been seen that there are many different possible applications of mycelium and mycelium-based materials in various fields as well as the wide range of mechanical and physical properties of mycelium-based materials.

In order to produce mycelium-based biocomposite materials, the following subjects and observations have been found crucial to take into account;

- Sterilization;
  - A sterile working environment is the first requirement to achieve success in mycelium growing. Best condition is to work with a laminar flow hood or with a glovebox during the mycelium generation, cloning mycelium and inoculating the substrates.
  - Keeping the tools which involve in all the stages of the process of mycelium generation as aseptic as possible is crucially important since tools can increase the risk of contamination between the mediums.
  - Sterilization of the substrate mediums prevents the contamination that can be caused by the bacteria or other living organisms that the substrate medium already may contain. For the substrates like agar extract, sawdust and woodchips sterilization should be under 15 Psi (121 °C) while straw substrates should be pasteurized.
- Specie of the mushroom;
  - Different species have different inoculation durations under different environmental conditions. During the experiments, it has been found that the species *Ganoderma lucidum* is really suitable to work with in order to produce mycelium-based composite materials due to its growth speed, low maintenance environmental condition requirements, and its mechanical properties.
  - Due to nutritional contents and molecular structures of each substrate type, and different capacities of different mushroom mycelium in order to break natural fiber into their molecules, different species of mushroom mycelium may perform variously with different substrate types.

- Substrate type;
  - Depending on the mushroom mycelium species, substrate types vary in order to create mycelium-based biocomposite materials. Sawdust and woodchips mixture creates the best substrate for the species *Ganoderma lucidum* while straw substrate works better for *Pleurotus eryngii*.
  - Different substrate types result with different mechanical and physical properties. Samples with sawdust and woodchips mixture presented a stiffer and durable result. On the other hand, samples with straw substrate presented a softer and deformable result.
- Gas exchange and moisture content;
  - During the mycelium growth, O<sub>2</sub> is absorbed and CO<sub>2</sub> is released. If the substrate does not have a proper gas exchange, the growth of the mycelium slows down exponentially till it stops. It has been observed that the mycelium grows faster on the exterior surfaces of the substrate in molds due to better gas exchange. Once the substrate is taken out from the mold and exposed to air in a sterile environment, the growth on the surfaces rapidly increases.
  - The moisture content is also critically important due to its effect on the growth speed as well as the mechanical and physical properties of the final mycelium-based biocomposite material. If the moisture content is too low or high, mycelium cannot grow properly.
- Drying conditions;
  - Drying conditions of the mycelium-based biocomposite materials affect the mechanical and physical properties of the final result. While artificial drying method using an oven creates more rigid and durable samples, natural drying methods create relatively flexible results.
  - Temperature and duration of drying in the artificial drying method also create a variety of mechanical behaviors and physical properties.
- Mold systems;
  - In order to have desired and unique shaped mycelium-based biocomposite materials, inoculated biomass with mycelium spawn should be placed into molds.
  - Molds should be designed in a way that it allows a proper gas exchange while it prevents contamination. Also, it should be easy to remove the colonized biomass from the mold without any damage. Thus, it has been found useful to have a mold system in an asunder from which pieces can be taken away when it's needed to remove the mycelium-based material.



The finite element analysis by using ANSYS software, for the catenary vault design as the case study, it has been simulated to show how the wide ranged material properties of the mycelium-based biocomposite materials affect the structural and static behavior. According to those simulations, among the database of the mechanical properties of the selected mycelium-based biocomposite from the literature, the most suitable mycelium-based biocomposite is the one, the mechanical and physical properties of which has been specified by Yang *et al.* (2017) with many laboratory tests.

The catenary vault designed with the hyperbolic paraboloid bricks by using the material data of Yang *et al.* (2017) represented a *maximum total deformation* of 3.9527 millimeters and an *average total deformation* of 1.872 millimeters. In order to understand the effect of the hyperbolic paraboloid brick shape on the deformation, a simulation has been applied to the catenary vault designed with the regular rectangular shaped bricks based on the material data of Yang *et al.* (2017). The catenary vault designed with the regular rectangular shaped bricks represented a *maximum total deformation* of 1.9912 millimeters and an *average total deformation* of 1.055 millimeters. It has been seen that the difference in the *average total deformation* values between the two designs is only 0.817 millimeters which have been found negligible.

Due to their constituents, mycelium-based biocomposite materials have a variable nature of the structure. The final mechanical behavior of the mycelium-based biocomposite materials depends on the variables which have been listed above. Therefore, it has been found hard to precisely predict the behavior of the mycelium-based biocomposites and also the behavior of the designs with them. Thus, it has been proved that using computational tools to design and analyze the structural and static performances of designs with mycelium-based biocomposite materials plays a critical role to prevent undesirable structural failures and to select the proper combination to design the mycelium-based biocomposite material.

It has been proven that it is possible to realize the designed catenary vault with the hyperbolic paraboloid bricks if the right mycelium-based biocomposite is developed and used.

### 6. Prospects

Based on the current experiments and developments on mycelium-based biocomposite materials, increasing interest in sustainability concepts and bio-based materials especially in the construction industry, a combination of computational tools to design and analyze the properties of materials and designs bring a high potential for mycelium-based biocomposite materials to be more commercially available in the market.

Some professional companies like *Ecovative Design* which already manufactures commercial packing and insulation products have had achieved to reduce the growth period of around five days to one week. During my personal experiences and experiments, it has been achieved to reduce the growth period from two months to two weeks by changing the fungi species, substrate types and nutritional supplements. Thus, it has been personally tested and proved that there is a high chance to tune the growth conditions and period by experimenting with different species and substrates in order to find the fastest growing recipe and combination of conditions.

In order to increase the mechanical properties of mycelium-based biocomposite materials, there are countless options and possibilities to test and to develop. For example, a mesh of gauze which is made of cotton can be used as reinforcement to increase the integrity of the substrate among itself as well as the binding behavior of the mycelium filament since, which possibly could increase the tensile strengths as well as the compressive strengths of the final product. Another idea to test is about a woven substrate mat like the wicker baskets which can be made out of straw or flax fibers and etc. and mycelium could grow around the mat and through the holes in the mat. Due to a large number of variables for the constituents of mycelium-based biocomposite materials, it has been found possible to propose and test numberless options and combinations like the examples.

Among many properties and different usage areas of mycelium-based biocomposite materials, acoustic features have a high potential in order to develop acoustic absorber panels. It has been found highly possible to create different acoustic panels for different sound frequencies by simply using different combinations of natural fibers and fungi species including with the geometry. During the thesis research and experiments, an acoustic absorber panel has been designed by using *Grasshopper* parametric design tool in order to represent the potential of the material.

Furthermore, based on the catenary vault design, there is a high potential of the suggested mold system which is an adaptable system by using a template like a mold frame with a flexible divider fabric. However, there are other possible techniques to create the hyperbolic paraboloid shaped bricks. For instance, hyperbolic paraboloid bricks can be cut out from a mass block of mycelium-based biocomposite by using two mutual robotic arms holding a cutting wire or a band saw. Although it might bring the question about the integrity of the mycelium-based biocomposite brick which has been cut out from a mass since the sliced

surfaces of the material would not have a mycelium mass that covers the surface and creates a bound.

A more futuristic approach in order to combine the existing fast prototyping tools and producing mycelium-based biocomposite materials can be proposed as well. 3D printing technologies can be adapted in order to create sawdust and woodchips layers in powder like form and after each layer of substrate, a liquid mycelium culture can be sprayed. In order to keep the shape stable in the desired form, before spraying the liquid mycelium culture a bio resin adhesive grid can be sprayed which enables the substrate to be inoculated with the liquid mycelium culture through the gaps of the grid.

## 7. Attachment/Appendix

In this appendix, an additional exploratory design of an acoustic absorption panel has been represented as well as some additional photos of the created mycelium-based biocomposite materials using different fungi species and various combinations of substrates.

The Grasshopper script below shows the simple parametric design of the acoustic panel.

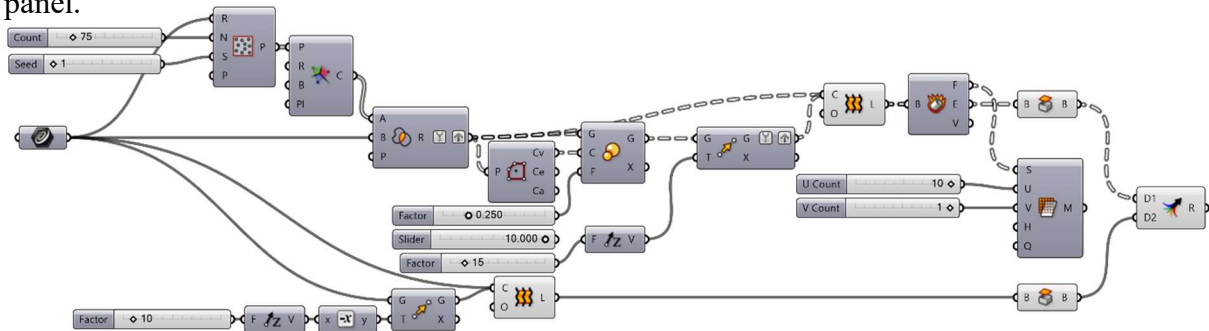
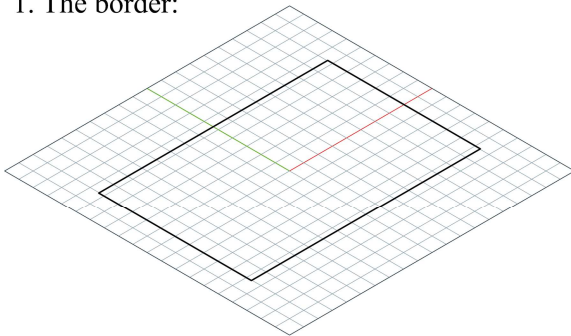
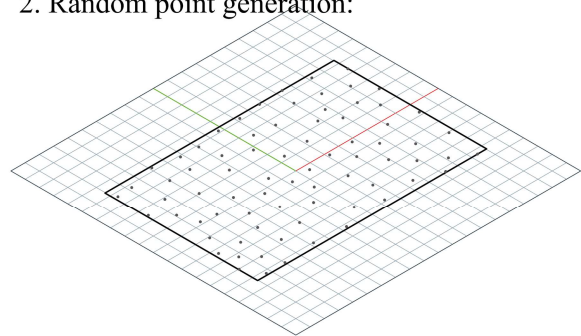


Figure 104: Grasshopper definition of the acoustic panel (Author's image)

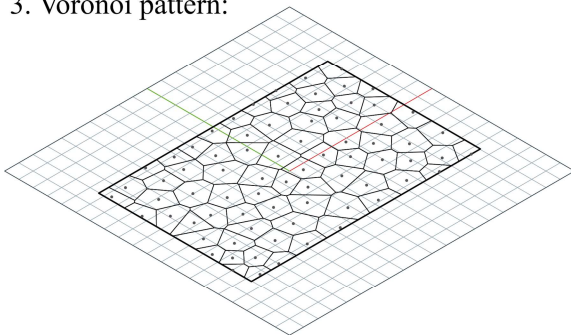
1. The border:



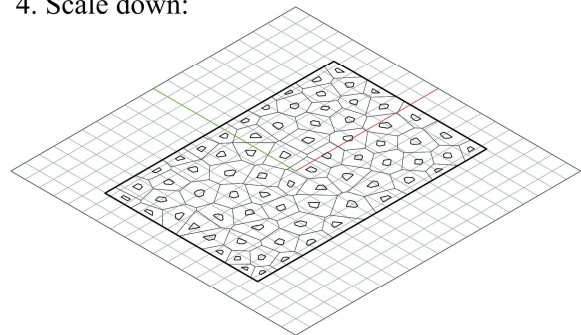
- ## 2. Random point generation:



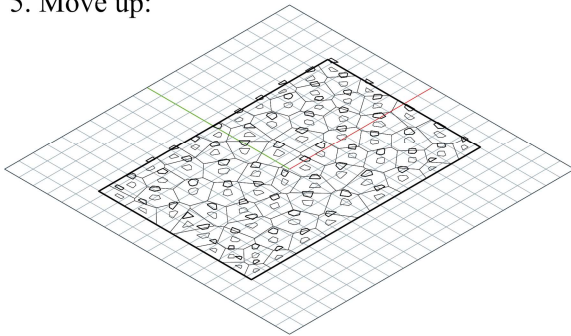
- ### 3. Voronoi pattern:



4. Scale down:



5. Move up:



- ## 6. Loft I:

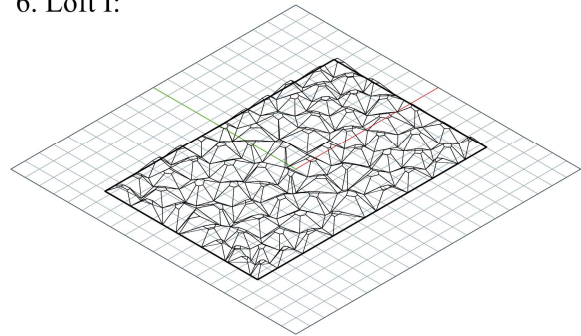
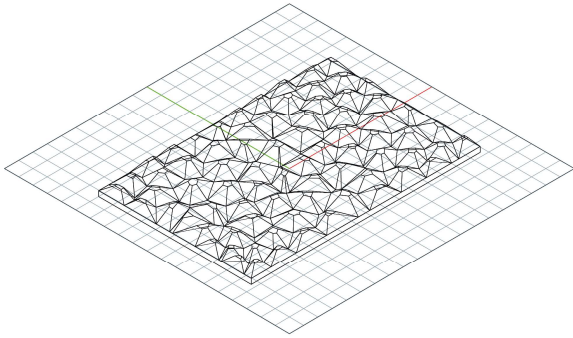


Figure 105: Steps 1 to 6 of the Grasshopper definition to generate the acoustic panel (Author's image)

7. Loft II:



8. Cap and shade:

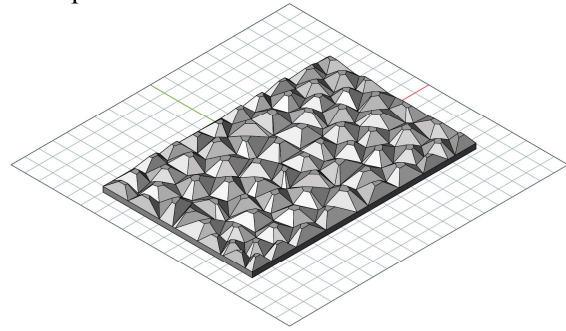


Figure 106: Steps 7 to 8 of the Grasshopper definition to generate the acoustic panel (Author's image)

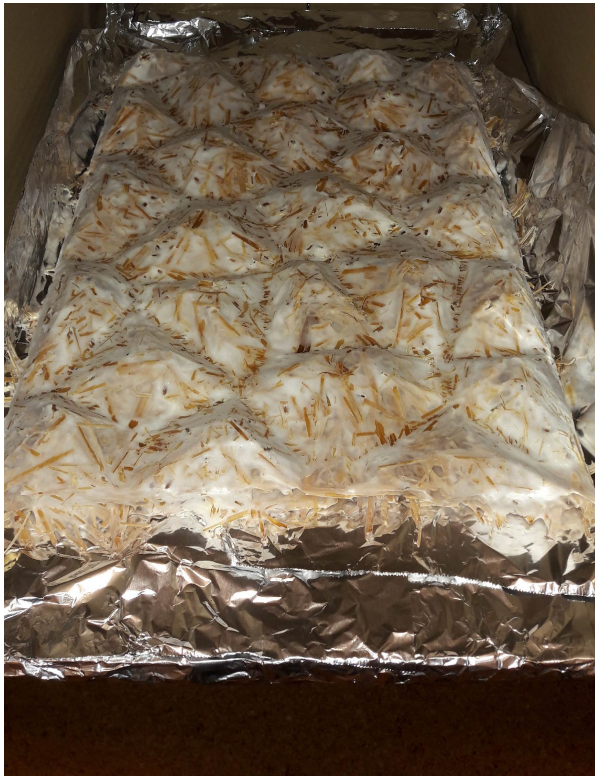
Due to parametric script, it has been enabled to generate random points and change the number of points in the border which brings a wider control on the shape of the acoustic absorber panel design. By randomizing the geometry, combined with the possible combinations different fungi species and substrate recipes and types, the efficiency of the acoustic panel under different sound sources which releases sound waves from different directions and frequencies can be increased and tuned. The following images represents the same acoustic absorber panel design created from different fungi species and substrate combinations.



Figure 107: Acoustic panel out of *Ganoderma lucidum* and sawdust-wood chips substrate mixture right after it has been taken out from the mold (Author's image)

The image above represents the acoustic absorber panel created with *Ganoderma lucidum* mycelium and sawdust and wood chips mixture substrate which has been taken out from its plastic mold. As it can be seen, there are some damages on the panel where some thin layers of material stick to the mold and peeled the mycelium mesh on the surface as well as some substrate. However, it has been observed that if the material kept in a protective environment with a high moisture level the mycelium keeps growing and starts to heal the damages by simply filling the gaps with mycelium tissue and actually the growth rate increases exponentially as it has been describes in the previous chapters. Thus, this sample is placed in a box where there is enough gas exchange which the moisture level can be kept a certain level.





*Figure 108: Acoustic absorber panel with Pleurotus eryngii and straw substrate (Author's image)*



*Figure 109: Various materials taken out from their molds (Author's image)*



*Figure 110: Mycelium growth of various materials after two days outside the molds (Author's image)*



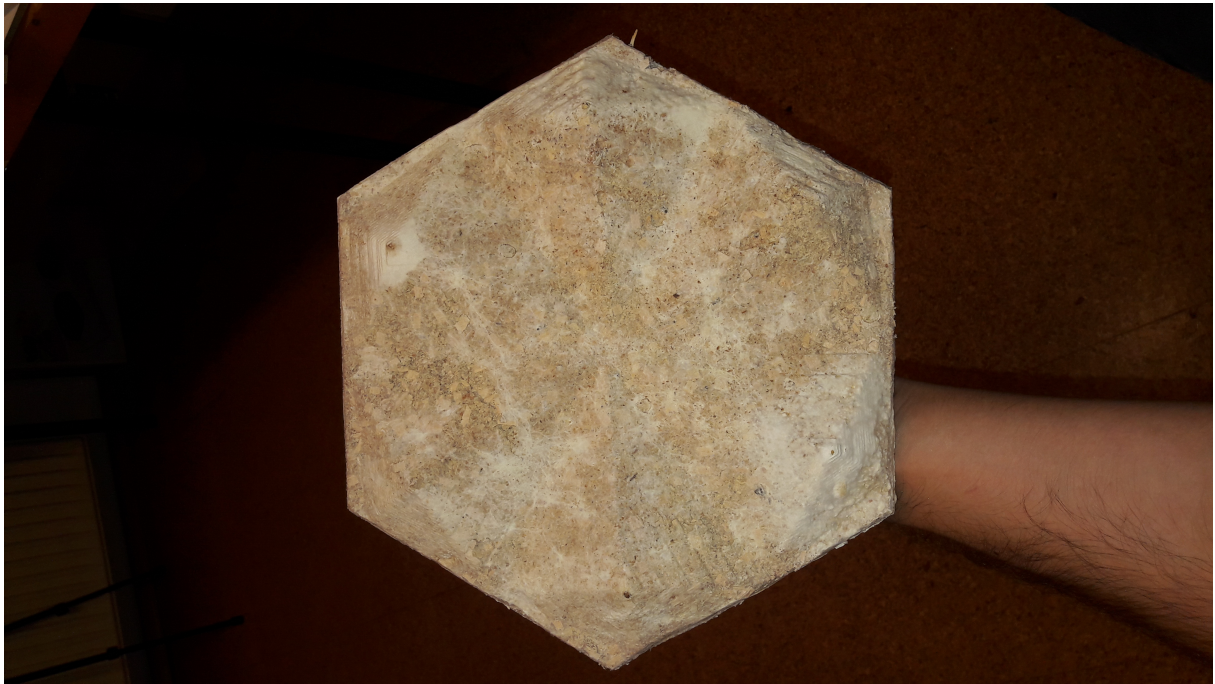


Figure 111: Another acoustic absorber panel (Author's image)

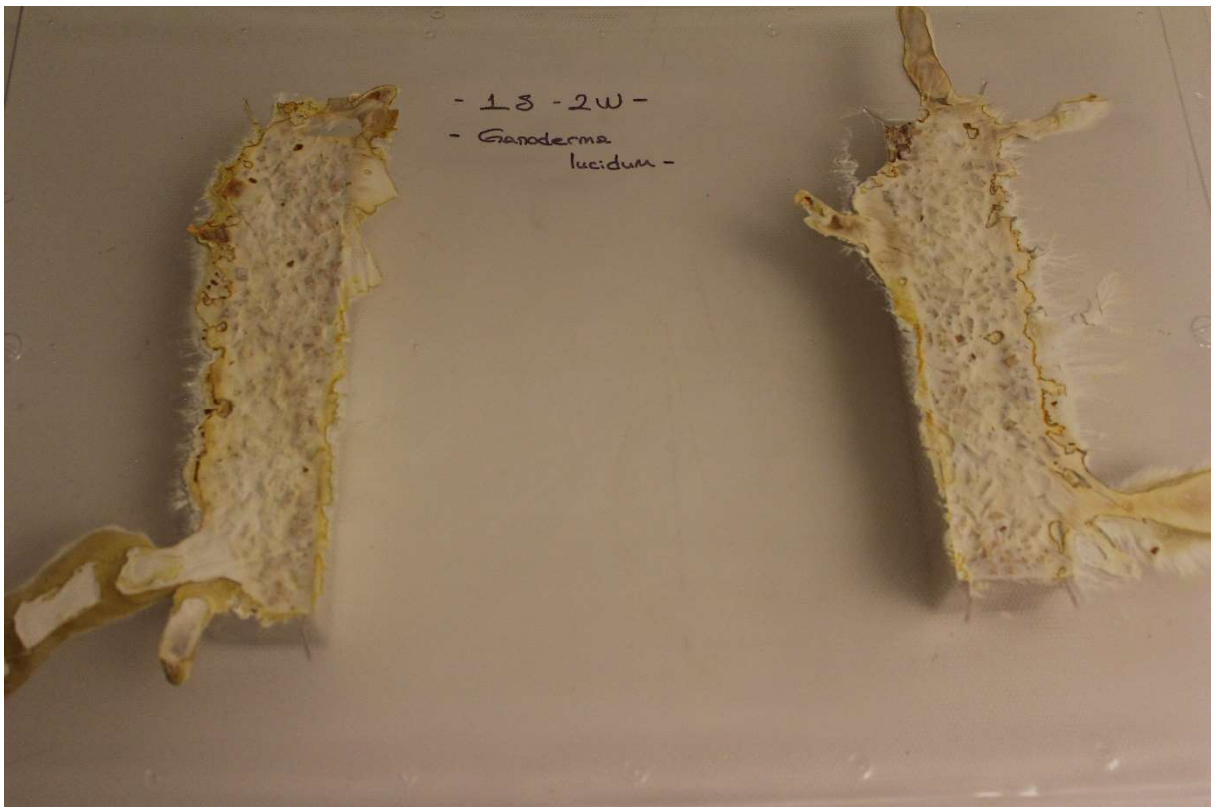


Figure 112: Mycelium-based biocomposite bricks growing in the molds (Author's image)



Figure 113: Mycelium-based biocomposite bricks growing in the molds (Author's image)



Figure 114: Hyperbolic paraboloid mycelium-based biocomposite brick growing in the molds (Author's image)

## Bibliography/References

- Albertsson, A. and Karlsson, S., 1994. Chemistry and Biochemistry of polymer degradation. In: G.J. Griffin, ed. *Chemistry and technology of biodegradable polymers*. London: Chapman & Hall, 7–17.
- Arifin, Y.H. and Yusuf, Y., 2013. Mycelium fibers as new resource for environmental sustainability. *Procedia Engineering*, 53, 504–508.
- Barnett, H.J. and Morse, C., 1963. Scarcity and Growth: The Economics of Natural Resource Availability. *Natural Resources Journal*, 288.
- Bayer, E. and McIntyre, G., 2012. Substrate Composition and Method for Growing Mycological Materials.
- Bergado, G., 2018. Mushrooms Are Helping Purify Dirty Waters [online]. *Popular Science*. Available from: <https://www.popsci.com/article/science/mushrooms-are-helping-purify-dirty-waters> [Accessed 13 Apr 2018].
- Block, P., Dejong, M., and Ochsendorf, J., 2006. As Hangs the Flexible Line : Equilibrium of Masonry Arches. *NEXUS NETWORK JOURNAL*, 8 (2), 9–19.
- Bordes, P., Pollet, E., and Avérous, L., 2009. Nano-biocomposites: Biodegradable polyester/nanoclay systems. *Progress in Polymer Science*, 34 (2), 125–155.
- Bos, H.L., Müssig, J., and van den Oever, M.J.A., 2006. Mechanical properties of short-flax-fibre reinforced compounds. *Composites Part A: Applied Science and Manufacturing*, 37 (10), 1591–1604.
- Clark, M. and Saporta, S., 2014. How Arup Engineered The Living's Mushroom Tower [online]. Available from: <http://www.metropolismag.com/ideas/technology/how-arup-engineered-the-livings-mushroom-tower/> [Accessed 10 Apr 2018].
- Cohen, R., Persky, L., and Hadar, Y., 2002. Biotechnological applications and potential of wood-degrading mushrooms of the genus *Pleurotus*. *Applied Microbiology and Biotechnology*, 58 (5), 582–594.
- Conversano, E., Mauro, F., Lorenzi, M., and Tedeschini-Lalli, L., 2011. Persistence of Form in Art and Architecture: Catenaries, Helicoids and Sinusoids. *APLIMAT Journal of Applied Mathematics*, 4, 101.
- Curtu, I., Brasov, U.T., Stanciu, M.D., Brasov, U.T., and Vasile, O., 2012. Assessment of Acoustic Properties of Biodegradable Composite Materials with Textile Inserts, (January).
- Diez, G., Gonzalez, E.M., Gonzalez, M.A.V., and Calderon, P.O., 2013. Design of prototype biosynthetic material for use as construction material [online]. *Seguridad y Medio Ambiente*. Available from: <https://www.mapfre.com/fundacion/html/revistas/seguridad/n132/docs/Article4.pdf> [Accessed 13 Apr 2018].
- Ecovative Design, MycoFoam [online], 2018. Available from: <https://shop.ecovativedesign.com/collections/packaging> [Accessed 4 May 2018].
- Ecovative Design, Press Kit [online], 2018. Available from: <https://ecovativedesign.com/press-kit> [Accessed 18 Jun 2018].
- Edvard, J., 2013. MYX [online]. Available from: <http://jonasedvard.dk/work/myx/> [Accessed 12 Apr 2018].
- Faruk, O., Bledzki, A.K., Fink, H.-P., and Sain, M., 2012. Biocomposites reinforced with natural fibers: 2000–2010. *Progress in Polymer Science*, 37 (11), 1552–1596.
- Ganotopoulou, E., 2014. Biodegradable materials. A research and design handbook; enhancing the use of biodegradable materials on building's envelopes in the Netherlands. Technical University of Delft.
- González, E.M. and Diez, I.G., 2015. Bacterial Induced Cementation Processes and Mycelium Panel Growth from Agricultural Waste. *Key Engineering Materials*, 663, 42–49.
- Güler, P., Kutluer, F., and Kunduz, İ., 2011. Screening to Mycelium Specifications of *Ganoderma lucidum* (Fr.) Karst (Reishi). *Hacettepe J. Biol. & Chem.*, 39 (4), 397–401.
- Haneef, M., Ceseracciu, L., Canale, C., Bayer, I.S., Heredia-Guerrero, J.A., and Athanassiou, A., 2017. Advanced Materials from Fungal Mycelium: Fabrication and Tuning of Physical Properties. *Scientific Reports*, 7 (January), 1–11.



- Hawksworth, D.L., 2001. The magnitude of fungal diversity: The 1.5 million species estimate revisited. *Mycological Research*, 105 (12), 1422–1432.
- He, J., Cheng, C.M., Su, D.G., and Zhong, M.F., 2014. Study on the Mechanical Properties of the Latex-Mycelium Composite. *Applied Mechanics and Materials*, 507, 415–420.
- Heyman, J., 1998. *Structural Analysis: A Historical Approach*. Cambridge University Press.
- Holt, G.A., McIntyre, G., Flagg, D., Bayer, E., Wanjura, J.D., and Pelletier, M.G., 2012. Fungal mycelium and cotton plant materials in the manufacture of biodegradable molded packaging material: Evaluation study of select blends of cotton byproducts. *Journal of Biobased Materials and Bioenergy*, 6 (4), 431–439.
- Islam, M.R., Tudryn, G., Bucinell, R., Schadler, L., and Picu, R.C., 2017. Morphology and mechanics of fungal mycelium. *Scientific Reports*, 7 (1), 1–12.
- Jacewicz, N., 2018. Making Furniture from Fungi [online]. Available from: <https://blogs.scientificamerican.com/guest-blog/making-furniture-from-fungi/> [Accessed 13 Apr 2018].
- Jones, M., Huynh, T., Dekiwadia, C., Daver, F., and John, S., 2017. Mycelium composites: A review of engineering characteristics and growth kinetics. *Journal of Bionanoscience*, 11 (4), 241–257.
- Kalisz, R.E. and Rocco, C.A., 2011. Method of making molded part comprising mycelium coupled to mechanical device.
- Khalil, H.P.S.A., Bhat, I.U.H., Jawaid, M., Zaidon, A., Hermawan, D., and Hadi, Y.S., 2012. Bamboo fibre reinforced biocomposites : A review Bamboo fibre reinforced biocomposites : A review. *Materials and Design*, 42 (July), 353–368.
- Klarenbeek, E., 2018. Myceliumchair [online]. Available from: <http://www.ericklarenbeek.com/> [Accessed 16 May 2018].
- Kralj, D. and Markič, M., 2008. Building materials reuse and recycle. *WSEAS Transactions on Environment and Development*, 4 (5), 409–418.
- Kropáček, K., Cudlín, P., and Mejstřík, V., 1990. The use of granulated ectomycorrhizal inoculum for reforestation of deteriorated regions. *Agriculture, Ecosystems & Environment*, 28 (1–4), 263–269.
- Larpernt, J.P., 1966. Caractèresetdéterminisme des correlations d'inhibition dans le mycelium jeune de quelques champignons. *Ann. Sci. Nat. Bot. Biol*, 7, 1–130.
- Lawson, B., 2006. *Embodied energy of building materials*. Environment design guide, PRO 2. Melbourne: Royal Australian Institute of Architects.
- Lelivelt, R., Lindner, G., Teuffel, P., and Lamers, H., 2015. The Production Process and Compressive Strength of Mycelium-based Materials. In: *First International Conference on Bio-based Building Materials*. Clermont-Ferrand, France, 1–6.
- Lelivelt, R.J.J., 2015. The mechanical possibilities of mycelium materials.
- López Nava, J.A., Mèndez Gonzàlez, J., Ruelas Chacòn, X., and Nàjiera Luna, J.A., 2016. Assessment of Edible Fungi and Films Bio-Based Material Simulating Expanded Polystyrene. *Materials and Manufacturing Processes*, 31 (8), 1085–1090.
- Matthews, F.L. and Rawlings, R.D. (Rees D., n.d. *Composite materials : engineering and science*. McGraw-Hill, 2016. Fungi [online]. Available from: <http://www.glencoe.com/sec/science/ose/bd012005/ca/docs/chap20.pdf> [Accessed 9 Apr 2018].
- Mohanty, A.K., Misra, M., and Hinrichsen, G., 2000. Biofibres, biodegradable polymers and biocomposites: An overview. *Macromolecular Materials and Engineering*, 276–277, 1–24.
- Montalti, M., 2010. Continuous Bodies. Design Academy Eindhoven.
- Morel, J.C., Mesbah, A., Oggero, M., and Walker, P., 2001. Building houses with local materials: Means to drastically reduce the environmental impact of construction. *Building and Environment*, 36 (10), 1119–1126.
- MycoWorks, 2017. MycoWorks Material [online]. Available from: <http://www.mycoworks.com/#product-section> [Accessed 13 Apr 2018].
- Nagy, D., Locke, J., and Benjamin, D., 2015. Computational Brick Stacking for Constructing Free-Form



- Structures. In: M.R. Thomsen, M. Tamke, C. Gengnagel, B. Faircloth, and F. Scheurer, eds. *Modelling Behaviour*. Springer, 203–213.
- Northwest Wild Foods [online], 2018. Available from: <https://nwwildfoods.com/product-tag/fresh-frozen-organic-shiitake-mushrooms/> [Accessed 19 Jun 2018].
- Pacheco Torgal, F. and Jalali, S., 2011. *Eco-efficient Construction and Building Materials*.
- Pavòn, J., 2018. Ganoderma lucidum, Invasión verde [online]. *Sustainable Living*. Available from: <https://www.invasionverde.com/blog/vida-sostenible/reishi-ganoderma-lucidum-hongo-juventud> [Accessed 19 Jun 2018].
- Rinaudo, M., 2007. Properties and degradation of selected polysaccharides: hyaluronan and chitosan. *Corrosion Engineering, Science and Technology*, 42 (4), 324–334.
- Sassi, P., 2006. Biodegradable building. *WIT Transactions on Ecology and the Environment*, 87, 91–102.
- Sathishkumar, T.P., Naveen, J., and Satheeshkumar, S., 2014. Hybrid fiber reinforced polymer composites - A review. *Journal of Reinforced Plastics and Composites*, 33 (5), 454–471.
- Satyanarayana, K.G., Carbajal Arizaga, G., and Wypych, F., 2009. *Biodegradable composites based on lignocellulosic fiber an overview*. Prog Polym Sci.
- Shields, T., 2018. FreshCap Mushrooms, Making Agar Plates [online]. Available from: <http://freshcapmushrooms.com/learn/agar-agar-so-nice-they-named-it-twice-5-steps-to-pouring-perfect-plates/> [Accessed 10 Apr 2018].
- Stamets, P., 2005. *Mycelium running*. Mycelium running: How mushrooms can help save the world. Berkeley, California: Ten Speed Press.
- Stamets, P. and Chilton, J.S., 1983. *The Mushroom Cultivator: A Practical Guide to Growing Mushrooms at Home*. Illustrate. Olympia, WA: Agarikon Press.
- Stone, M., 2018. The Plan to Mop Up the World's Largest Oil Spill With Fungus [online]. Available from: [https://motherboard.vice.com/en\\_us/article/jp5k9x/the-plan-to-mop-up-the-worlds-largest-oil-spill-with-fungus](https://motherboard.vice.com/en_us/article/jp5k9x/the-plan-to-mop-up-the-worlds-largest-oil-spill-with-fungus) [Accessed 13 Apr 2018].
- Stott, R., 2014. Hy-Fi, The Organic Mushroom-Brick Tower Opens At MoMA's PS1 Courtyard [online]. Available from: Hy-Fi, The Organic Mushroom-Brick Tower Opens At MoMA's PS1 Courtyard [Accessed 12 May 2018].
- Su, C.H., Sun, C.S., Juan, S.W., Hu, C.H., Ke, W.T., and Sheu, M.T., 1997. Fungal mycelia as the source of chitin and polysaccharides and their applications as skin substitutes. *Biomaterials*, 18 (17), 1169–1174.
- Swain, S.N., Biswal, S.M., Nanda, P.K., and L. Nayak, P., 2004. *Biodegradable Soy-Based Plastics: Opportunities and Challenges*. Journal of Polymers and the Environment.
- Symington, M.C., Banks, W.M., West, O.D., and Pethrick, R.A., 2009. Tensile testing of cellulose based natural fibers for structural composite applications. *Journal of Composite Materials*, 43 (9), 1083–1108.
- Thakur, V.K. and Singha, A.S., 2013. *Biomass-based Biocomposites*. Shrewsbury, U.K.: Smithers Rapra.
- The Auroville Earth Institute, Stability calculations, Catenary Method [online], 2018. Available from: [http://www.earth-auroville.com/stability\\_calculations\\_en.php#](http://www.earth-auroville.com/stability_calculations_en.php#) [Accessed 29 May 2018].
- Thepinsta.com [online], 2018. Available from: [http://www.thepinsta.com/mushroom-king-oyster-200g-pack-harris-farm-markets\\_4D29Qm2Vd4TybvGw7XSnn3nrawYIkjBLTNiBWcfxN7ztzOkjtqTSEuMxPfxCLiXjoRBZb395vl0wx7E2LKUmwA/zdCMU6%7C8moCy907CI7it\\*CPryv1TWmQOkWYi8lbFk2\\*uP7qJbXflgzGwV6g9TSY6JqlkdxQQfbEZQRTsBMiijswO3](http://www.thepinsta.com/mushroom-king-oyster-200g-pack-harris-farm-markets_4D29Qm2Vd4TybvGw7XSnn3nrawYIkjBLTNiBWcfxN7ztzOkjtqTSEuMxPfxCLiXjoRBZb395vl0wx7E2LKUmwA/zdCMU6%7C8moCy907CI7it*CPryv1TWmQOkWYi8lbFk2*uP7qJbXflgzGwV6g9TSY6JqlkdxQQfbEZQRTsBMiijswO3) [Accessed 19 Jun 2018].
- Travaglini, S., Dharan, C.K.H., and Ross, P.G., 2014. Mycology Matrix Sandwich Composites Flexural Characterization. In: *Proceedings of the American Society for Composites 2014-Twenty-ninth Technical Conference on Composite Materials*. DEStech Publications, Inc, 222–236.
- Travaglini, S., Noble, J., Ross, P.G., and Dharan, C.K.H., 2013. Mycology matrix composites. In: *Proceedings of the American Society for Composites 28th Technical Conference*. Red Hook, NY: Curran Associates, Inc., 517–535.

- Trinici, A.P.J. and Collinge, A.J., 1975. Hyphal Wall Growth in *Neurospora crassa* and *Geotrichum candidum*. *Journal of General Microbiology*, 91, 355–361.
- Tuzcu, T.M., 2007. Hygro-Thermal Properties of Sheep Wool Insulation. Delft University of Technology.
- Tyroler, Glückspilze, Making of spore prints [online], 2018. Available from: <https://gluckspilze.com/1sporenabdruck-1> [Accessed 20 Jun 2018].
- Tyroler, Glückspilze, Mushroom cloning [online], 2018. Available from: <https://gluckspilze.com/5klonen-1> [Accessed 20 Jun 2018].
- Vega, K. and Kalkum, M., 2012. Chitin, chitinase responses, and invasive fungal infections. *International Journal of Microbiology*, 2012.
- Viitanen, H., Vinha, J., Salminen, K., Ojanen, T., and Peuhkuri, R., 2010. Moisture and biodeterioration risk of building materials and structures. *Journal of Building Physics*, 33 (3), 1–14.
- Visual Dictionary Online, Structure of a mushroom [online], 2018. Available from: <http://www.visualdictionaryonline.com/plants-gardening/plants/mushroom/structure-mushroom.php> [Accessed 5 Feb 2018].
- Wambua, P., Ivens, J., and Verpoest, I., 2003. Natural fibres: Can they replace glass in fibre reinforced plastics? *Composites Science and Technology*, 63 (9), 1259–1264.
- Watkinson, S.C., Boddy, L., Money, N.P., and Carlile, M.J., 2016. *The Fungi*. 3rd ed. Amsterdam; Boston: Elsevier B.V.
- Webster, J. and Weber, R., 2007. *Introduction to Fungi*. Cambridge: Cambridge University Press.
- Weisstein, E.W., 2008. Catenary [online]. *MathWorld - A Wolfram Web Source*. Available from: <http://mathworld.wolfram.com/Catenary.html> [Accessed 3 Jun 2018].
- Wikipedia, Taq Kasra [online], 2018. Available from: [https://en.wikipedia.org/wiki/Taq\\_Kasra](https://en.wikipedia.org/wiki/Taq_Kasra) [Accessed 8 Jun 2018].
- Wool, R.P. and Sun, X.S., 2005. *Bio-based polymers and composites*. 1st ed. Elsevier Academic Press.
- Workshop Residence, Yamanaka McQueen [online], 2018. Available from: <https://workshopresidence.com/products/yamanaka-mcqueen> [Accessed 12 May 2018].
- Yang, Z. (Joey), Zhang, F., Still, B., White, M., and Amstislavski, P., 2017. Physical and Mechanical Properties of Fungal Mycelium-Based Biofoam. *Journal of Materials in Civil Engineering*, 29 (7), 04017030.